Nuclear Safety
NEA/CSNI/R(2016)9
April 2016
www.oecd-nea.org

PREMIUM: A Benchmark on the Quantification of the Uncertainty of the Physical Models in System Thermal-hydraulic Codes

Methodologies and Data Review

OECD
BETTER POLICIES FOR BETTER LIVES

NEA
NUCLEAR ENERGY AGENCY

Unclassified **NEA/CSNI/R(2016)9**

Organisation de Coopération et de Développement Économiques
Organisation for Economic Co-operation and Development **28-Apr-2016**

English text only

NUCLEAR ENERGY AGENCY
COMMITTEE ON THE SAFETY OF NUCLEAR INSTALLATIONS

PREMIUM, a benchmark on the quantification of the uncertainty of the physical models in the system thermal-hydraulic codes: methodologies and data review

JT03394989

NEA/CSNI/R(2016)9
Unclassified
English text only

ORGANISATION FOR ECONOMIC CO-OPERATION AND DEVELOPMENT

The OECD is a unique forum where the governments of 34 democracies work together to address the economic, social and environmental challenges of globalisation. The OECD is also at the forefront of efforts to understand and to help governments respond to new developments and concerns, such as corporate governance, the information economy and the challenges of an ageing population. The Organisation provides a setting where governments can compare policy experiences, seek answers to common problems, identify good practice and work to co-ordinate domestic and international policies.

The OECD member countries are: Australia, Austria, Belgium, Canada, Chile, the Czech Republic, Denmark, Estonia, Finland, France, Germany, Greece, Hungary, Iceland, Ireland, Israel, Italy, Japan, Luxembourg, Mexico, the Netherlands, New Zealand, Norway, Poland, Portugal, the Republic of Korea, the Slovak Republic, Slovenia, Spain, Sweden, Switzerland, Turkey, the United Kingdom and the United States. The European Commission takes part in the work of the OECD.

OECD Publishing disseminates widely the results of the Organisation's statistics gathering and research on economic, social and environmental issues, as well as the conventions, guidelines and standards agreed by its members.

NUCLEAR ENERGY AGENCY

The OECD Nuclear Energy Agency (NEA) was established on 1 February 1958. Current NEA membership consists of 31 countries: Australia, Austria, Belgium, Canada, the Czech Republic, Denmark, Finland, France, Germany, Greece, Hungary, Iceland, Ireland, Italy, Japan, Luxembourg, Mexico, the Netherlands, Norway, Poland, Portugal, the Republic of Korea, the Russian Federation, the Slovak Republic, Slovenia, Spain, Sweden, Switzerland, Turkey, the United Kingdom and the United States. The European Commission also takes part in the work of the Agency.

The mission of the NEA is:

- to assist its member countries in maintaining and further developing, through international co-operation, the scientific, technological and legal bases required for a safe, environmentally friendly and economical use of nuclear energy for peaceful purposes;
- to provide authoritative assessments and to forge common understandings on key issues, as input to government decisions on nuclear energy policy and to broader OECD policy analyses in areas such as energy and sustainable development.

Specific areas of competence of the NEA include the safety and regulation of nuclear activities, radioactive waste management, radiological protection, nuclear science, economic and technical analyses of the nuclear fuel cycle, nuclear law and liability, and public information.

The NEA Data Bank provides nuclear data and computer program services for participating countries. In these and related tasks, the NEA works in close collaboration with the International Atomic Energy Agency in Vienna, with which it has a Co-operation Agreement, as well as with other international organisations in the nuclear field.

COMMITTEE ON THE SAFETY OF NUCLEAR INSTALLATIONS

The NEA Committee on the Safety of Nuclear Installations (CSNI) is an international committee made up of senior scientists and engineers with broad responsibilities for safety technology and research programmes, as well as representatives from regulatory authorities. It was created in 1973 to develop and co-ordinate the activities of the NEA concerning the technical aspects of the design, construction and operation of nuclear installations insofar as they affect the safety of such installations.

The committee's purpose is to foster international co-operation in nuclear safety among NEA member countries. The main tasks of the CSNI are to exchange technical information and to promote collaboration between research, development, engineering and regulatory organisations; to review operating experience and the state of knowledge on selected topics of nuclear safety technology and safety assessment; to initiate and conduct programmes to overcome discrepancies, develop improvements and reach consensus on technical issues; and to promote the co-ordination of work that serves to maintain competence in nuclear safety matters, including the establishment of joint undertakings.

The priority of the CSNI is on the safety of nuclear installations and the design and construction of new reactors and installations. For advanced reactor designs, the committee provides a forum for improving safety-related knowledge and a vehicle for joint research.

In implementing its programme, the CSNI establishes co-operative mechanisms with the NEA Committee on Nuclear Regulatory Activities (CNRA), which is responsible for issues concerning the regulation, licensing and inspection of nuclear installations with regard to safety. It also co-operates with other NEA Standing Technical Committees, as well as with key international organisations such as the International Atomic Energy Agency (IAEA), on matters of common interest.

ACKNOWLEDGEMENTS

Coordinators of this activity: Francesc Reventós (UPC), Elsa de Alfonso (UPC) and Rafael Mendizábal Sanz (CSN).

Participants

Belgium	Bel V	Christine Sarrette
	Tractebel Engineering (ENGIE Energy Services)	Jinzhao Zhang, Andriy Kovtonyuk, Adrien Dethioux, Maxim Janssens, Claudio Léna, Jacobo Segurado
China	Shanghai Jiao Tong University (SJTU)	Xiaojing Liu, Li Dong
Czech Republic	Centrum Výzkumu Řež (CVRez)	Milos Kyncl, Rostislav Pernica, Vit Kopecek, Radim Meca
Finland	Technical Research Centre of Finland (VTT)	Joona Kurki, Torsti Alku
France	Commissariat à l'énergie atomique et aux énergies alternatives (CEA)	Agnès de Crécy, Pascal Bazin
	Institut de Radioprotection et de Sûreté Nucléaire (IRSN)	Pierre Probst, Jean Baccou, Fabrice Fouet, François Barré
Germany	Gesellschaft für Anlagen- und Reaktorsicherheit (GRS)	Tomasz Skorek
	Karlsruhe Institute of Technology (KIT)	Wadim Jaeger, Victor Sánchez
Italy	Nuclear and Industrial Engineering (N.IN.E)	Alessandro Petruzzi
	San Piero a Grado Nuclear Research Group (GRNSPG), Univ. of Pisa	Francesco D'Auria
Korea (Republic of)	Korea Atomic Energy Research Institute (KAERI)	Bub-Dong Chung, Jae Seok Heo
	Korea Institute of Nuclear Safety (KINS)	Deog-Yeon Oh
Russia	OKB Mechanical Engineering (OKBM)	Alexey Gusev, Alexander Falkov, Yuri Shvetsov
Spain	Universitat Politècnica de Catalunya (UPC)	Francesc Reventós, Elsa de Alfonso
	Consejo de Seguridad Nuclear (CSN), Spain	Rafael Mendizábal Sanz
Switzerland	Paul Scherrer Institute (PSI)	Omar Zerkak, Damar Wicaksono

The NEA official supporting this activity was firstly A. Amri then M.P. Kissane.

EXECUTIVE SUMMARY

The objective of the Post-BEMUSE Reflood Model Input Uncertainty Methods (PREMIUM) benchmark is to progress on the issue of the quantification of the uncertainty of the physical models in system thermal-hydraulic codes by considering a concrete case: the physical models involved in the prediction of core reflooding.

The present document was initially conceived as a final report for the Phase I "Introduction and Methodology Review" of the PREMIUM benchmark. The objective of Phase I is to refine the definition of the benchmark and publish the available methodologies of model input uncertainty quantification relevant to the objectives of the benchmark. In this initial version the document was approved by WGAMA and has shown its usefulness during the subsequent phases of the project.

Once Phase IV was completed, and following the suggestion of WGAMA members, the document was updated adding a few new sections, particularly the description of four new methodologies that were developed during this activity. Such developments were performed by some participants while contributing to PREMIUM progress (which is why this report arrives after those of other phases). After this revision the document title was changed to "PREMIUM methodologies and data review".

The introduction includes first a chapter devoted to contextualization of the benchmark in nuclear safety research and licensing, followed by a description of the PREMIUM objectives. Next, a description of the Phases in which the benchmark is divided and its organization is explained.

Chapter two consists of a review of the involvement of the different participants, making a brief explanation of the input uncertainty quantification methodologies used in the activity.

The document ends with some conclusions on the development of Phase I, some more general remarks and some statements on the benefits of the benchmark, which can be briefly summarized as it follows:

- Contribution to development of tools and experience related to uncertainty calculation and promotion of the use of BEPU approaches for licensing and safety assessment purposes;
- Contribution to prioritization of improvements to thermal-hydraulic system codes;
- Contribution to a fluent and close interaction between the scientific community and regulatory organizations.

Appendices include the complete description of the experimental data FEBA/SEFLEX used in the benchmark and the methodologies CIRCÉ and FFTBM and the general requirements and description specification used for Phase I. Due to the revision of the document, four extra appendixes have been added related to the methods developed during the activity, MCDA DIPE, Tractebel IUQ and PSI methods.

TABLE OF CONTENTS

LIST OF ABBREVIATIONS AND ACRONYMS

AA	Average amplitude
BAF	Bottom of active fuel
BE	Best estimate
BEPU	Best estimate plus uncertainty
BEMUSE	Best estimate methods – uncertainty and sensitivity evaluation (see NEA/CSNI/R(2011)3)
BIC	Boundary and initial conditions
BWR	Boiling-water reactor
CCFL	Counter-current flow limiting
CDF	Cumulative density function
CHF	Critical heat flux
CIRCÉ	Calcul des incertitudes relatives aux corrélations élémentaires
CSNI	Committee on the Safety of Nuclear Installations
DBA	Design-basis accident
DFFB	Dispersed-flow film boiling
DIPE	Determination of Input Parameters Empirical properties
DNB	Departure from nucleate boiling
DP	Pressure drop
ECC	Emergency core cooling
FEBA	Flooding Experiment with Blocked Arrays
FFTBM	Fast-Fourier Transformation Based Method
HPIS	High pressure injection system
HT	Heat transfer
HTC	Heat transfer coefficient
IAEA	International Atomic Energy Agency
IAFB	Inverted Annular Film Boiling
IBP	Input Basic Parameter
ICP	Input Coefficient Parameter
ID	identification
IGP	Input Global Parameter
IP	Input Parameter
ITF	Integral Test Facility
IUQ	Inverse uncertainty quantification
LB	Large break
LOCA	Loss-of-coolant accident

LP	Lower plenum
LPIS	Low pressure injection system
LWR	Light-water reactor
MCDA	Model Calibration through Data Assimilation
NA	Not available
NLLS	Non-linear least square
NPP	Nuclear Power Plant
PDF	Probability density function
PERICLES	Large-scale experimental facility for thermal hydraulics (reflood in this case)
PREMIUM	Post-BEMUSE REflood Models Input-Uncertainty Methods
PWR	Pressurized-water reactor
QF	Quench front
REM	Realistic evaluation methodology
RTA	Relevant Thermal-hydraulic Aspect
SB	Small break
SEFLEX	Fuel-rod Simulator Effects in Flooding Experiments
SET	Separate-effect test
SM2A	Safety-margin assessment and application (see NEA/CSNI/R(2011)3)
SUSA	Software for Uncertainty and Sensitivity Analysis
TH	Thermal hydraulic
TH-SYS	Thermal-hydraulic system (referred to computer code)
UP	Upper plenum
UAM	Uncertainty Analysis in Modelling (see NEA/NSC/DOC(2013)7)
UMAE	Uncertainty Method based on Accuracy Extrapolation
UMS	Uncertainty Methods Study
WF	Weighted frequency
WGAMA	Working Group on Analysis and Management of Accidents (CSNI group)

APROS, ATHLET, CATHARE, COBRA, KORSAR MARS-KS, RELAP and TRACE are all thermal-hydraulic computer codes.

1 INTRODUCTION

1.1 Context

In the framework of nuclear safety, computer codes are used in order to assess event/accident analysis, nuclear power plants design or improvement, and licensing review. The models used by these codes are only an approximation of real physical phenomena. Moreover the data used to run these codes is known with limited accuracy. Therefore, the predictions resulting from code simulation are not exact but uncertain. To deal with these uncertainties, two different approaches can be distinguished as described below.

- Conservative approach: this first approach, well-adopted in licensing practices, uses conservative codes, which contain deliberate pessimistic and unphysical assumptions in relation to acceptance criteria. Its predictions are considered conservative but its meaningfulness remains very limited.

- Best-estimate approach: this second approach is in full development and uses best-estimate codes, which are designed to model all the relevant processes in a physically realistic way without bias (either in a pessimistic or optimistic direction). A single calculation with a best-estimate code is then considered as the best estimation of the reality but cannot be used directly for safety purposes, due to the uncertainty attached to its results. The development of accuracy evaluation techniques is therefore necessary.

Taking into account the features of both approaches, the use of best-estimate thermal-hydraulic system codes is mainly motivated by four reasons as described below.

- The conservatism of results obtained with conservative codes is questionable due to the complexity of the phenomena involved in a nuclear safety calculation (e.g. the possibility of counter-reactions when using penalizing assumptions).

- The relaxation of technical specifications and core operating limits set by conservative calculations results in more economical operation of reactors and, moreover, more financially stimulating projects of new and safer developments.

- Realistic calculations can give a better understanding of accident progress, contributing to the improvement of accident management procedures.

- An insight into the phenomena relevant to an accident and into the quality of code predictions, resulting in a conscious analysis of the sufficiency of the different models used in codes increases the confidence in nuclear power plant safety and the adequacy of safety procedures for accidents.

For all these reasons, Best-Estimate Plus Uncertainty (BEPU) methods are gaining increased interest in the licensing process. In particular, improvements of classical BEPU approaches are currently the driving force to promote their use instead of the conservative or mixed conservative-BE approaches.

In order to progress on the issue of BEPU approach, several international initiatives, such as the UMS or BEMUSE, have arisen, consolidating methods, stimulating working groups and developing a common understanding. BEMUSE has shown that uncertainty methods have now a good maturity for the evaluation of uncertainty on a LB-LOCA transient. However, as mentioned in the final BEMUSE report; important efforts have to be done on the quantification of input uncertainties which is a compulsory step when performing for example a probabilistic uncertainty analysis. More precisely, high requirements are needed on the determination and the justification of the uncertainty range associated with each uncertain parameter. This quantification is often performed by subjective engineering judgement and therefore requires further development to provide a common understanding on this key issue.

1.2 The PREMIUM objectives

The general objective of PREMIUM (Post BEMUSE Reflood Models Input Uncertainty Methods project, endorsed by CSNI and WGAMA, is to progress on the issue of the quantification of the uncertainty of the physical models in system thermal-hydraulic codes, having as final goals:

- Assessment of advanced methods and tools used for event/accident analysis.

- Review of current analytical tools as well as risk assessment approaches regarding their applicability to safety assessments of new designs, and their further development and validation where needed.

There are different kinds of input parameters that can bring uncertainty to a BE calculation: initial and boundary conditions, material properties, physical models (involving the solution of numerical techniques, empirical data, or validity ranges of correlations, among others), etc. The physical models often involve the most influential input parameters. Nevertheless estimating their uncertainty is a difficult challenge since the majority of physical models predictions cannot be directly measured, and in many cases there is no Separate Effect Test (SET) that can describe the isolated phenomena.

PREMIUM is aimed at using State of the Art statistic methodologies and improving expert judgement and common understanding in order to face this challenge. To this end, it considers a concrete case: the physical models involved in the prediction of core reflooding. Examples of such physical models are: heat transfer downstream from the quench front (post-CHF heat transfer), enhancement to the heat transfer very close to the quench front, relative velocity downstream from the quench front, etc.

At the end of the benchmark, each participant will have determined the uncertainty of the input parameters associated with the physical models that he considers as influential in the reflood calculation for the chosen system code. Methodologies and experimental data used have to be put in common, using FEBA/SEFLEX experiment as main experimental data for the quantification of uncertainties. A confirmation step will be performed at the end of the project to evaluate the quality of the information provided by each participant. It will be achieved after uncertainty propagation in the case of the PERICLES experiments, which are yet unpublished.

The main expected results are:

- A State of the Art, included in the synthesis report, of the existing methods devoted to the quantification of the uncertainty of the physical models, including a comparison of methods and recommendations for future work.

- An improvement of expert judgment if the user does not have at his disposal a specific method, as well as an increase of common understanding.

1.3 Brief description of PREMIUM Phases

Within the frame of the PREMIUM benchmark, the quantification of the uncertainties will be performed for the influential physical models in the reflooding. More precisely, the participants will:

- Determine the uncertain parameters of their code associated with these physical models;
- Quantify the uncertainties of these parameters using FEBA/SEFLEX experimental result or own reflood experiment;
- Confirm the found uncertainties by uncertainty propagation in the case of the 2-D reflood PERICLES experiment. This part will be performed blindly (except for the coordinators: CEA and IRSN).

The benchmark will be concluded by a synthesis report with recommendations.
PREMIUM is divided into five chronological Phases, each one lead by a coordinating institution from the Organizing Committee, and following this general pattern:

1. The coordinating institution produces a specification defining the activities expected by the participants during the Phase
2. A period is given to the participants in order to fulfil these activities
3. A meeting is organized in which the participants put in common their results and analytical experience
4. A final report compiling all the information produced during the Phase is written by the coordinating institution and reviewed by all the participants

Each of these Phases is described below:

1.3.1 Phase I: introduction and methodology review

Coordinating institution: UPC, Spain (with the support of CSN, Spain)

This first Phase of PREMIUM consists of a precise definition of the benchmark and a review of the available methodologies concerning the objectives of the benchmark (see Appendix D). In this Phase, participants will put in common the methodologies and the experimental data they intend to use or make available for other participants.

- Regarding methodology, as described in Phase I Specifications [1], specific methods will be used, if available. Otherwise, expert judgment can also be used, complemented by classic methods like fitting of data.
- Regarding experimental data, FEBA/SEFLEX data is proposed since the beginning of the benchmark to be used during the identification and quantification of uncertainties.
- Regarding system thermal-hydraulic code, there is no particular restriction.

The coordinating institution distributes at the end of the Phase the present report, including final specification of the benchmark, the involvement of participants, and a methodology review.

1.3.2 Phase II: identification of important input uncertainties and their initial quantification

Coordinating institution: UNIPI, Italy

In this Phase, the participants are asked to identify which physical models of their codes can be considered as influential in the reflooding scenario using data from the FEBA/SEFLEX experiment, select the related uncertain input parameters and propose the quantification of range of variation of associated parameters through a series of sensitivity calculations.

The coordinating institution will distribute among the participants at the beginning of the Phase a guideline containing recommendations, examples and criteria for the uncertain parameters selection.

Participants will have to present their results in Phase II meeting, featuring the following steps:

1. Identification of influential phenomena
2. Identification of the associated physical models and parameters depending on the used code
3. Quantification of the range of variation of identified input uncertainties through a series of sensitivity calculations

1.3.3 Phase III: quantification of physical model uncertainties

Coordinating institution: GRS, Germany

During this Phase, participants are asked to perform the quantification of uncertainties, with their chosen code, methodology and experimental data described in Phase I. FEBA/SEFLEX experiments (series without blockage) are proposed by the coordinator for this phase but participants can use own reflood data provided that it is sufficiently validated and they agree to make available the results of their experiment for the other participants. The participants can use the sets of measurements of FEBA/SEFLEX (or own experiment) of their choice, if they think that these measurements are relevant for accuracy estimation of physical models influential in the reflood prediction. For instance, they can consider differential pressure drops for accuracy estimation of relative velocity upstream from the quench front if they think that this relative velocity is an influential parameter for the prediction of cladding temperatures downstream from the quench front.

The participants, who have in their disposal a tool for quantification of input uncertainties on the basis of intermediate experiments, should apply it using measured data from the FEBA/SEFLEX or another experiment.

Other participants should control their preliminary defined uncertainty ranges (defined in Phase II) by comparison of results of calculations with varied uncertain input parameters with measured data. This should enable to improve the uncertainty ranges estimated in previous step (e.g., by engineering judgement), or confirm their validity for the reflooding experiment.

The results of the quantification will have to be presented in Phase III meeting.

1.3.4 Phase IV: confirmation/verification

Coordinating institutions: CEA and IRSN, France

During this Phase, participants are asked in first place to use the input uncertainty ranges found in Phase III in order to perform an uncertainty analysis in the case of the 2-D reflood PERICLES experiment (that is

not used in the quantification step). Secondly, a verification of the input uncertainties will take place, consisting in evaluating if the output uncertainty ranges (obtained after propagation through the code) of selected output parameters like cladding temperature or quench front propagation encompass their corresponding measured values. These measured values will not be provided to the participants. The differential pressure drops along the test section will not be considered for this confirmation phase unlike the previous quantification phase.

Coordinating institutions will have to evaluate the quality of the results provided by each participant, according to their system code and the chosen methodology. A first qualitative comparison between participants' results will be performed by CEA, using time trends. In order to guarantee a clear and common understanding of the verification process, the formal IRSN method for information evaluation will be then used for a quantitative evaluation. This method is based on the combination of two criteria (calibration and informativeness) and, in the framework of the PREMIUM project, it will be applied to scalar outputs. The results should enable to elaborate some conclusions concerning the applicability and quality of methodologies used for input uncertainties quantification.

1.3.5 Phase V: conclusions

Coordinating institution: CSN, Spain (with the support of UPC, Spain)

During Phase V, all the information produced by the benchmark will be put in common in order to analyse the accomplishment of the objectives, the experience gained and the benefits of the benchmark. As stated in the Objectives section (§1.2), the final output of the benchmark will be a State of the Art report on quantification of the uncertainty of the physical models. If it will appear of interest from the point of view safety significance, it might be followed by the writing of a Best Practice Guidelines report.

2 PARTICIPATION AND METHODOLOGY REVIEW

2.1 Participation review

End users of PREMIUM benchmark are research institutes, vendors, utilities and safety authorities. In other words, they are the developers and the users of BEPU approaches, as well as the organizations in charge of evaluating these approaches.

The wide participation achieved includes participants of BEMUSE [11] and other benchmarks such as UAM [2] and SM2A [19], as well as countries having answered the WGAMA questionnaire on the Use of Best-Estimate Methodologies.

The 16 participating institutions are:

- Bel V, Belgium;
- Tractebel Engineering, Belgium;
- Shanghai Jiao Tong University (SJTU), China;
- Research Centre Rez (CVRez), Czech Republic;
- Technical Research Centre Of Finland (VTT), Finland;
- Commissariat à l'énergie atomique et aux énergies alternatives (CEA), France;
- Institut de Radioprotection et de Sûreté Nucléaire (IRSN), France;
- Gesellschaft für Anlagen- und Reaktorsicherheit (GRS), Germany;
- Karlsruhe Institute of Technology (KIT), Germany;
- San Piero a Grado Nuclear Research Group (GRNSPG), University of Pisa (UNIPI), Italy;
- Korea Atomic Energy Research Institute (KAERI), Republic of Korea;
- Korea Institute of Nuclear Safety (KINS), Republic of Korea;
- OKB Mechanical Engineering (OKBM), Russia;
- Universitat Politècnica de Catalunya (UPC), Spain;
- Consejo de Seguridad Nuclear (CSN), Spain;
- Paul Scherrer Institute (PSI), Switzerland.

A description of the participation of each of the 15 teams (UPC and CSN participate as a single team) can be read in the following table, the type of participation ranging from I to IV being explained in §2.2.

Table 1: details of the participating teams involved in the PREMIUM benchmark (updated at the end of Phase IV of the benchmark)

Team	Country	Type	Method	Code	Access
Bel V	Belgium	II	CIRCÉ	CATHARE	YES
Tractebel	Belgium	IV	Own methodology	RELAP5/MOD3.3	YES
SJTU	China	II	FFTBM	RELAP5/SCDAP/MOD3.4	YES
CVRez	Czech Republic	II	CIRCE	RELAP5/MOD3.3	YES
VTT	Finland	II-IV	CIRCE+FFTBM	APROS	YES
CEA	France	I	CIRCÉ	CATHARE	YES
IRSN	France	IV	Own methodology (DIPE)	CATHARE	YES
GRS	Germany	IV	Own methodology	ATHLET	YES
KIT	Germany	II	FFTBM	TRACE	YES
UNIPI	Italy	I	FFTBM	RELAP5/MOD3.3	YES
KAERI	Republic of Korea	II, IV	CIRCÉ and own methodology (MCDA)	COBRA-TF (MARS-KS1.3 Module)	YES
KINS	Republic of Korea	II	CIRCÉ	MARS-KS 003 and RELAP5/MOD3.3 as support	YES
OKBM	Russian Federation	II	CIRCÉ	RELAP/SCDAPSIM/MOD3.4 and KORSAR/BR	YES
UPC & CSN	Spain	II	CIRCÉ	RELAP5/MOD3.3	YES
PSI	Switzerland	III, IV	Expert judgement	TRACE	YES

The words “expert judgement” are used in this table in a wider sense. Organizations using expert judgement are following a method based on expert opinion supplemented by the so-called fitting data as well as using sensitivity calculations in order to avoid too much subjective decisions. The words “own methodology” are also used specifically for those organizations intending to perform additional tasks connected with Separate Effect Tests and the know-how of code developers.

As it can be observed in the table above, several system codes are involved in this benchmark, including TRACE, RELAP, CATHARE, ATHLET, COBRA, MARS-KS, KORSAR and APROS. All the participants have confirmed to be able to access to the source of their thermal-hydraulic system code to vary physical model parameters. Such modifications have to be performed following an adequate coding and keeping the traceability of the changes performed. Although different degrees of experience can be distinguished among participants, not all of them have the experience to modify the source files to vary the uncertainty parameters. In this sense guidance for code modifications will be provided by sharing knowledge among participants.

Regarding the experimental data, all the participants have agreed to use FEBA/SEFLEX data for Phases II and III, and PERICLES data for Phase IV, as initially proposed by the organization committee. Some participants will use additional data from other reflood experiments for their private use.

The detailed description of FEBA/SEFLEX experimental data written by GRS addressing all PREMIUM participants is included in the Appendix A.

2.2 Methodology review

According to their involvement regarding the used methodologies, four different types of participants can be distinguished in PREMIUM:

i. Participants who have at their disposal methodologies for quantification of uncertainties of the physical models

ii. Participants willing to become users of the available methodologies

iii. Participants willing to use an expert-judgment based method improved with methods of fitting of data

iv. Participants willing to develop their own method in parallel with PREMIUM participation.

Among participating organisations, only two have at their disposal a methodology for quantification of uncertainties of the physical models (type 1), which are the CEA, having a the statistical method CIRCÉ, and UNIPI, having a sensitivity method based in an accuracy calculation by the FFTBM. The Table 1, reviewed at the end of Phase IV of PREMIUM activity, reveals that the majority of teams (type 2) used these available methodologies (most of them have chosen the CIRCÉ method).

Only one team, PSI, used an expert-judgement based method (type 3), essentially using empirical fitting of data and sensitivity calculations based on the FEBA/SEFLEX data set. This method has been employed by PSI as the preparation step of an ongoing method development based on data assimilation using Bayesian inference, which requires a prior estimate of the input uncertainties (hence based on expert-judgement).

KAERI and IRSN developed their own methodologies during the benchmark (type 4), named “Estimation of Parameter Distributions through Model Calibration” and DIPE respectively.

Other methods referenced by PREMIUM participants are the KIT method [15,16], which served as a depart for developing KAERI own methodology, and a PSI-SUSA method [13] and the DAKOTA non-linear least square (NLLS) optimization method [14] which was used by Tractebel Engineering (ENGIE Energy Services) as alternative to CIRCÉ.

The next sections provide a quick overview of the input uncertainty quantification methodologies CIRCÉ and FFTBM, as well as the ones developed during the activity (MCDA, DIPE, Tractebel IUQ and PSI method). It should be kept in mind that before performing this step, an important effort has to be done to construct an experimental data base that should be sufficiently representative and exhaustive of the considered physical phenomena.

2.2.1 CIRCÉ method

CIRCÉ (Calcul des Incertitudes Relatives aux Corrélations Élementaires) is an inverse method of quantification of uncertainty of the parameters associated to the physical models of the thermal-hydraulic system code. This tool has been developed as part of a work programme defined in France by Areva, EDF,

IRSN and CEA for the CATHARE code. The software and source data is available to the participants of the PREMIUM benchmark, as well as support and documentation.

CIRCÉ is a statistical tool of data analysis that uses measured data sensitive to some particular physical models to determine a probabilistic representation of their associated parameters.

Before the use of this method, responses and influential parameters have to be chosen, performing sensitivity calculations. Next, the derivatives of each code response to each parameter have to be calculated. For CATHARE 2 these are obtained using the ASM (Adjoint Sensitivity Method) if the experiment is described with only 1-D elements without reflood. Nevertheless, as it will be the case for reflood experiments considered in PREMIUM, finite differences are calculated to estimate the derivatives. CIRCÉ approach considers as a virtual "observation" a combination of values of the considered parameters that result in an exact (equal to experimental measure) calculation of each selected response. These observations of the parameters are virtual because they cannot be quantified if several parameters are considered. But the use of the well-known in statistics E-M (Expectation-Maximization) algorithm based on the principle of maximum of likelihood and Bayes' theorem makes it possible to estimate the mean value (also called bias) and the standard deviation of each parameter. .

CIRCÉ can be used with different system codes, though it must not be applied as a black box, as it is a complex statistical tool that must be understood. Its main hypothesis are normality of the parameters associated to the physical models (resulting in a normal or log-normal law for the multipliers of the physical models), and linearity between the code responses and each of these parameters. CIRCÉ can additionally be used in an iterative mode, which works with a less strong hypothesis of linearity between parameters and responses. In the studies performed up to now, the different parameters are assumed statistically independent (covariance terms equal to zero).

The detailed description of the method prepared by CEA addressing the PREMIUM participants, including a step-by-step guideline on how to choose the responses and influential parameters, and how to apply the method using CIRCÉ software, can be found in the Appendix B.

2.2.2 FFTBM method

UNIPI has proposed a methodology for characterizing the range of input uncertainty parameters by the use of the Fast Fourier Transform Based Method (FFTBM), which was already part of the Uncertainty Method based on the Accuracy Extrapolation (UMAE).

The methodology has been developed by San Piero a Grado Nuclear Research Group of University of Pisa (GRNSPG-UNIPI).

The methodology is currently available for the application within the framework of the PREMIUM benchmark. The documentation of the methodology and the associated software must not be disclosed to third parties without written consensus received by GRNSPG.

This methodology consists on a quantification of variation ranges of input parameters for physical models using FFTBM to quantify the accuracy of sensitivity calculations applied to relevant experiments.

A preliminary step of the methodology consists in performing single-parameter sensitivity in order to determine the most influential parameters for the dimensionless figure of merit Average Amplitude (AA), which evaluates the discrepancies between code and experimental data. For each of parameters which are observed to be the most influential in the quality of the calculation:

1. A criterion is established for maximum allowed deviation of an AA from the reference case.

2. A range in which this criterion is accomplished for each considered response is determined through a single-parameter sensitivity analysis

3. All the ranges obtained for each response are finally reduced to the most restrictive final range.

The output of this methodology is range of variation for each parameter which is observed to be influential for the calculation quality.

This method can be used with different system codes, and it is independent of the type of investigated input parameter and analysed responses. The methodology is based on rather engineering considerations and previous experience from the application of FFTBM than on statistical methods. Its main hypothesis is a uniform probability distribution of the parameters uncertainty, independence between parameters.

The description of the method prepared by UNIPI addressing the PREMIUM participants including a step-by-step guideline on how to apply the method can be found in the Appendix C.

2.2.3 MCDA method

The Model Calibration through Data Assimilation (MCDA) method is a statistical method which consists in adjusting the input parameter values to achieve better agreement between measured and predicted response values (i.e. selected output parameters). This method has been developed during the PREMIUM activity by the participant KAERI and therefore it was not available for the rest of participants. It must be also noted that it was used only as an alternative method to CIRCÉ.

MCDA integrates experimental data and computational results, including their mean values and uncertainties, for the purpose of updating the parameters of the computational models. The fundament of this method is Bayesian statistics which indicate how the degree of belief changes after utilizing the additional information. The mathematical approach used to obtain the calibrated parameter distribution (called the a posteriori distribution of the parameters) depends on the linearity of the system. Therefore, after identifying uncertainties on the measured values and the parameters, linearity test is conducted to determine whether the system responses are or are not linearly dependent upon the parameters. Deterministic approach will be used for a linear system to obtain the mean value and standard deviation of the parameters, and probabilistic method will be utilized for a nonlinear system to estimate the a posteriori distributions of the parameters.

The deterministic approach is based upon a first-order truncated Taylor series for the responses. The parameters and observables uncertainties are considered Gaussian. In order to address the nonlinear responses in MCDA, a sampling approach is employed by propagating the parameter uncertainties to predict the a posteriori distributions of the parameters. This is conducted using the Markov Chain Monte Carlo (MCMC) method [17], [18] and the Metropolis algorithm is used for a MCMC implementation.

Uncertainty quantification is followed determining the response distributions and the safety margins to complete the safety analysis. The method has been developed with COBRA code during the PREMIUM activity but is not code-dependent. More detail can be found in Appendix E.

2.2.4 DIPE method

DIPE (Determination of Input Parameters Empirical properties) is a method that gives information on uncertain input parameters permitting the coverage of selected output parameters of a considered set of

experiments. It was developed during the PREMIUM activity by the participant IRSN and therefore it was not available for the rest of participants.

The method evaluates the code performance of a deterministic sample of sets of values of the considered uncertain input parameters in order to find the combined ranges that will allow code simulation to cover 95% of the selected experimental data.

It is important to state that this method cannot give the intrinsic uncertainties of the input parameters; it gives only information on these parameters permitting the "coverage" of the chosen experimental data. This is true for all methods based on comparison between code results and a set of experimental data. The extrapolation to other devices or other physical conditions must be carefully checked.

The most basic application of the method is DIPE 1D, where only one uncertain input parameter is considered and a Pseudo-CDF (Cumulative Distribution Function) is obtained by evaluating the coverage range using single-parameter sensitivity. Differentiating this function, a PDF (Probability Distribution Function) can be easily found. The results of different experiments or different output parameters of interest can be aggregated in order to obtain a global result.

The application to more complex problems with several input parameters considered (DIPE 2D for two parameters and DIPE 2D+ for more) is also possible through a more complex sampling by repeating the DIPE 1D evaluation fixing the rest of the parameters and then constructing a surface of 95% cover range.

Three assumptions made in this method: (1) measurement error is negligible, (2) for each considered point of time-trend there exists a calculated value obtained with a combination of input parameters that is equal to the experimental value and (3) the calculated curve is monotonous (curves must not cross).

The method has been developed with CATHARE code during the PREMIUM activity but is not code-dependent. More detail can be found in Appendix F.

2.2.5 TRACTABEL IUQ method

Tractebel has developed a sampling-based inverse uncertainty quantification (IUQ) approach with DAKOTA tool.

It uses DAKOTA sampling based uncertainty quantification (UQ) functionality to quantify the model uncertainty.

The DAKOTA code has such functionality based on random sampling. The approach should be in principle used for "propagation" of the "known" input uncertainties into the "unknown" output uncertainties, which can be quantified based on the desired probability and confidence level.

More detail can be found in Appendix G.

2.2.6 PSI method

The PSI participation to the PREMIUM benchmark was made as part of the development of a new methodology, which is still at an early stage of development. The new methodology is essentially based on the use of Bayesian inference to derive the parameters of the PDF of relevant code input and parameters out of a set of representative experimental Separate-Effect-Test database for bottom reflooding. More detail can be found in Appendix H.

3 CONCLUSIONS

The contribution of PREMIUM to the development of tools and experience related to uncertainties calculation is a step forward in the promotion of the use of BEPU approaches for licensing and safety assessment purposes. The participation in the benchmark of several national nuclear regulatory bodies is very encouraging in that sense. Moreover KINS, the nuclear regulatory body in the Republic of Korea, is supposed to utilize CIRCÉ method as a tool quantifying the uncertainty ranges in their KINS-REM methodology.

The scenario chosen for PREMIUM is the reflood that takes place at the end of a Large Break LOCA, which not only complies with the requirements set by the benchmark objectives, but it is one of the key issues of a very relevant Design Base Accident (DBA), whose studies have been taken place since the beginning of nuclear safety history. Therefore, all the experience gained in the past contributes to the excellence of the results obtained by PREMIUM participants. At the same time, the exercise set out by the benchmark improves the experience and understanding of this essential accident, as well as the dissemination in the scientific community of sound quantitative information (e.g., probability distribution functions) on the uncertainty in the reflood models of current thermal-hydraulic system codes.

Another immediate application of PREMIUM findings is the improvement of thermal-hydraulic system codes, as the experience and results obtained will result in identifying the physical models where further development and assessment is required in priority. The great variety of system codes involved in the benchmark (TRACE, RELAP, CATHARE, ATHLET, COBRA, MARS-KS, KORSAR and APROS), and the participation of institutions in charge of code development are very encouraging in that sense.

For all these reasons, the progress on the issue of the quantification of the uncertainty of the physical models in system thermal-hydraulic codes that represents PREMIUM benchmark will result in the assessment of advanced methods and tools used for event/accident analysis and a review, development and validation of current analytical tools as well as risk assessment approaches regarding their applicability to safety assessments of new designs.

The main results expected for PREMIUM benchmark is a State of the Art of the existing methods devoted to the quantification of the uncertainty of the physical models. The performance of each participant will be put in common and evaluated according to their system code and methodology used, resulting in the development of a common understanding, conclusions concerning the applicability and quality of methodologies used for input uncertainties quantification, recommendations for future work, and an analysis of the objectives accomplishment and the benefits of the benchmark.

4 REFERENCES

[1] Reventós F., de Alfonso E., Mendizábal R.: *General requirements and description specification of methodologies and experimental data to be used in PREMIUM benchmark*, PREMIUM Kick-Off Meeting, Paris, February 2012.

[2] OECD, "OECD Benchmark for Uncertainty Analysis in Best-Estimate Modelling (UAM) for Design, Operation and Safety Analysis of LWRs (OECD LWR UAM Benchmark): Expert Group on Uncertainty Analysis Third Workshop (UAM-3)", NEA/NSC/DOC(2013)7, https://www.oecd-nea.org/science/docs/2009/nsc-doc2009-11.pdf

[3] de Crécy A., Skorek T.: *PREMIUM – Benchmark on the quantification of the uncertainty of the physical models in the system thermal-hydraulic codes*, Workshop on Best-estimate Methods and Uncertainty Evaluations, Barcelona, November 2011.

[4] Ihle P., Rust K.: *FEBA – Flooding Experiments with Blocked Arrays, Evaluation Report*, Kfk Karlsruhe, Rep. KfK 3657, March 1984

[5] Ihle P., Rust K.: *FEBA – Flooding Experiments with Blocked Arrays, Data Report 1, Test Series I through IV*, Kfk Karlsruhe, Rep. KfK 3658, March 1984

[6] Ihle P., Rust K.: *SEFLEX – Fuel Rod Simulator Effects in Flooding Experiments, Part 1: Evaluation Report*, Kfk Karlsruhe, Rep. KfK 4024, March 1986

[7] Ihle P., Rust K.: *SEFLEX – Fuel Rod Simulator Effects in Flooding Experiments, Part 2: Unblocked Bundle Data*, Kfk Karlsruhe, Rep. KfK 4025, March 1986

[8] de Crécy A. *"Determination of the uncertainties of the constitutive relationships of the CATHARE 2 code"*, M&C 2001, Salt Lake City, Utah, USA, September 2001.

[9] de Crécy A., Bazin P. *"Quantification of the Uncertainties of the Physical Models of CATHARE"*, BE2004, Washington D.D., USA, November 2004.

[10] Kovtonyuk A., Petruzzi A., D'Auria F., *Details of the FFTBM method for PREMIUM Phase – III*, PREMIUM Coordination Meeting, Pisa, Italy, October 2011.

[11] OECD, "*BEMUSE Phase VI report, Status report on the area, classification of the method, conclusions and recommendations*", NEA/CSNI/R(2011)4, 2011. https://www.oecd-nea.org/nsd/docs/2011/csni-r2011-4.pdf

[12] Destercke S., Chojnacki E. "*Methods for the evaluation and synthesis of multiple sources of information applied to nuclear computer codes*", Nuclear Engineering and Design, 238, pp 2484-2493, 2008.

[13] Vinai P., Macian-Juan R., Chawla R.: *"A statistical methodology for quantification of uncertainty in best estimate code physical models"*, Annals of Nuclear Energy 34 (2007) 628–640.

[14] Swiler L.P., Adams B.M., Eldred M.S.: *"Model Calibration under Uncertainty: Matching Distribution Information"*, SAND Report 2008-0632A, AIAA Paper AIAA-2008-5944.

[15] Cacuci D.G., Ionescu-Bujor M.: *"Best-Estimate Model Calibration and Prediction Through Experimental Data Assimilation—I: Mathematical Framework"*, Nuclear Science and Engineering: 165, 18–44 (2010).

[16] Petruzzi A., Cacuci D.G., D'Auria F.: *"Best-Estimate Model Calibration and Prediction Through Experimental Data Assimilation—II: Application to a Blowdown Benchmark Experiment"*, NUCLEAR SCIENCE AND ENGINEERING: 165, 45-100 (2010).

[17] Metropolis N., Rosenbluth A.W., Rosenbluth, M.N., Teller A.H., Teller E.: "*Equation of State Calculation by Fast Computing Machines*", Journal of Chemical Physics, vol. 21, No.2, pp. 1087-1092, 1953.

[18] Higdon D., Kennedy M., Cavendish J.C., Cafeo J.A., Ryne R.D.: "*Combining Field Data and Computer Simulation for Calibration and Prediction*", SIAM J. Sci. Comput. Vol. 26, No. 2, pp. 448-466, 2004.

[19] OECD, "Safety Margin Evaluation - SMAP Framework Assessment and Application", NEA/CSNI/R(2011)3, https://www.oecd-nea.org/nsd/docs/2011/csni-r2011-3.pdf

APPENDIX A: DESCRIPTION OF THE FEBA TEST FACILITY AND FEBA/SEFLEX EXPERIMENTAL PROGRAMME

For the evaluation step of the PREMIUM benchmark the tests from the FEBA/SEFLEX programme have been chosen. However, if any participants prefer, they can use their own reflood experiment, provided that it is sufficiently validated and they accept to make their experimental results available for other participants.

The test runs of the FEBA experiment seems to be sufficient for performing of quantification (or evaluation) of the selected input uncertainties. If any participants found that more experimental data are needed or they would like to extend the evaluation on fuel rod simulators of different construction (with gap and different cladding material) the measured data of SEFLEX experiment can be used in addition.

FEBA/SEFLEX Programme

The purpose of the FEBA/SEFLEX programme was to obtain an insight into the most important heat transfer mechanisms during reflood phase of LOCA and to broaden the data base for the development and assessment of improved thermal-hydraulics models. The FEBA/SEFLEX programme has been performed at KfK Karlsruhe, Germany. The FEBA and SEFLEX experiment were published inclusive experimental results. A detailed description of the FEBA experiment series I and II can be found in KfK reports: KfK 3657 [A.1] and KfK 3658 [A.2]. Description of SEFLEX experiment with unblocked arrays in is available in KfK reports: KfK 4024 [A.3] and KfK 4025 [A.4]. The concise description of the experimental programme presented in this paper is based on the above reports.

The FEBA experiment as well as SEFLEX experiment was performed on the FEBA test facility using different heater rods. The test facility was designed for the reflooding tests with possibility of maintaining constant flooding rates and constant back pressure. The test section consists of a full-length 5 x 5 rod bundle of PWR fuel rod dimensions utilizing electrically heated rods with a cosine power profile approximated by 7 steps of different power density in axial direction. The rod bundle is placed in housing made of stainless steel and insulated with Triton Kao Wool to reduce heat losses to environment. The cross-section of the FEBA test section is shown in the Figure A.1.

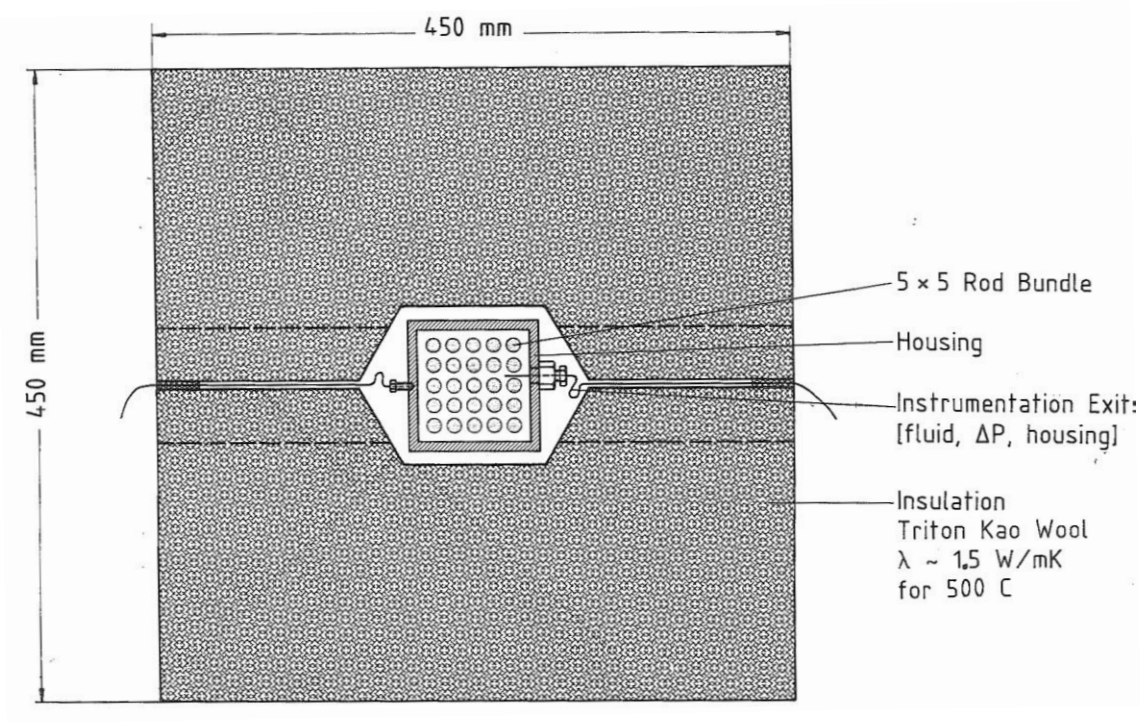

Figure A.1: FEBA test section – cross-section view [A.1]

During test runs cladding temperatures at several axial positions have been measured. Cladding temperatures were measured with 0.5 mm sheath diameter thermocouples. The fluid temperature measurements were performed with unshielded thermocouples of 0.25 mm outer sheath diameter. Radiation effect of the unshielded thermocouples was not detected. However, the shielding led to slightly earlier quenching of the shielded thermocouples, while the unshielded thermocouples showed predominance of superheated steam for a longer time span. Fluid temperature and housing temperature measurement taps were installed at numerous elevations along the test section. However, during individual tests only few of them were used. Pressure and pressure differences were measured with pressure transducers. In addition to inlet and outlet pressure, the pressure differences were measured along the bottom middle and upper part of the channel as well as along the whole channel. The flooding rate was measured with a turbo flow-meter. The amount of the water carried over was measured continuously by a pressure transducer at the water collecting tank.

The cladding and housing temperatures can be expected to be of high accuracy. A typical accuracy of chromel-alumel thermocouple is about ± (0.4% – 0.5%) *Temp. [°C]. For the measured temperature range it is about ±5 °C. In addition it has to be taken into account that the thermocouples measure not exactly the temperature of the cladding surface. The accuracy of the pressure drop measurement was not reported. However, a typical error of pressure transducers is about 1% of measured pressure range by constant temperature. Since, the temperature in the FEBA experiments varies strongly along the test section the error can be much higher. The accuracy of the pressure drop measurements in another test with similar bundle configuration was estimated as ±10%. It could be a reasonable estimation also for the FEBA pressure drop measurements.

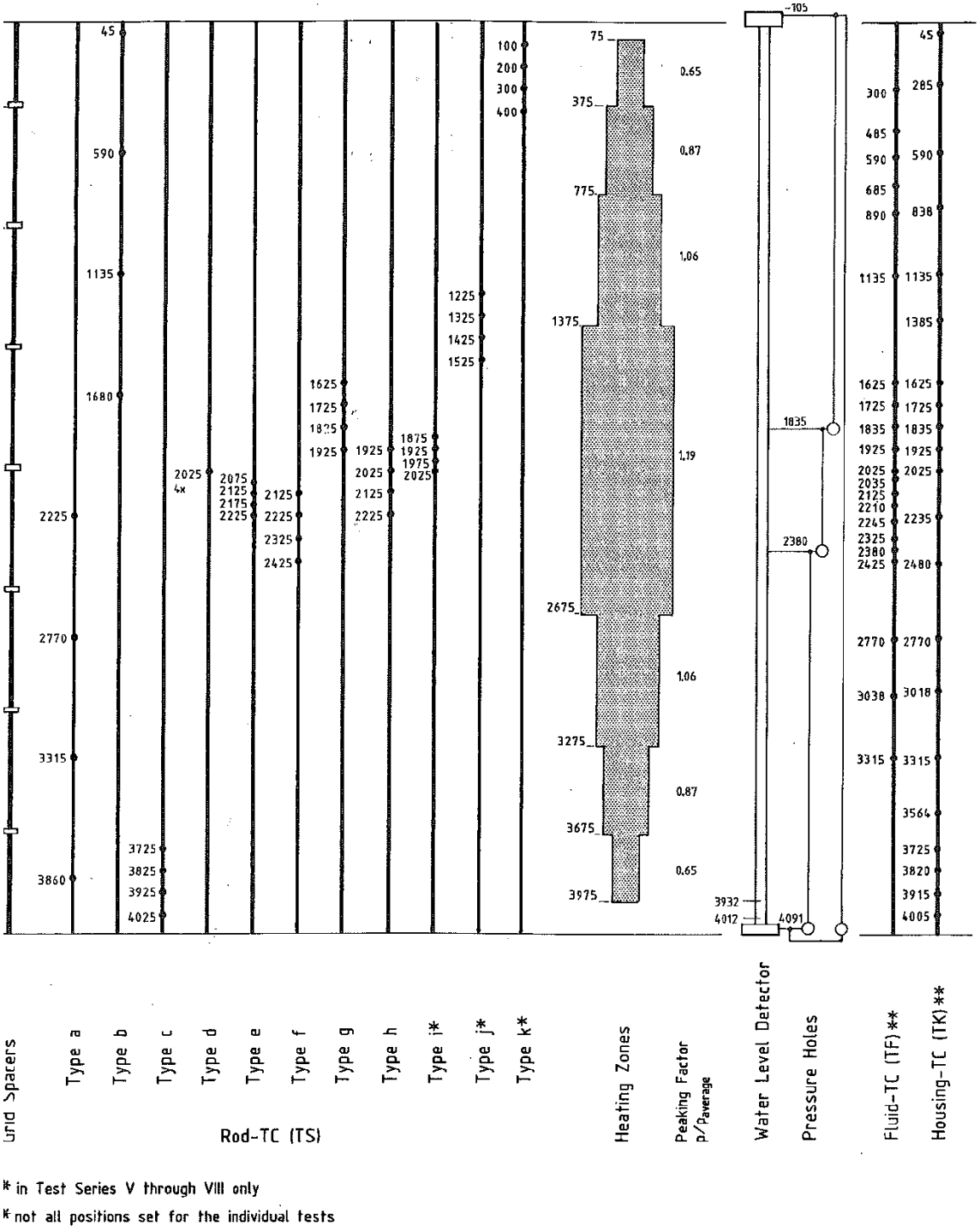

Figure A.2: axial levels of the measuring taps in the rod bundle [A.1].

The overview of the measuring taps in the test section is shown in the Figure A.2. As can be seen in the figure the pressure drops at the lower and middle part of the channel were measured in the channel inside the rod bundle. The pressure drop in the upper part of the channel was measured across the upper grid plate.

The cross section of the rod bundle with housing and the axial view of the FEBA heater rod are shown in the Figures A.3 and A.4.

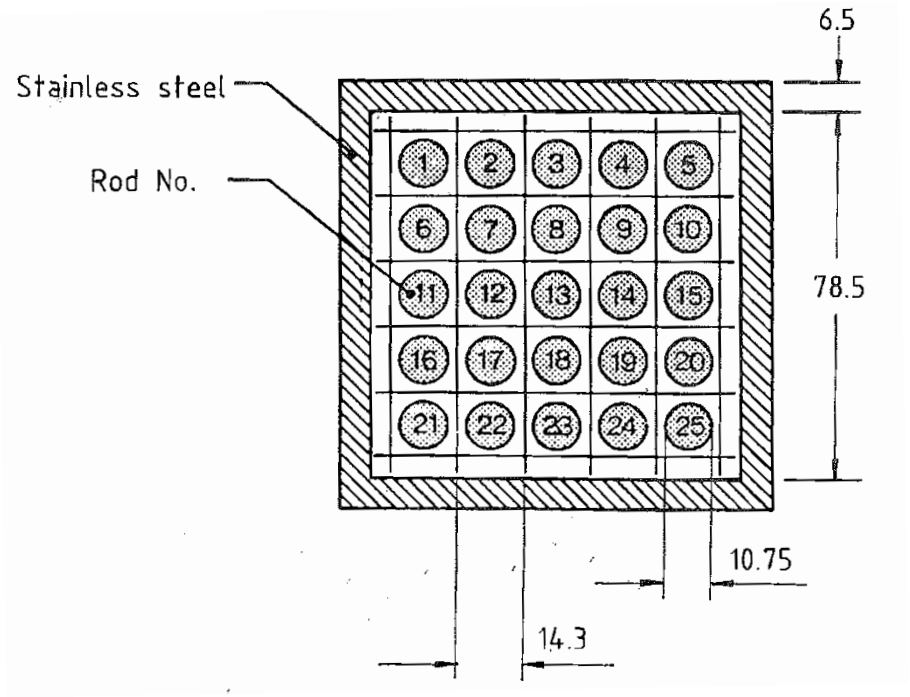

Figure A.3: 5 x5 rod bundle with housing – cross section [A.2]

The outer diameter of the heater rod is 10.75 mm. The pitch of the rod grid is 14.3 mm. The dimensions of the quadratic housing are: inner side length 78.5 mm and wall thickness 6.5 mm. The inner size of the housing is chosen in such a way that the hydraulic diameter of the bundle array for all rods is the same and equal 13.47 mm. The heated length is 3900 mm.

In the Figure A.4 the location of spacer grids is shown. The spacers decree the flow cross section about 20%. The applied spacers were original PWR spacers as used by KWU. The location of the spacers can be found in the Figure A.4.

The inlet and outlet conditions are measured during each test run. The inlet conditions (in particular inlet pressure) are measured at the inlet to the test section in the rod bundle geometry. The outlet pressure is measured in the upper plenum 81 mm above the upper grid plate. The thickness of the upper grid plate is 24 mm. The coolant flows through 36 holes of 10 mm diameters. The upper plenum has dimensions of the rod bundle housing, i.e.: square of length 78.5 mm, without any installations. The main reason for the use of thick-wall housing was to simulate surrounding heat generating rods (as it is the case in much larger reactor array) by having sufficient heat storage in the wall prior to the test run.

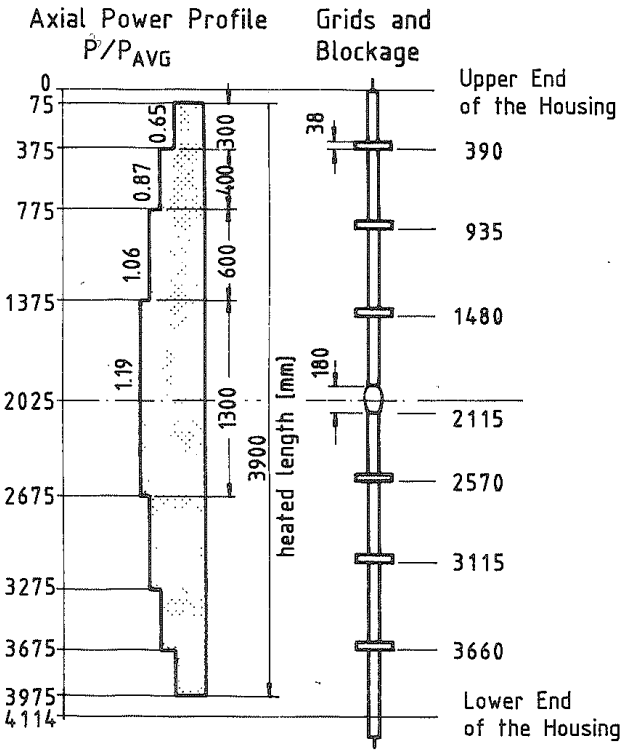

Figure A.4: axial view of the FEBA heater rod and axial power profile distribution [A.1].

FEBA Experiment

The FEBA experiment (Flooding Experiments with Blocked Array) consisted of tests performed on a full-length 5 x 5 rod bundle of PWR fuel rod dimensions utilizing electrically heated rods without fuel gap simulation. The cross-section of the FEBA heater rod is shown in the Figure A.5. The thermal properties of the FEBA test facility materials were obtained in a review of technical literature and made available to PREMIUM participants.

Eight test series were performed under idealized reflood conditions using forced feed and system pressure as fixed boundary conditions, without taking into account the effects of reactor cooling system. The tests series were conducted to study the effect of grid spacers and of coplanar blockages with different blockage rates.

The test series I and II (see Table A.1 and A.2) were performed for unblocked rod arrays and they are suitable as a basis for quantification of uncertainties of flooding simulation in PERICLES test facility.

The results of the both test series showed a significant effect of grid spacers on reflood heat transfer. The cooling enhancement downstream of the grid spacers occurs mainly during the early portion of the reflood. A similar effect could be observed for coplanar coolant channel blockages with moderate reduction of cross section.

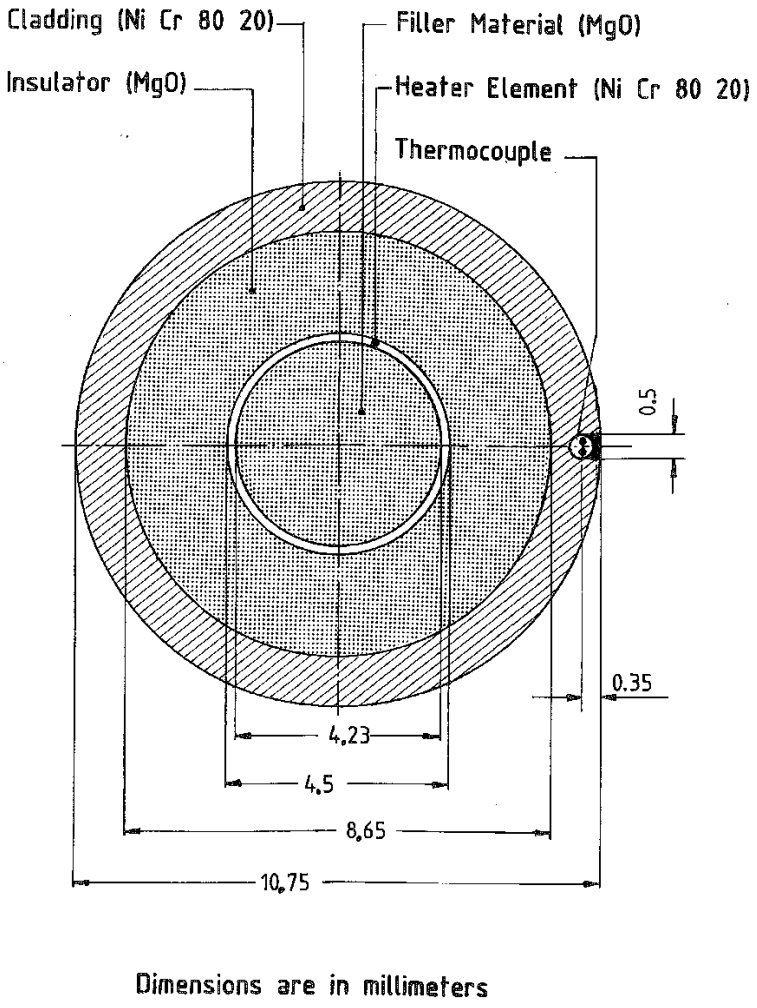

Figure A.5: cross section of the FEBA heater rod [A.1].

Operational procedure

Prior to the test run the fuel rod simulators were heated in stagnant steam to desired initial cladding temperature, using a low rod power. In the meantime the test bundle housing was being heated up passively to the requested initial temperature by radiation from the rods. The aim of choosing the thick wall ("active wall") was to prevent premature quenching of the wall relative to the bundle quench front progression.

During the heat up period the inlet plenum was cooled by circulating water to maintain the desired temperature. The steam filled ducts were heated up to a temperature slightly above the saturation temperature.

By starting of the test run the bundle power was increased to the required level simulating decay heat according to 120% ANS-Standard about 40 s after reactor shut down. The electrical power of the bundle was measured for each test run. The measured curves are practically identical. The bundle power digitalised from the measured curves is given in the Table A.3.

Table A.1: Series I, base-line tests with undisturbed bundle geometry with 7 grid spacers

Test No.	Inlet velocity (cold), cm/s	System pressure, Bar	Feed water temperature, °C		Bundle power, kW	
			0-30 s	End	0 s	Transient
223	3.8	2.2	44	36	200	120% ANS
216	3.8	4.1	48	37	200	120% ANS
220	3.8	6.2	49	37	200	120% ANS
218	5.8	2.1	42	37	200	120% ANS
214	5.8	4.1	45	37	200	120% ANS
222	5.8	6.2	43	36	200	120% ANS

Table A.2: Series II, investigation of the effect of a grid spacer, with 6 grid spacers (without grid spacer at the bundle midpoint)

Test No.	Inlet velocity (cold), cm/s	System pressure, Bar	Feed water temperature, °C		Bundle power, kW	
			0-30 s	End	0 s	Transient
234	3.8	2.0	46	37	200	120% ANS
229	3.8	4.1	53	38	200	120% ANS
231	3.8	6.2	54	40	200	120% ANS
233	5.8	2.0	47	37	200	120% ANS
228	5.7	4.1	50	37	200	120% ANS
230	5.8	6.2	48	37	200	120% ANS

Simultaneously the water supply was activated with mass flow rates as previewed in the test matrix. In the experiment documentation no information has been found on the initial water level during the time of power increase and start of the test run (time = 0 sec.). The analysis of cladding temperature plots at level 3860 mm indicates that the initial liquid level by start of data collection can be different:

- in test no. 218 according to temperature measurements the cladding is quenched at 0 sec., what indicates high water level, may be at the beginning of the heated part of the rod;
- in test no. 216 on the contrary cladding temperature curve shows quenching several seconds after the start, what indicates low initial water level.

Therefore, it can be supposed that the start of the test run (time 0 sec.) varies in the range: lower end of housing (top of lower plenum) – beginning of the heated part of the rod. The difference between those two levels is 254 mm and with flooding velocity 3.8 cm/s it would take 6.7 sec. and with flooding velocity 5.8 cm/s it would take only 4.4 sec. to cover this distance. This leads to uncertainty of quench front progression of the same range. I can be assumed as uncertainty of the experiment. This uncertainty must be regarded in the context of limited accuracy of plotted curves digitalization. The accuracy of the digitalization can be estimated rather ±2 sec. then ±1 sec. The inaccuracy of the initial water level position appears not considerably larger than inaccuracy of experimental curve digitalization.

Table A.3: bundle power

Time, sec.	Electrical power, kW
0.0	187.5
2.5	200.0
5.0	192.5
10.0	190.0
20.0	180.0
30.0	175.0
50.0	167.5
75.0	160.0
100.0	152.5
150.0	141.25
200.0	132.5
250.0	126.25
300.0	121.25
400.0	121.25
500.0	121.25

Measured data

For each test run a huge amount of data were measured and recorded. From the experimental data the following measurements, which could be applied for quantification and evaluation of reflood models in the frame of the phase III of PREMIUM benchmark have been selected:

- Initial axial cladding temperature distribution;
- Boundary conditions for the test runs:
  - System pressure
  - Flooding (inlet) velocity
  - Bundle power
  - Feed water temperature
- Time trends of cladding temperature at 8 axial levels;
- Pressure drops along the test section in the lower, middle and upper part of the bundle;
- Fluid temperature in the middle of the test section;
- Housing temperature in the middle of the test section;
- Water carry over test section;
- Coolant temperature at the outlet of the test section.

The sets of selected measurement plots of FEBA Series I and II can be of interest for model uncertainties quantification. The selected measured values for the test run no 216 are shown as plotted curves in the following pictures.

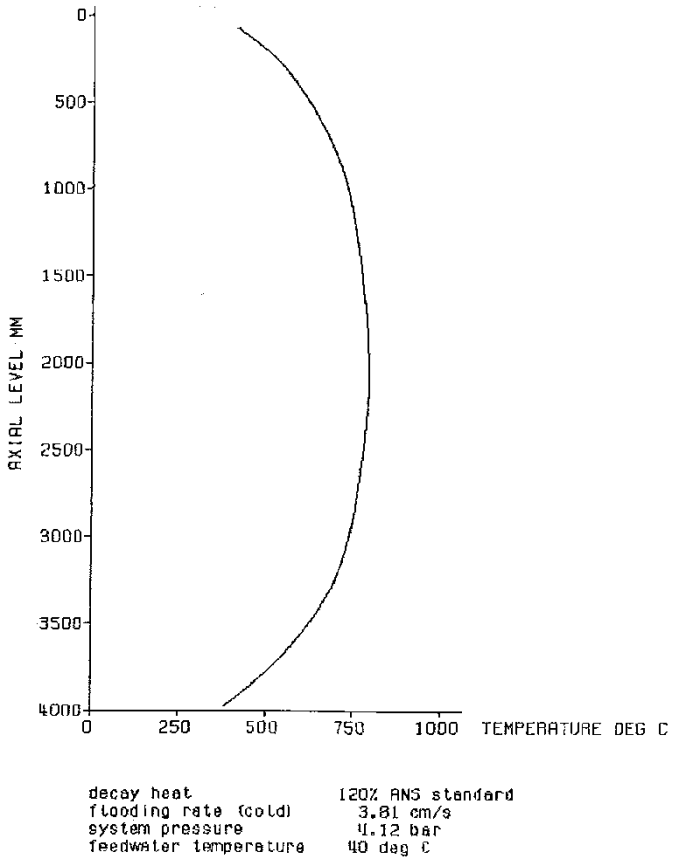

Figure A.6: initial axial temperature profile of the cladding [A.1]

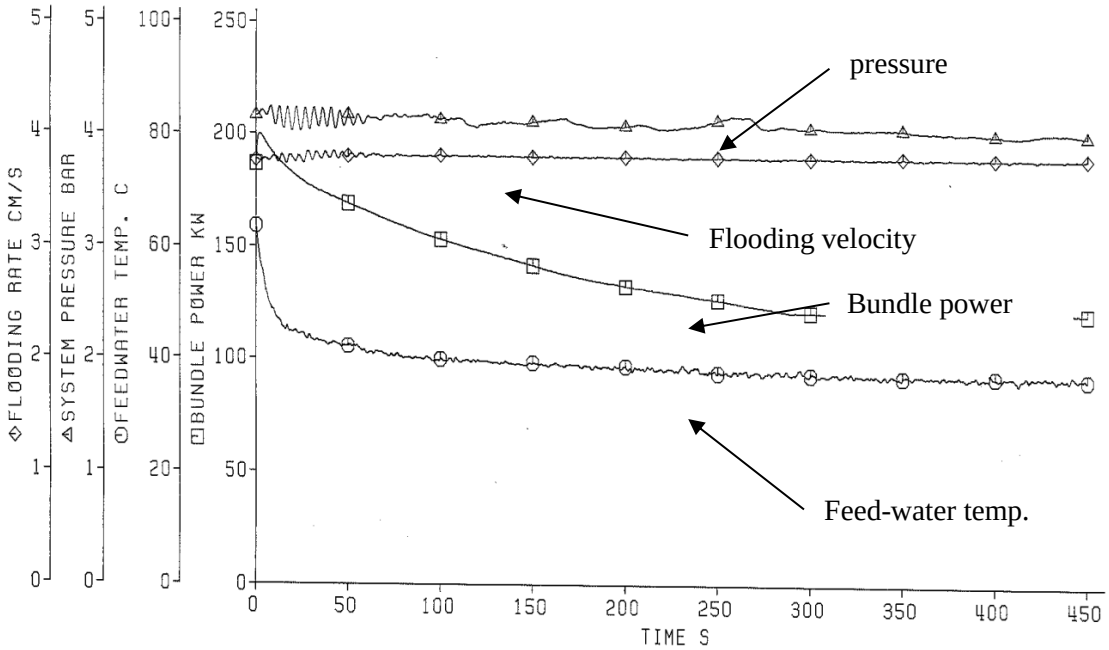

Figure A.7: boundary conditions for the flooding test no 216 [A.1]

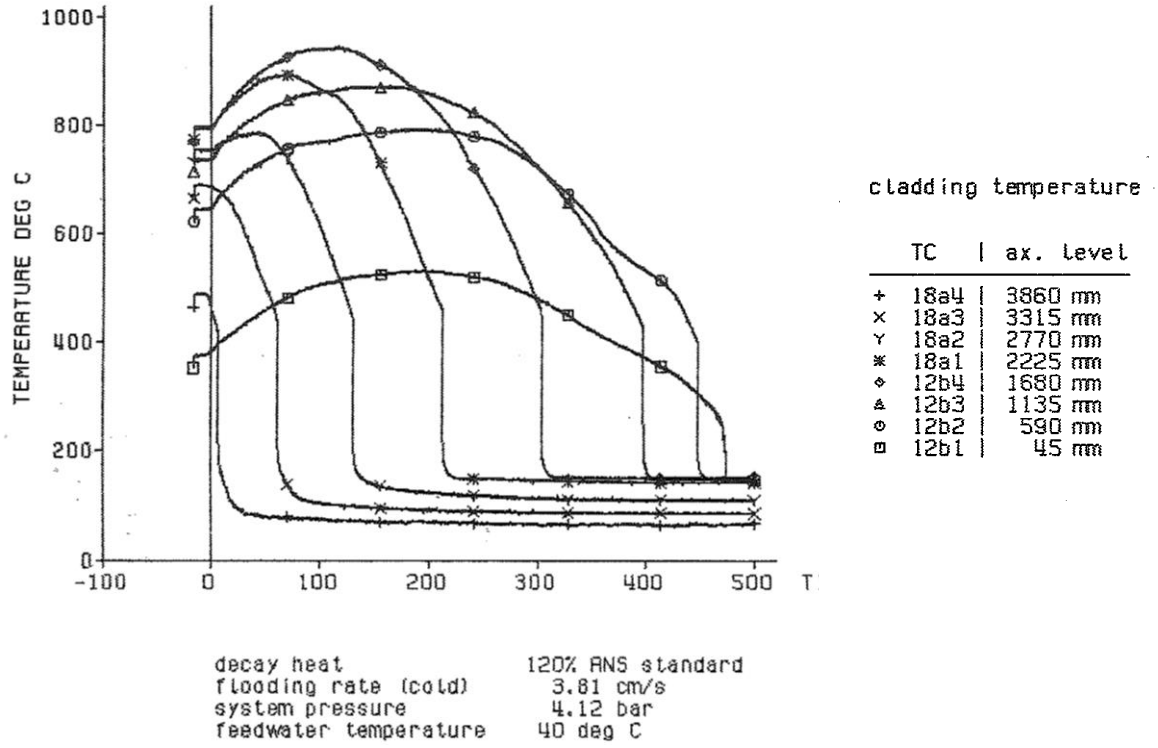

Figure A.8: cladding temperatures along the test rod bundle [A.1]

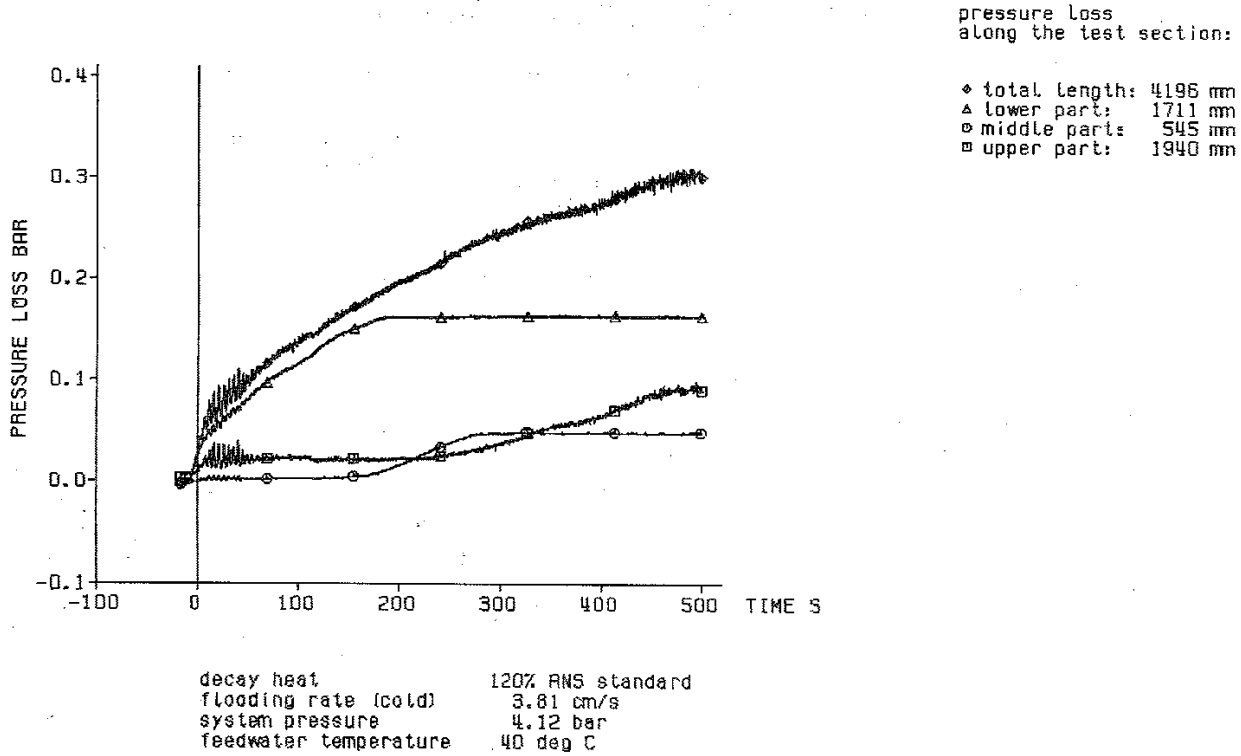

Figure A.9: pressure drop along the test section [A.2]

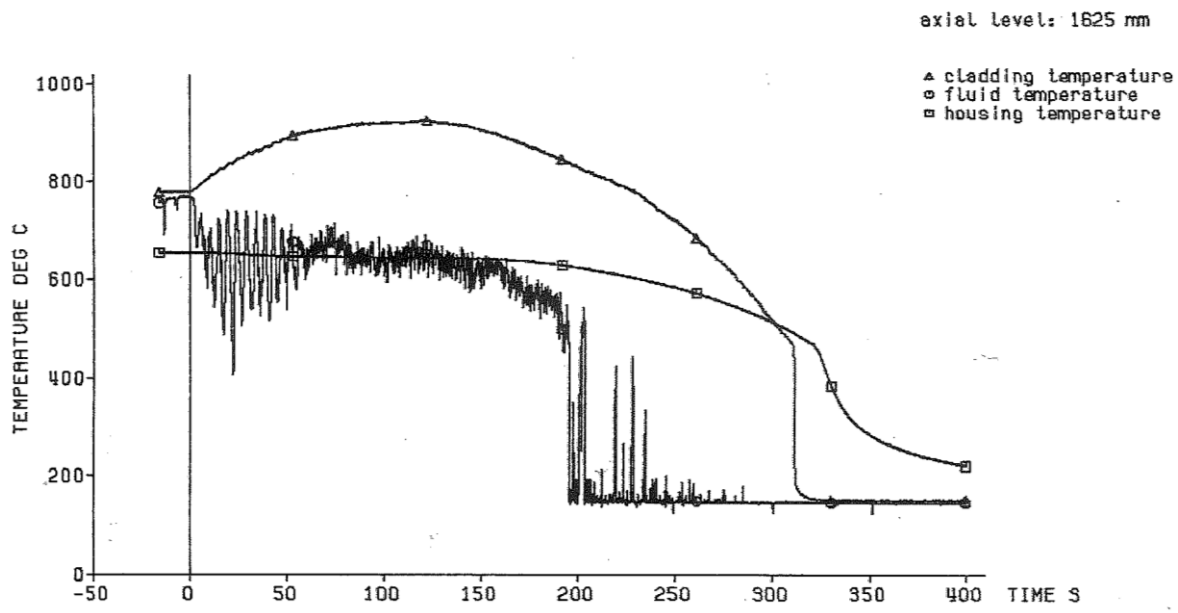

Figure A.10: measurements of housing temperature, fluid temperature and cladding temperature performed at axial level 1625 mm [A.2]

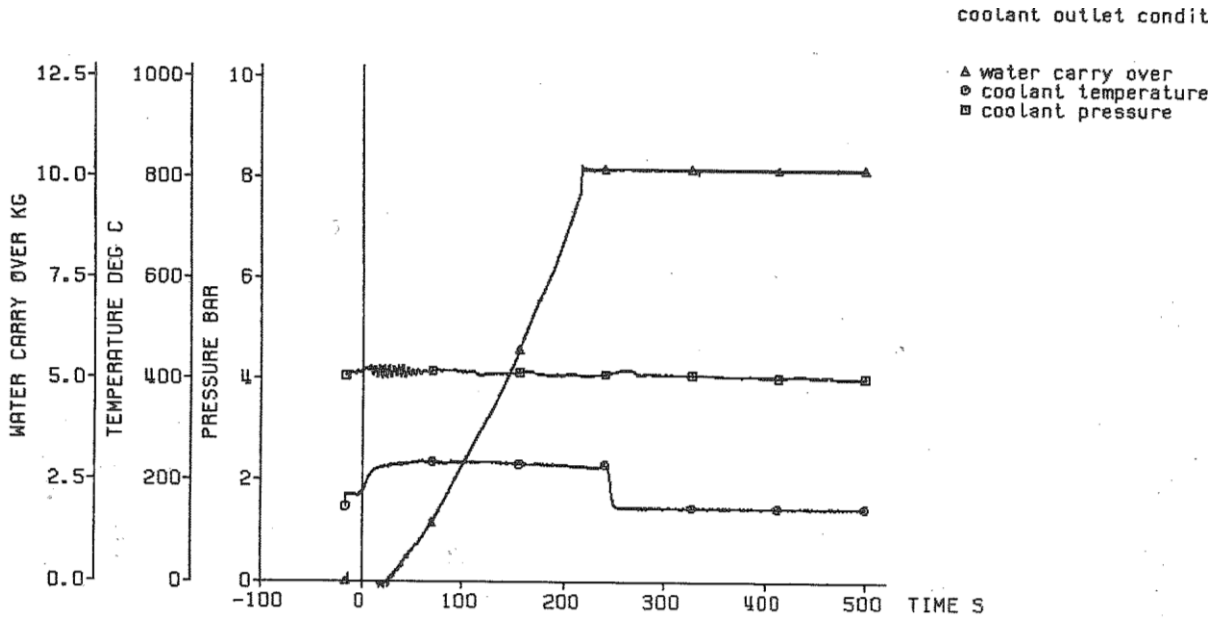

Figure A.11: coolant outlet conditions measured in the upper plenum of the test section [A.2]

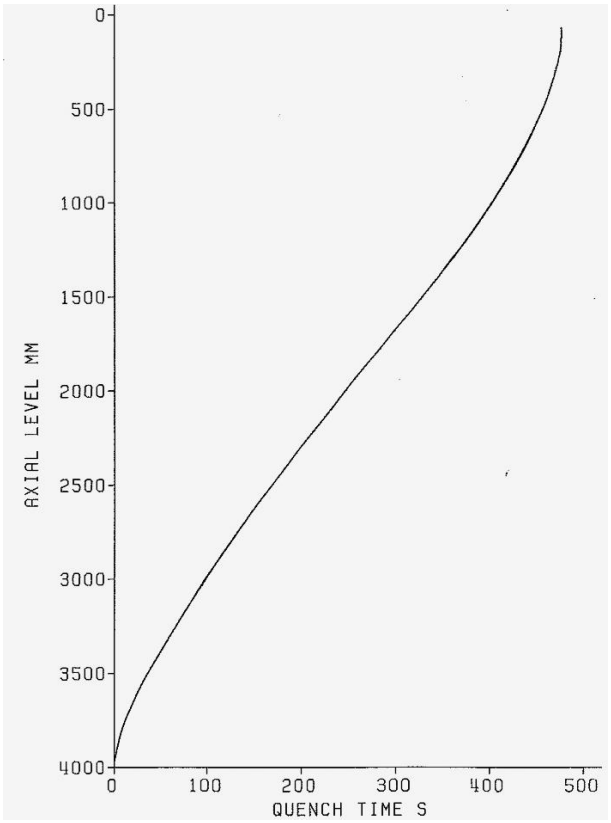

Figure A.12: quench time obtained for test run 216 [A.1]

SEFLEX Experiment

The aim of the SEFLEX (fuel rod Simulator Effects in FLooding EXperiments) [A.3] experiment was investigation of the influence of the design and the physical properties of different fuel rod simulators on heat transfer and quench front progression in unblocked und blocked rod bundles during the reflood phase of LOCA in a PWR reactor. The cross section of the heater rod used in SEFLEX experiment is shown in the Figure A.13. The configuration of the test section in axial direction as well as measurement taps arrangement was identical with those in the FEBA experiment.

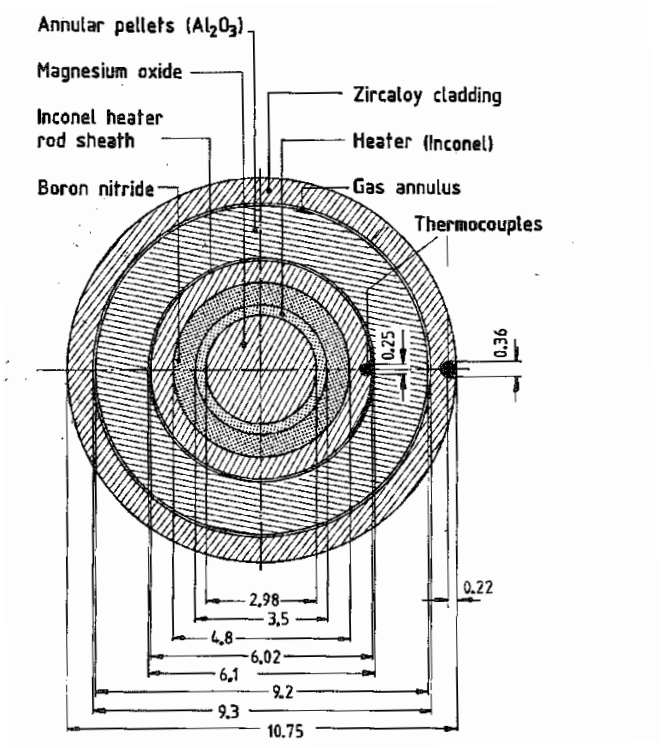

Figure A.13: cross section of the heater rod used in the SEFLEX experiment

In the frame of SEFLEX experiment 4 test series were performed. Test series I and II were performed without blockage:

- Series I, rods with helium-filled gaps between Zircaloy claddings, alumina pellets and 7 grid spacers;
- Series II, rods with argon-filled gaps between Zircaloy claddings, alumina pellets and 7 grid spacers.

Fuel rod simulators with Zircaloy claddings and gas-filled gap between claddings and pellets showed lower peak cladding temperature and shorter quench times than gapless heater rods with stainless steel claddings.

Comparison of SEFLEX tests Series I and II boundary conditions with FEBA tests is shown in Table A.4.

Table A.4: characteristic of SEFLEX tests series I and II

Experiment/Test series	Test No.	Cladding material	Gap gas	Inlet velocity, cm/s	System pressure, bar	Feed water temperature, °C
SEFLEX/I	05	Zircaloy	Helium	3.8	2.1	40
SEFLEX/I	03	Zircaloy	Helium	3.8	4.1	40
SEFLEX/I	06	Zircaloy	Helium	5.8	2.1	40
SEFLEX/I	04	Zircaloy	Helium	5.8	4.1	40
SEFLEX/II	07	Zircaloy	Argon	3.8	2.1	40
FEBA		stainless steel	gapless	3.8 – 5.8	2.1 – 6.2	40

REFERENCES

[A.1] Ihle P., Rust K.: FEBA – Flooding Experiments with Blocked Arrays, Evaluation Report, Kfk Karlsruhe, Rep. KfK 3657, March 1984

[A.2] Ihle P., Rust K.: FEBA – Flooding Experiments with Blocked Arrays, Data Report 1, Test Series I through IV, Kfk Karlsruhe, Rep. KfK 3658, March 1984

[A.3] Ihle P., Rust K.: SEFLEX – Fuel Rod Simulator Effects in Flooding Experiments, Part 1: Evaluation Report, Kfk Karlsruhe, Rep. KfK 4024, March 1986

[A.4] Ihle P., Rust K.: SEFLEX – Fuel Rod Simulator Effects in Flooding Experiments, Part 2: Unblocked Bundle Data, Kfk Karlsruhe, Rep. KfK 4025, March 1986

APPENDIX B: CIRCÉ, A METHODOLOGY TO QUANTIFY THE UNCERTAINTY OF THE PHYSICAL MODELS OF A CODE

B.1 INTRODUCTION

CIRCÉ, or "Calcul des Incertitudes Relatives aux Corrélations Élementaires" (which can be translated into English as Calculation of the Uncertainties Related to the Elementary Correlations), is a method and a tool developed by CEA. It has been extensively applied to the physical models of the CATHARE 2 code via a work programme defined in France by Areva, EDF, IRSN and CEA. But it can be applied to any code, without specific developments since it works in a stand-alone way. CIRCÉ estimates the mean value and the standard deviation, as well as the type of probability density function (PDF), normal or log-normal, of the parameters associated with the physical models for which uncertainty must be quantified. Thus it is apparent that the uncertainty representation made by CIRCÉ is of probabilistic type. For the CATHARE studies, CIRCÉ has been applied to the dimensionless multipliers of the physical models, but it would be possible to consider also single coefficients inside the physical models or even additive parameters.

This Appendix comprehensively describes the CIRCÉ tool covering: the CIRCÉ algorithm, detailed user's guidelines, the software and the structure of an input data deck and some recommendations for calculation of the derivatives used by CIRCÉ. The Appendix is structured in two parts. Part B.2 is a rapid presentation of: the method; the problem solved by CIRCÉ; the main principles of CIRCÉ; parameters considered and the final multipliers; a rapid description of assumptions; an example of results; and a rapid description of the user guidelines. Part B.3 is a detailed description of the CIRCÉ method and its application followed by some conclusions. There are also some acknowledgements and two addenda on (i) the principal of maximum likelihood and (ii) an example of bias calculation comparing CIRCÉ with the E-M algorithm.

This Appendix constitutes the CEA contribution to Phase I of the PREMIUM benchmark: this benchmark is devoted to the problem solved by CIRCÉ, the different participants having to describe for Phase I their uncertainty method (if they have one).

CIRCÉ is a statistical tool of data analysis: it must not be applied as a black box; indeed, this is the only difficulty to use it. To this end, a specific methodology for a proper use of CIRCÉ, including validation of the obtained results, has been developed by CEA during the studies performed with CIRCÉ for CATHARE. This methodology is rapidly explained in Part I, in the form of a kind of user guidelines

Conference papers have already been published on CIRCÉ[1] but the present description is by far the most complete.

[1] A description of the algorithm: A. de Crécy, "Determination of the uncertainties of the constitutive relationships of the CATHARE 2 code", M&C 2001, Salt Lake City, Utah, USA, September 2001.

User guidelines, A. de Crécy, P. Bazin, "Quantification of the Uncertainties of the Physical Models of CATHARE 2", BE 2004, Washington DC, USA, 14-18 November 2004.

Updated guidelines: A. de Crécy, P. Bazin, "CIRCÉ, a tool to quantify the uncertainty of the physical models", Technical Meeting on the Application of Deterministic Best Estimate Safety Analysis, organized by IAEA and OECD/NEA, Pisa, Italy, 21-25 Sept. 2009.

B.2 RAPID PRESENTATION OF THE CIRCÉ METHOD AND ITS APPLICATION

B.2.1 The CIRCÉ method

B.2.1.1 The problem solved by CIRCÉ

The CIRCÉ method is a statistical approach of data analysis and is applied as an alternative to the expert judgment often used to determine the uncertainty of the physical models. Estimating these uncertainties is a difficult problem because these models are, in the majority of the cases, not directly measurable: for instance, interfacial friction between liquid and vapour phases cannot be measured. However, there are SET (separate-effect tests) experiments, the results of which are a priori sensitive to the considered models. That is the case, for example, of the "Vertical Canon" experiment, which is devoted to the study of the depressurization of a pipe initially filled with liquid. In this experiment, void fractions and remaining liquid masses are measured, which depend directly on interfacial friction.

In a case of very simple SET experiments where only one physical phenomenon, described by one physical model, is clearly dominant, the quantification of its uncertainty is rather simple. It is sufficient to shift the parameter associated with the involved physical model in order to fit the code value with each experimental data, and after that to do statistics with the different values of the parameter obtained with all the experimental data. But in the most frequent case, several physical models must be considered together, and this method does not apply any more. Such experiments are called "intermediate". Examples of intermediate experiments are the reflood experiments such as FEBA or PERICLES reflood 2-D considered for PREMIUM.

CIRCÉ is devoted to this problem: quantify the uncertainty of the parameters associated with physical models, when these physical models are not measurable (e.g., interfacial friction) and when the considered experiment is of intermediate type, i.e. with several influential physical models (e.g., reflood experiments). CIRCÉ is an inverse method of quantification of uncertainty: as explained in next §B.2.1.2, it is aimed at estimating the uncertainty of non-measurable physical models (via parameters associated with these physical models), and for that, it uses measured data sensitive to these physical models.

B.2.1.2 Main principles of CIRCÉ

For a given experiment of intermediate type, the user determines the physical models describing the physical phenomena potentially influential on the experimental data. This choice is made by expert judgment and with the help of sensitivity calculations. On this basis, CIRCÉ uses the measured quantities of the intermediate experiment, called experimental responses, and the corresponding code values, called code responses.
More precisely, let us denote as α_i (i = 1, I, with I = 1, 2 or 3, rarely more) the parameters considered by CIRCÉ and associated with the physical models relevant in the considered experiment. The α_i parameters are assumed to follow a normal law. CIRCÉ gives an estimation of the b_i mean value (also called bias) and the σ_i standard deviation of each α_i parameter. To obtain these results, CIRCÉ combines the differences between the experimental results and the corresponding code results, denoted as $\left(R_j^{exp} - R_j^{code}\right)$ (j = 1, J, with J typically equal to several tens) and the derivatives of each code response with respect to each parameter: $\frac{\partial R_j^{code}}{\partial \alpha_i}$. It is also possible to take into account the experimental uncertainties of the responses, denoted as δR_j^{exp}.This process is summarized below in Figure B.1.

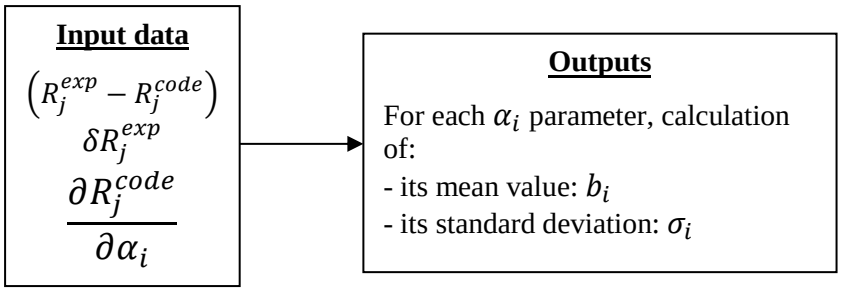

Figure B.1: inputs and outputs of CIRCÉ

For CATHARE 2, the derivatives are obtained with the ASM (Adjoint Sensitivity Method[2]) if the description of the experiment requires the use of only 1-D modules, without reflood and fuel. In other cases, finite differences are used with some precautions. §B.4.1 of this document is devoted to this issue.

A well-known algorithm in statistics, the E-M (expectation-maximization) algorithm[3], is applied in CIRCÉ4. This algorithm is based on the principle of maximum of likelihood and Bayes' theorem.

B.2.1.3 α_i parameters considered by CIRCÉ and final p_i multipliers

In its algorithm, CIRCÉ supposes that the nominal value of the α_i parameters, considered for the calculation of R_j^{code} and $\frac{\partial R_j^{code}}{\partial \alpha_i}$ in its input data deck, is equal to 0. Consequently a change of variable is needed if, for instance, the CIRCÉ study is aimed at determining the uncertainty of dimensionless multipliers of the correlations, denoted as p_i 5, since their nominal value is obviously equal to 1. Let us denote as f the relationship between α_i and p_i: $p_i = f(\alpha_i)$. The f function must satisfy: $f(0) = 1$. Besides, the ASM and the finite differences provide the derivatives of R_j^{code} with respect to the p_i multipliers: $\frac{\partial R_j^{code}}{\partial p_i}$, calculated for $p_i = 1$ and not the derivatives considered by CIRCÉ: $\frac{\partial R_j^{code}}{\partial \alpha_i}$ for $\alpha_i = 0$. As the following relationship holds:

$$\frac{\partial R_j^{code}}{\partial \alpha_i}(\alpha_i = 0) \quad = \quad \frac{\partial R_j^{code}}{\partial p_i}(p_i = 1) \times f'(\alpha_i = 0)$$

the f function must be such as: $f'(0) = 1$ so that $\frac{\partial R_j^{code}}{\partial p_i}(p_i = 1)$ can be directly used for $\frac{\partial R_j^{code}}{\partial \alpha_i}(\alpha_i = 0)$.

Both conditions: $f(0) = 1$ and $f'(0) = 1$ are verified for f defined by either $f(\alpha_i) = p_i = 1 + \alpha_i$ or $f(\alpha_i) = p_i = exp(\alpha_i)$. It will be shown later on that both formulations have other advantages. The choice among both changes of variable is based on considerations of linearity and the values found for the bias, b_i, and standard deviation, σ_i, as explained in §B.2.3.3 and in §B.3.4.3. In any case, the change of variable is performed after obtaining the CIRCÉ results that concern only the α_i parameters as shown in Figure B.1.

[2] Cacuci, D.G. (1981), "Sensitivity Theory for Nonlinear Systems: I. Nonlinear Functional Analysis Approach", J. Math. Phys. 22, 2794.

[3] Dempster, A.P., Rubin, D. B., Tsutakawa, R.K. (1981), "Estimation in Covariance Components Models", Journal of the American Statistical Association 76 (374).

[4] A. de Crécy, "Determination of the uncertainties of the constitutive relationships of the CATHARE 2 code", M&C 2001, Salt Lake City, Utah, USA, September 2001.

[5] It would also be theoretically possible to use CIRCÉ for parameters such as single coefficients inside the correlations or additive parameters. But this possibility was never used in the CIRCÉ studies performed up to now for CATHARE.

B.2.1.4 Rapid description of the hypotheses made by CIRCÉ

Two main hypotheses are made by CIRCÉ. The first hypothesis is the normality of the α_i parameters. A hypothesis on the PDF of the parameters is compulsory since the principle of maximum of likelihood is applied in the E-M algorithm. This hypothesis results in a hypothesis of normality for the p_i multiplier if the $p_i = 1 + \alpha_i$ change of variable is selected. In the other case, with the $p_i = exp(\alpha_i)$ change of variable, the p_i multiplier obeys a log-normal law. One out of the interests of both proposed changes of variable becomes apparent: with other changes of variable, making it possible to have $f(0) = 1$ and $f'(0) = 1$, the p_i multiplier will not obey a classical law.

The second hypothesis is the linearity between the code responses and each α_i parameter. Without giving a detailed description of the E-M algorithm, this hypothesis seems fairly obvious since first-order derivatives $\frac{\partial R_j^{code}}{\partial \alpha_i}$ are used. Thanks to an iterative use of CIRCÉ explained in §B.3.3, this linearity hypothesis is made for values of the α_i parameter ranging in its final variation interval, i.e., $[b_i - 2\sigma_i;\ b_i + 2\sigma_i]$ for a 95% variation interval and by considering the first hypothesis of normality. Consequently the hypothesis of linearity is checked even with high b_i biases, but is more challenging for high σ_i standard deviations.

The linearity and normality hypotheses must be systematically checked: this is an important part of the methodology developed for proper use of CIRCÉ and explained in the part "user guidelines" (cf. §B.2.3.3, §B.3.4.3 and §B.3.4.4).

Three other hypotheses, less relevant, are also made by CIRCÉ and will be explained below in §B.3:

- the δR_j^{exp} experimental uncertainties must be independent of the $R_j^{real} - R_j^{code}$ differences, where R_j^{real} is the real value of the R_j response, that the experimenter tries to measure (he/ she obtains R_j^{exp}) and the code user to calculate (he/she obtains R_j^{code});
- the $R_j^{exp} - R_j^{code}$ differences must be globally higher than the δR_j^{exp} experimental uncertainties: otherwise CIRCÉ calculates σ_i standard deviations equal to 0;
- the R_j responses must be as independent as possible: two dependent responses will be considered by CIRCÉ as only one response, with a double weight. Too many dependent responses lowers the precision of CIRCÉ results, precision increases with the number of independent responses.

B.2.2 An example of CIRCÉ results

A rather outstanding work programme has been achieved with CIRCÉ for CATHARE 2 physical models: roughly 15 studies corresponding to more than 15 man-years work have been performed since 1999. Considered physical models for these studies are those which are influential either for SB- or LB-LOCA.

One of these studies concerns the quantification of the uncertainties of the physical models of CATHARE 2 influential for the film-wise condensation in the presence of incondensable gases in the SG (Steam Generator) tubes. This phenomenon occurs in the primary side of the SG, especially for Intermediate Break LOCA. The experimental data are taken from the qualification data base of CATHARE 2 and concern the 82 COTURNE single vertical tube tests with nitrogen or helium[6].

[6] Chataing, T., Clément, P., Excoffon, J., Geffraye, G. (1999), "A general correlation for steam condensation in case of wavy laminar flow along vertical tubes", NURETH 9, San Francisco, California, USA, 3-8 Oct. 1999.

In the presence of incondensable gases, film condensation is controlled by two phenomena: the heat transfer through the liquid film (as in pure steam conditions) and the steam diffusion through the gas mixture boundary layer, rich in incondensable gas. The first phenomenon is described by the modified Chen correlation for the heat transfer coefficient, denoted as hfilm and the second one is described by a correlation of the Sherwood number, denoted as Sh. Figure B.2 sums up both phenomena.

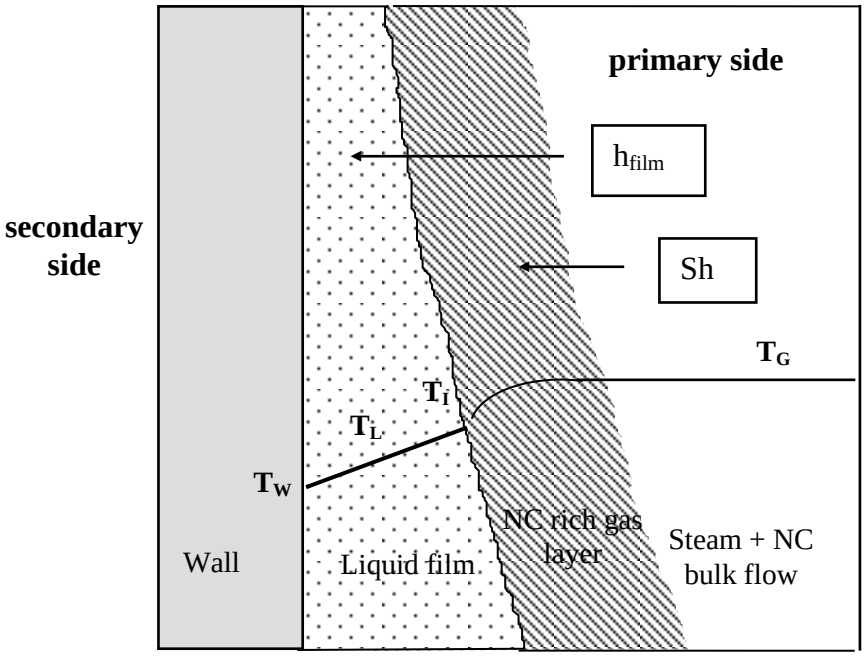

Figure B.2: film-wise condensation with incondensable gases in the primary part of SG

Let us denote as α_1 and α_2 the parameters associated with hfilm and Sh correlations, not measurable. For each test, two experimental results are considered: the overall heat transfer coefficient in condensation located at the gas inlet and at the middle length of the tube. It is h_{cond} deduced from the local measurement of the global condensation flux $\varphi_{cond} = h_{cond} \times (T_{sat}(P_v) - T_w)$ through both layers and from the T_w wall temperature. As 82 tests are considered, a total of 164 responses are available.

The raw CIRCÉ results, concerning the α_i parameters, are the followings:

- for h_{film}: α_1 has a mean value b_1 equal to -0.046 and a standard deviation σ_1 equal to 0.350;
- for Sh: α_2 has a mean value b_2 equal to -0.152 and a standard deviation σ_2 equal to 0.290.

For the p_i multipliers, which are the parameters finally considered, the results are:

- for h_{film}: the formulation $p_1 = 1 + \alpha_1$ is chosen; consequently, p_1 the multiplicative factor of h_{film}, follows a normal law, with a bias equal to 0.95 and a 95% variation interval equal to [0.25 ; 1.65] = $[1 + b_1 - 2\sigma_1 \; ; \; 1 + b_1 + 2\sigma_1]$.
- for Sh: the formulation $p_2 = \exp(\alpha_2)$ is chosen. Consequently, p_2 the multiplicative factor of the Sh number, follows a log-normal law with a bias equal to $e^{-0.152}$ = 0.86 and a 95% variation interval equal to [0.48 ; 1.53] = $[\exp(b_2 - 2\sigma_2) \; ; \; \exp(b_2 + 2\sigma_2)]$.

Both mean values for the multiplicative factors p_1 and p_2, equal to 0.95 and 0.86, are rather close to 1. It means that both correlations are rather well centred.

B.2.3 Rapid description of the user guidelines of CIRCÉ

B.2.3.1 Introduction

CIRCÉ is a statistical tool, and it can lead to spurious results if it is used as a black box. In addition, CIRCÉ relies on two main hypotheses, linearity and normality, described in §B.2.1.4, which must be checked. Therefore, a methodology has been developed for a proper use of CIRCÉ and the most important main features are briefly recalled here. They make up a kind of user guidelines. These guidelines are extensively described in the §B.3.4.

B.2.3.2 Before using CIRCÉ

Representativeness of the considered experiment

The experimental conditions of the tests of the considered intermediate experiment must be similar or close to those encountered during the reactor transient for which uncertainty analysis is carried out. In the rare cases where the experimental conditions of some tests strongly differ from the reactor conditions, the question of whether or not to consider these tests must be raised.

This verification partly answers to the issue of the representativeness of the CIRCÉ results. If, in the reactor case, boundary conditions cover a more extended field than that of the experiment used in the CIRCÉ study, other experiments must be found and used by CIRCÉ.

Distribution of the derivatives vectors

The problem solved with the CIRCÉ algorithm must be well posed from a mathematical point of view, in other words must be identifiable. Indeed, in the calculation of the bi biases, a matrix has to be inverted (cf. §B.3.1.3, equation 16), which is impossible if the different derivative vectors $\frac{\partial R_j}{\partial \alpha} = \begin{pmatrix} \frac{\partial R_j}{\partial \alpha_1} \\ \vdots \\ \frac{\partial R_j}{\partial \alpha_I} \end{pmatrix}$ (for j ranging from 1 to J) are collinear. Practically and more generally, the b_i biases, but also the σ_i standard deviations will be poorly estimated if the distribution of these vectors is close to a collinear configuration. Nevertheless this condition is generally well respected if the considered parameters are correctly chosen, in other words if they are independent (see the end of §B.3.1.3).

B.2.3.3 Checking the hypotheses made by CIRCÉ

Checking the hypothesis of linearity

One recalls that, due to an iterative use of CIRCÉ, this hypothesis is made inside the final variation interval found for each α_i parameter, whatever the value found for the biases (particularly even for high biases in absolute values).

Therefore, in order to check the hypothesis of linearity, each $\alpha_i$parameter is regularly varied inside its 95% variation interval found by CIRCÉ, equal to $[b_i - 2\sigma_i;\ b_i + 2\sigma_i]$. The dependence between the R_j^{code} code responses and the α_i parameter is observed. This dependence is different according to the type of change of variable between the α_i parameters considered by CIRCÉ and the p_i multipliers. One reminds that two changes of variable are used in the CIRCÉ studies: $p_i = 1 + \alpha_i$ and $p_i = exp(\alpha_i)$. With both changes of variables, both values of the R_j^{code} code responses are different for a given α_i value, since the physical

models are multiplied by $1 + \alpha_i$ in a case, by $\exp(\alpha_i)$ in the other case. The change of variable for which the hypothesis of linearity is the best verified, is selected.

This verification of the hypothesis of linearity between R_j^{code} and α_i shows another interest of both formulations: $p_i = 1 + \alpha_i$ and $p_i = exp(\alpha_i)$. If the first formulation is the best one for the linearity, it means that the dependence between R_j^{code} and the p_i multiplier is of linear type, like the dependence between R_j^{code} and α_i. If the second formulation is the best one, the dependence between R_j^{code} and the p_i multiplier (and not the α_i parameter) is of logarithmic type since $\alpha_i = ln(p_i)$. Both types of dependences are the most frequent in physics and considering them seems to be a reasonable choice.

One will note that the retained formulations are not necessarily the same for all the correlations, as shown in the example §B.2.2.

It is therefore apparent that the choice among both formulations, $p_i = 1 + \alpha_i$ and $p_i = \exp(\alpha_i)$ is the result of this linearity study. There is nevertheless a case where the $p_i = \exp(\alpha_i)$ formulation must be kept, whatever the result of the linearity study is. Indeed the sign of a physical model cannot change: negative values of the p_i multiplier are forbidden. The interest of the $p_i = \exp(\alpha_i)$ formulation is that p_i is always strictly positive, whereas it is not necessarily the case with the $p_i = 1 + \alpha_i$ formulation, depending of the b_i and σ_i values found by CIRCÉ.

At first sight, this hypothesis of linearity can be viewed as quite restrictive. But in all the studies performed with CIRCÉ for CATHARE 2, this hypothesis is generally well verified, for one among both formulations.

Checking the hypothesis of normality

If several parameters are considered, the empirical distribution of each α_i parameter cannot be plotted, because the algorithm does not provide the individual realizations of α_i (corresponding with each experimental response). However, a global check can be performed, via the residuals of each R_j response, defined by[7]:

$$r_j = \frac{R_j^{\exp} - R_j^{code} - \sum_{i=1}^{I} \frac{\partial R_j^{code}}{\partial \alpha_i} b_i}{\sum_{i=1}^{I} \left(\frac{\partial R_j^{code}}{\partial \alpha_i} \right)^2 \sigma_i^2 + \left(\sigma_j^{\exp}\right)^2}$$

. If the α_i parameters obey a normal law, then the residuals obey a standardized normal law (m = 0, σ= 1), denoted as $N(0,1)$. Their empirical distribution is plotted to see if it is close to $N(0,1)$.

B.2.3.4 Final checks: the so-called bounding calculations

The first check consists in performing an uncertainty analysis of the experiment used in the CIRCÉ study, following by this way the specifications of Phase III of PREMIUM. The outputs are the responses considered in the CIRCÉ study. The parameters considered for the study (generally 2 or 3) are sampled following their PDF, the features of which have been estimated by CIRCÉ. A high number of code runs, denoted as *N*, is carried out for the propagation step, generally 100 but sometimes higher, for example 1000. For each value of the parameters, the corresponding CATHARE response is calculated.

[7] $\sigma_j^{\exp}$ is the standard deviation of the experimental uncertainty of the R_j^{exp} response. Moreover, this definition of the residuals is given, initially, for the case where the α_i parameters are assumed independent. A more general definition is given by equation 17.

Consequently N values of each response are obtained. Order statistics are used to derive quantities such as the 2.5% and 97.5% percentiles of each R_j^{code} response, denoted as $R_j^{0.025}$ and $R_j^{0.975}$. One must check that:

- for roughly 2.5% of the responses, the following relationship holds: $R_j^{exp} \leq R_j^{0,025}$
- for also roughly 2.5% of the responses, the following relationship holds: $R_j^{exp} \geq R_j^{0.975}$.

In other words, one checks that the $[R_j^{0.025}; R_j^{0.975}]$ variation intervals envelop 95% of the R_j^{exp} experimental responses, what explains the name of bounding calculations used for this check.

The biases estimated by CIRCÉ are also checked: without having absolute mathematical proof, we have noticed that taking into account the biases in the CATHARE calculations decreases significantly the mean quadratic deviation between code and experimental results defined by $\sqrt{\frac{1}{J}\sum_{j=1}^{J}(R_j^{exp} - R_j^{code})^2}$, J being the number of considered responses.

Both checks can be viewed as a validation of the CIRCÉ method. They were systematically performed in all the CIRCÉ studies, and the obtained results were always satisfactory. Nevertheless, this validation is only a verification of the consistency of the CIRCÉ results. They do not give indications about the extrapolability of these results to the reactor case: that is why verification such as that performed with the Phase IV of PREMIUM, using the PERICLES reflood 2-D results will be especially of interest.

B.2.3.5 Accuracy of the results

This last item is more an additional information than a supplementary check. Thanks to the bootstrap technique, accuracy can be associated to the results of CIRCÉ. A standard deviation is given for each CIRCÉ result, that is to say each b_i bias and each σ_i standard deviation. The lower the standard deviation is, the more accurate the result is.

This accuracy becomes better when J, the number of considered responses, is increased. It also partly answers to the issue of the influence of the choice of the responses on the CIRCÉ results.

B.3: DETAILED DESCRIPTION OF THE CIRCÉ METHOD AND ITS APPLICATION

B.3.1 CIRCÉ Algorithm

B.3.1.1 Introduction

In this part, the notations are the same as those of §B.2.1.2:

- α_i, i = 1, I for the parameters considered by CIRCÉ,
- R_j, j = 1, J for the responses.

The p_i parameters, dimensionless multipliers of the correlations, are considered outside from the CIRCÉ algorithm. Consequently they do not appear in its description. One reminds that these p_i parameters depend on the α_i parameters by one out of both formulations: $p_i = 1 + \alpha_i$ or $p_i = exp(\alpha_i)$, the choice of the formulation being made in order to respect at best the hypothesis of linearity (§B.2.3.3).

CIRCÉ is aimed at calculating the statistical features of the α vector defined by $\alpha = \begin{pmatrix} \alpha_1 \\ \vdots \\ \alpha_I \end{pmatrix}$. Thus CIRCÉ calculates a mean value vector, also called bias vector: $b = \begin{pmatrix} b_1 \\ \vdots \\ b_I \end{pmatrix}$ and a covariance matrix, denoted as C. By definition, a covariance matrix is symmetric; its diagonal terms are the variances of the parameters, i.e. the square of the σ_i standard deviations and its extra-diagonal terms are the covariance terms, related to the correlation coefficients of the parameters considered two by two. In the studies performed up to now with CIRCÉ, the covariance terms are considered as equal to 0. It means that, in these studies, the different parameters are assumed statistically independent. This hypothesis is nevertheless not compulsory. However, to sum up and simplify, one can say that the C matrix is defined by:

$$C = \begin{pmatrix} \sigma_1^2 & \cdots & 0 \\ \vdots & \ddots & \vdots \\ 0 & \cdots & \sigma_I^2 \end{pmatrix} \qquad \textbf{Equation 1}$$

In order to explain step by step the CIRCÉ algorithm, it is firstly described for the case where the b bias vector is supposed equal to 0, then in the more general case where it does not equal 0. All the CIRCÉ studies were performed in this second case.

B.3.1.2 Case without bias calculation

<u>The α_j realizations and the estimation of C by the maximum of likelihood</u>

For each R_j response, the notion of α_j realization can be defined. This realization is the value of the α vector of the parameters such as the code response calculated with $\alpha = \alpha_j$ equals the real value, unknown, of the response R_j. Of course, these α_j realizations are unknown. In addition, if more than one parameter is considered, several α_j exist for each R_j response.

The CIRCÉ algorithm uses this notion of α_j realizations, via the principle of maximum of likelihood[8]. This principle gives an estimation of the C matrix, denoted as $\hat{C}$:

$$\hat{C} = \frac{1}{J}\sum_{j=1}^{J} \boldsymbol{\alpha_j}\,\boldsymbol{\alpha_j^T} \qquad \textbf{Equation 2}$$

<u>The linear model</u>

But as written before, the α_j realizations are unknown. However they depend on known quantities: the R_j^{exp} and R_j^{code} responses, via a first order development around the nominal value of the α vectorial parameter, equal to 0. For each R_j response, one can write:

$$R_j^{exp} - R_j^{code} = \left(R_j^{exp} - R_j^{real}\right) + \left(R_j^{real} - R_j^{code}\right) = e_j + \frac{\boldsymbol{\partial R_j}^T}{\boldsymbol{\partial \alpha}} \times \boldsymbol{\alpha_j} \qquad \textbf{Equation 3}$$

Where:

- R_j^{real} is the real value of the R_j response, that the experimenter tries to measure (he obtains R_j^{exp}) and the code user to calculate (he obtains R_j^{code});

[8] This principle is quite usual in statistics and is explained in Addendum B1.

- e_j is a realization of δR_j^{exp}, the experimental uncertainty of R_j^{exp}. e_j is not explicitly known but it is supposed to obey a centred normal law, with a known standard deviation, denoted as σ_j^{exp};
- $\frac{\partial R_j}{\partial \boldsymbol{\alpha}}$ is the vector of the derivatives of R_j^{code} with respect to the I α_i parameters: $\frac{\partial R_j}{\partial \boldsymbol{\alpha}}^T = \left(\frac{\partial R_j}{\partial \alpha_1} \quad \cdots \quad \frac{\partial R_j}{\partial \alpha_I}\right)$;
- $\boldsymbol{\alpha_j}$ is the unknown realization of the $\boldsymbol{\alpha}$ vector for the R_j response, as explained above. One can write: $R_j^{code}(\boldsymbol{\alpha_j}) = R_j^{real}$.

In the equation 3, $\left(R_j^{exp} - R_j^{real}\right)$ and $(R_j^{real} - R_j^{code})$ are supposed to be independent random variables. Consequently, one can write the following sum of variances:

$$var(R_j^{exp} - R_j^{code}) = var\left(R_j^{exp} - R_j^{real}\right) + var(R_j^{real} - R_j^{code}) \qquad \textbf{Equation 4}$$

In other words, by taking into account the equation 3, one obtains:

$$var(R_j^{exp} - R_j^{code}) = var(e_j) + var\left(\frac{\partial R_j}{\partial \boldsymbol{\alpha}}^T \boldsymbol{\alpha_j}\right) = \left(\sigma_j^{exp}\right)^2 + \frac{\partial R_j}{\partial \boldsymbol{\alpha}}^T \boldsymbol{C} \frac{\partial R_j}{\partial \boldsymbol{\alpha}} \qquad \textbf{Equation 5}$$

This last equation 5 will be useful later on.
The first order development (equation 3) does not allow explicitly calculating the $\boldsymbol{\alpha_j}$ realizations, if more than one parameter is considered, because it is a scalar equation whereas $\boldsymbol{\alpha_j}$ is a vectorial unknown. Nevertheless, it makes it possible to use Bayes' theorem.

Bayes' theorem

This theorem deals with the conditional probabilities and is explained in any statistics manual. Its general idea is to start from an initial estimation of the $\boldsymbol{C}$ covariance matrix, referred to as $\boldsymbol{C}$ *a priori*, and denoted as $\boldsymbol{C^{(m-1)}}$. This first estimation is corrected after "observation" of each $\boldsymbol{\alpha_j}$ realization of $\boldsymbol{\alpha}$, or more precisely, since these $\boldsymbol{\alpha_j}$ are impossible to determine, after "observation" of the $R_j^{exp} - R_j^{code}$ differences. A new matrix is obtained, referred to as *a posteriori* matrix, and denoted as $\boldsymbol{C^{(m)}}$. The process is continued until both *a priori* and *a posteriori* matrices are very close. It is consequently an iterative process. The (m) exponent used for the *a posteriori* matrix indicates the number of the iteration performed by CIRCÉ. Generally, the iterative process is started with the identity matrix, and around 1000 iterations are necessary to converge.
More precisely, if the $\boldsymbol{\alpha}$ vectorial random variable is assumed to obey a normal law, then each $\boldsymbol{\alpha_j}$ can be considered as a random variable that itself obeys a normal law depending on j. Bayes' theorem gives an estimation of the $\overline{\boldsymbol{\alpha}}_{\boldsymbol{j}}$ mean vector and of the $\boldsymbol{C_j}$ covariance matrix of each $\boldsymbol{\alpha_j}$, after observation of $R_j^{exp} - R_j^{code}$ and from the *a priori* $\boldsymbol{C^{(m-1)}}$ matrix. They are:

$$\overline{\boldsymbol{\alpha}}_{\boldsymbol{j}} = \boldsymbol{C^{(m-1)}} \times \frac{\partial R_j}{\partial \boldsymbol{\alpha}} \times \frac{R_j^{exp} - R_j^{code}}{\frac{\partial R_j}{\partial \boldsymbol{\alpha}}^T \boldsymbol{C^{(m-1)}} \frac{\partial R_j}{\partial \boldsymbol{\alpha}} + \left(\sigma_j^{exp}\right)^2} \qquad \textbf{Equation 6}$$

$$\boldsymbol{C_j} = \boldsymbol{C^{(m-1)}} - \frac{\boldsymbol{C^{(m-1)}} \frac{\partial R_j}{\partial \boldsymbol{\alpha}} \frac{\partial R_j}{\partial \boldsymbol{\alpha}}^T \boldsymbol{C^{(m-1)}}}{\frac{\partial R_j}{\partial \boldsymbol{\alpha}}^T \boldsymbol{C^{(m-1)}} \frac{\partial R_j}{\partial \boldsymbol{\alpha}} + \left(\sigma_j^{exp}\right)^2} \qquad \textbf{Equation 7}$$

Final iterative formula

It is apparent that Bayes' theorem does not calculate explicitly each $\boldsymbol{\alpha_j}$ but gives only an estimation of its mean vector and its covariance matrix. The $\boldsymbol{\alpha_j \alpha_j^T}$ products are needed in the equation 2 to calculate the *a posteriori* $\boldsymbol{C^{(m)}}$ matrix. They are replaced by their expectation value, given by the equation 8:

$$E\left(\boldsymbol{\alpha_j \alpha_j^T}\right) = \bar{\boldsymbol{\alpha}}_j \bar{\boldsymbol{\alpha}}_j{}^T + \boldsymbol{C_j} \qquad \textbf{Equation 8}$$

Finally, the following iterative relationship between the $\boldsymbol{C^{(m-1)}}$ *a priori* matrix and the $\boldsymbol{C^{(m)}}$ *a posteriori* matrix is obtained, by combining the equations 6, 7 and 8 in the equation 2:

$$\boldsymbol{C^{(m)}} = \boldsymbol{C^{(m-1)}} + \frac{1}{J}\sum_{j=1}^{J} \frac{\boldsymbol{C^{(m-1)}} \frac{\partial \boldsymbol{R_j}}{\partial \boldsymbol{\alpha}} \frac{\partial \boldsymbol{R_j}^T}{\partial \boldsymbol{\alpha}} \boldsymbol{C^{(m-1)}}}{\frac{\partial \boldsymbol{R_j}^T}{\partial \boldsymbol{\alpha}} \boldsymbol{C^{(m-1)}} \frac{\partial \boldsymbol{R_j}}{\partial \boldsymbol{\alpha}} + \left(\sigma_j^{exp}\right)^2} \left(\frac{\left(R_j^{exp} - R_j^{code}\right)^2}{\frac{\partial \boldsymbol{R_j}^T}{\partial \boldsymbol{\alpha}} \boldsymbol{C^{(m-1)}} \frac{\partial \boldsymbol{R_j}}{\partial \boldsymbol{\alpha}} + \left(\sigma_j^{exp}\right)^2} - 1 \right) \qquad \textbf{Equation 9}$$

Comments

The iterative process therefore consists of two parts:

- A "maximization" part where the principle of maximum likelihood is applied. It gives the equation 2, involving the $\boldsymbol{\alpha_j \alpha_j^T}$ products.
- An "expectation" part, where each $\alpha_j \alpha_j^T$ product is replaced by an estimation of its expectation value, thanks to Bayes' theorem.

That is the reason why this algorithm, well-known in statistics, is called E-M algorithm, E for Expectation part, and M for Maximization.

This algorithm has two valuable features:

- It warrants that the $\boldsymbol{C^{(m)}}$ matrix is always defined and positive, which is a compulsory condition for a covariance matrix (with or without covariance terms). Consequently, one obtains always positive values of the variances.
- The likelihood of the $(R_j^{exp} - R_j^{code})$ observed data increases with the iterations of the algorithm.

Nevertheless, it must be noted that the maximum found with the E-M algorithm is only a local maximum, depending on the initial $C^{(0)}$ matrix. The $C^{(0)}$ initial matrix considered by default by CIRCÉ is the identity matrix. In some cases, it can be advisable to run CIRCÉ with other initial $C^{(0)}$ matrices, what can be made without difficulty with the CIRCÉ software.

B3.1.3 Case with bias calculation

Calculation of the $\boldsymbol{C}$ covariance matrix

At each (m) iteration, $C^{(m)}$ is firstly calculated, using the estimations of $b^{(m-1)}$ and $C^{(m-1)}$ of the previous iteration. One defines the new centred variable $\alpha'_j = \alpha_j - b^{(m-1)}$. The equation 2 becomes:

$$\widehat{\boldsymbol{C}}^{(\boldsymbol{m})} = \frac{1}{J}\sum_{j=1}^{J} \boldsymbol{\alpha}'_j \ \boldsymbol{\alpha}'^{\boldsymbol{T}}_{\boldsymbol{j}} \qquad \textbf{Equation 10}$$

Bayes' theorem gives the $\bar{\alpha}'_j$ mean vector of α'_j, its covariance matrix being always C_j. The difference of the $\bar{\alpha}'_j$ mean vector with the $\bar{\alpha}_j$ mean vector is that the $(R_j^{exp} - R_j^{code})$ difference is replaced by $\left(R_j^{exp} - R_j^{code} - \frac{\partial R_j}{\partial \alpha}^T b^{(m-1)}\right)$, as it is apparent in the equation 11:

$$\overline{\boldsymbol{\alpha}}'_{\boldsymbol{j}} = \boldsymbol{C}^{(\boldsymbol{m-1})} \times \frac{\boldsymbol{\partial R_j}}{\boldsymbol{\partial \alpha}} \times \frac{R_j^{exp} - R_j^{code} - \frac{\boldsymbol{\partial R_j}^{\boldsymbol{T}}}{\boldsymbol{\partial \alpha}} \boldsymbol{b}^{(\boldsymbol{m-1})}}{\frac{\boldsymbol{\partial R_j}^{\boldsymbol{T}}}{\boldsymbol{\partial \alpha}} \boldsymbol{C}^{(\boldsymbol{m-1})} \frac{\boldsymbol{\partial R_j}}{\boldsymbol{\partial \alpha}} + \left(\sigma_j^{exp}\right)^2} \qquad \textbf{Equation 11}$$

The equation 12 for $E\left(\boldsymbol{\alpha}'_{\boldsymbol{j}} \boldsymbol{\alpha}'^{\boldsymbol{T}}_{\boldsymbol{j}}\right)$ is similar to the equation 8:

$$E\left(\boldsymbol{\alpha}'_{\boldsymbol{j}} \boldsymbol{\alpha}'^{\boldsymbol{T}}_{\boldsymbol{j}}\right) = \overline{\boldsymbol{\alpha}}'_{\boldsymbol{j}} \overline{\boldsymbol{\alpha}}'^{\boldsymbol{T}}_{\boldsymbol{j}} + \boldsymbol{C_j} \qquad \textbf{Equation 12}$$

The final iterative formula is given by the equation 13, identical to the equation 9 except that $(R_j^{exp} - R_j^{code})$ is replaced by $\left(R_j^{exp} - R_j^{code} - \frac{\boldsymbol{\partial R_j}^{\boldsymbol{T}}}{\boldsymbol{\partial \alpha}} \boldsymbol{b}^{(\boldsymbol{m-1})}\right)$:

$$\boldsymbol{C}^{(\boldsymbol{m})} = \boldsymbol{C}^{(\boldsymbol{m-1})} + \frac{1}{J} \sum_{j=1}^{J} \frac{\boldsymbol{C}^{(\boldsymbol{m-1})} \frac{\boldsymbol{\partial R_j}}{\boldsymbol{\partial \alpha}} \frac{\boldsymbol{\partial R_j}^{\boldsymbol{T}}}{\boldsymbol{\partial \alpha}} \boldsymbol{C}^{(\boldsymbol{m-1})}}{\frac{\boldsymbol{\partial R_j}^{\boldsymbol{T}}}{\boldsymbol{\partial \alpha}} \boldsymbol{C}^{(\boldsymbol{m-1})} \frac{\boldsymbol{\partial R_j}}{\boldsymbol{\partial \alpha}} + \left(\sigma_j^{exp}\right)^2} \left(\frac{\left(R_j^{exp} - R_j^{code} - \frac{\boldsymbol{\partial R_j}^{\boldsymbol{T}}}{\boldsymbol{\partial \alpha}} \boldsymbol{b}^{(\boldsymbol{m-1})}\right)^2}{\frac{\boldsymbol{\partial R_j}^{\boldsymbol{T}}}{\boldsymbol{\partial \alpha}} \boldsymbol{C}^{(\boldsymbol{m-1})} \frac{\boldsymbol{\partial R_j}}{\boldsymbol{\partial \alpha}} + \left(\sigma_j^{exp}\right)^2} - 1 \right) \qquad \textbf{Equation 13}$$

Calculation of the $\boldsymbol{b}$ bias vector

Once $C^{(m)}$ is calculated, $b^{(m)}$ is calculated by using too the principle of maximum of likelihood, but applied to the $(R_j^{exp} - R_j^{code})$ realizations. If α follows a normal law, with a b bias and a C covariance matrix, each $(R_j^{exp} - R_j^{code})$ follows a scalar normal law with the following statistical parameters:

- Mean value: $\frac{\boldsymbol{\partial R_j}^{\boldsymbol{T}}}{\boldsymbol{\partial \alpha}} \boldsymbol{b}$
- Variance: $\frac{\boldsymbol{\partial R_j}^{\boldsymbol{T}}}{\boldsymbol{\partial \alpha}} \boldsymbol{C} \frac{\boldsymbol{\partial R_j}}{\boldsymbol{\partial \alpha}} + \left(\sigma_j^{exp}\right)^2$ (as already expressed in the equation 5)

The logarithm of the likelihood of the J-sample $(R_j^{exp} - R_j^{code})$ (j = 1, J) is given by the equation 14:

$$\ln(L) = -\frac{J}{2}\ln(2\pi) - \frac{1}{2}\sum_{j=1}^{J} ln\left(\frac{\boldsymbol{\partial R_j}^{\boldsymbol{T}}}{\boldsymbol{\partial \alpha}} \boldsymbol{C}^{(\boldsymbol{m})} \frac{\boldsymbol{\partial R_j}}{\boldsymbol{\partial \alpha}} + \left(\sigma_j^{exp}\right)^2\right) - \frac{1}{2}\sum_{j=1}^{J} \frac{\left(R_j^{exp} - R_j^{code} - \frac{\boldsymbol{\partial R_j}^{\boldsymbol{T}}}{\boldsymbol{\partial \alpha}} \boldsymbol{b}^{(\boldsymbol{m})}\right)^2}{\frac{\boldsymbol{\partial R_j}^{\boldsymbol{T}}}{\boldsymbol{\partial \alpha}} \boldsymbol{C}^{(\boldsymbol{m})} \frac{\boldsymbol{\partial R_j}}{\boldsymbol{\partial \alpha}} + \left(\sigma_j^{exp}\right)^2} \qquad \textbf{Equation 14}$$

ln(L) is maximized with respect to each component b_i of the b mean vector: The I scalar equations 15 are written :

$$\frac{\partial \ln(L)}{\partial b_i} = \sum_{j=1}^{J} \frac{\left(R_j^{exp} - R_j^{code} - \frac{\boldsymbol{\partial R_j}^{\boldsymbol{T}}}{\boldsymbol{\partial \alpha}} \boldsymbol{b}^{(\boldsymbol{m})}\right) \frac{\partial R_j}{\partial \alpha_i}}{\frac{\boldsymbol{\partial R_j}^{\boldsymbol{T}}}{\boldsymbol{\partial \alpha}} \boldsymbol{C}^{(\boldsymbol{m})} \frac{\boldsymbol{\partial R_j}}{\boldsymbol{\partial \alpha}} + \left(\sigma_j^{exp}\right)^2} = 0 \qquad \textbf{Equation 15}$$

They lead to the linear system 16, which has to be solved to obtain $\boldsymbol{b}^{(\boldsymbol{m})}$:

$$\begin{pmatrix} \sum_{j=1}^{J} \frac{\left(\frac{\partial R_j}{\partial \alpha_1}\right)^2}{\frac{\partial \boldsymbol{R_j}^T}{\partial \boldsymbol{\alpha}} \boldsymbol{C^{(m)}} \frac{\partial \boldsymbol{R_j}}{\partial \boldsymbol{\alpha}} + \left(\sigma_j^{exp}\right)^2} & \cdots & \sum_{j=1}^{J} \frac{\frac{\partial R_j}{\partial \alpha_1}\frac{\partial R_j}{\partial \alpha_I}}{\frac{\partial \boldsymbol{R_j}^T}{\partial \boldsymbol{\alpha}} \boldsymbol{C^{(m)}} \frac{\partial \boldsymbol{R_j}}{\partial \boldsymbol{\alpha}} + \left(\sigma_j^{exp}\right)^2} \\ \vdots & \ddots & \vdots \\ \sum_{j=1}^{J} \frac{\frac{\partial R_j}{\partial \alpha_I}\frac{\partial R_j}{\partial \alpha_1}}{\frac{\partial \boldsymbol{R_j}^T}{\partial \boldsymbol{\alpha}} \boldsymbol{C^{(m)}} \frac{\partial \boldsymbol{R_j}}{\partial \boldsymbol{\alpha}} + \left(\sigma_j^{exp}\right)^2} & \cdots & \sum_{j=1}^{J} \frac{\left(\frac{\partial R_j}{\partial \alpha_I}\right)^2}{\frac{\partial \boldsymbol{R_j}^T}{\partial \boldsymbol{\alpha}} \boldsymbol{C^{(m)}} \frac{\partial \boldsymbol{R_j}}{\partial \boldsymbol{\alpha}} + \left(\sigma_j^{exp}\right)^2} \end{pmatrix} \begin{pmatrix} b_1^{(m)} \\ \vdots \\ b_I^{(m)} \end{pmatrix} = \begin{pmatrix} \sum_{j=1}^{J} \frac{\frac{\partial R_j}{\partial \alpha_1}\left(R_j^{exp} - R_j^{code}\right)}{\frac{\partial \boldsymbol{R_j}^T}{\partial \boldsymbol{\alpha}} \boldsymbol{C^{(m)}} \frac{\partial \boldsymbol{R_j}}{\partial \boldsymbol{\alpha}} + \left(\sigma_j^{exp}\right)^2} \\ \vdots \\ \sum_{j=1}^{J} \frac{\frac{\partial R_j}{\partial \alpha_I}\left(R_j^{exp} - R_j^{code}\right)}{\frac{\partial \boldsymbol{R_j}^T}{\partial \boldsymbol{\alpha}} \boldsymbol{C^{(m)}} \frac{\partial \boldsymbol{R_j}}{\partial \boldsymbol{\alpha}} + \left(\sigma_j^{exp}\right)^2} \end{pmatrix} \quad \textbf{Equation 16}$$

Comments on the CIRCÉ algorithm with bias calculation

Unlike the case without bias calculation, the CIRCÉ algorithm slightly differs from the E-M algorithm in the case of bias calculation. The differences are precisely explained in Appendix B. They are minor enough so that CIRCÉ and pure E-M results are the same.

The b bias vector is estimated by the solving of a linear system (equation 16). As a consequence, the matrix in the left term of this system must be invertible. One can easily show that it is not the case if all the $\frac{\partial \mathrm{R_j}}{\partial \alpha}$ derivative vectors are collinear. This configuration of the derivatives vectors must also be avoided even in the case without bias calculation, whereas, in this case, the E-M algorithm is strictly used. Indeed, the covariance matrix of the C matrix (i.e. the variances and the covariances of the σ_i^2) tends to infinity in case of collinear derivative vectors: it means that, in this case, the precision of the σ_i standard deviations becomes very poor. Consequently, the configuration of the derivative vectors must be checked before beginning a CIRCÉ study, as explained in §B.2.3.2. Nevertheless the case of almost collinear vectors is not met in CIRCÉ studies performed for CATHARE: the physics described by CATHARE is too complex for that. Nevertheless, even with a complex physics, the choice of the parameters and of the responses must be suitable. Indeed the $\frac{\partial \mathrm{R_j}}{\partial \alpha}$ vectors will be almost collinear in two cases:

- the parameters are dependent: in this case, it is more advisable to consider only one parameter;
- the R_j responses are dependent and consequently the derivatives of a given response are very similar to those of another response: it must be avoided since CIRCÉ lies on a hypothesis of independence of the responses (cf. §B.2.1.4 and next §B.3.2).

B.3.2 The CIRCÉ hypotheses explained from its algorithm

When reading the description of its algorithm, the hypotheses made by CIRCÉ become obvious. The two major hypotheses are:

i. The hypothesis of linearity between the R_j^{code} responses and the α_i parameters: this is compulsory since a first-order development is used: that is equation 3 of §B.3.1.2. An iterative use of CIRCÉ makes it possible to limit this hypothesis of linearity to the case where the α_i parameter is varied

inside its final range of variation, i.e. $[b_i - 2\sigma_i;\ b_i + 2\sigma_i]$ if considering a 95% variation interval. This iterative use of CIRCÉ, so-called "iterative CIRCÉ" is explained in the next §B.3.3.

ii. The hypothesis of normality of the α_i parameters: The principle of maximum of likelihood, used by CIRCÉ, requires making a hypothesis on the type of PDF of the α_i parameters. The CIRCÉ algorithm (like the E-M algorithm) chooses to make the hypothesis of normality. It leads to the equation 2 of the case without bias (§B.3.1.2), the equation 10 for the C calculation and the equation 14 for the b calculation in the case with bias calculation (§B.3.1.3).

Three other hypotheses are made.

iii. The $\left(R_j^{exp} - R_j^{real}\right)$ and the $\left(R_j^{real} - R_j^{code}\right)$ differences are two independent random variables. That is what allows writing the equation 4 on the sum of variances, and then the expressions of $\bar{\boldsymbol{\alpha}}_{\boldsymbol{j}}$ and $\boldsymbol{C_j}$ resulting from the application of Bayes' theorem (equations 6 and 7). It means that the differences of the code with reality do not depend on the δR_j^{exp} experimental uncertainties. This hypothesis seems quite plausible, in any case more plausible than another hypothesis such as the independence of the $\left(R_j^{exp} - R_j^{real}\right)$ experimental uncertainties with the $\left(R_j^{exp} - R_j^{code}\right)$ differences. It has consequences on the consideration of experimental uncertainties, explained in the §B.3.4.2.

iv. The $\left(R_j^{exp} - R_j^{code}\right)$ differences must be not negligible with respect to the experimental uncertainties. In the opposite case, one will have both $var\left(R_j^{exp} - R_j^{code}\right) \cong 0$ and $var\left(R_j^{exp} - R_j^{real}\right) > 0$. Considering the equation 4, reminded below:

v. $$var(R_j^{exp} - R_j^{code}) = var\left(R_j^{exp} - R_j^{real}\right) + var(R_j^{real} - R_j^{code}) \qquad \textbf{Equation 4}$$

it appears that the calculation of $var(R_j^{real} - R_j^{code})$**,** i.e. the calculation of C, will be difficult since, by definition, a variance is always positive. In this case, CIRCÉ converges with a very high number of iterations to σ_i standard deviations very close to 0. In addition, the r_j residuals (defined in §B.2.3.3) do not follow a standardized normal law *N(0,1)* and the precision of the σ_i, given by the bootstrap (cf. §B.2.3.5), is very bad. All these indications show that CIRCÉ does not really apply in such a case. Fortunately, this case is rarely met: the most frequent configuration is: $\left(R_j^{exp} - R_j^{code}\right) \gg \delta R_j^{exp}$.

vi. It is strongly advisable to have significantly different R_j responses. Theoretically, CIRCÉ can be used even with some dependent responses: for example, in a steady-state, the same quantity at two close locations, or in a transient, the same quantity considered at the same location and at two close times. But it is not really interesting because two dependent responses will be considered by CIRCÉ as only one response, with a double weight. The precision of CIRCÉ results increases with the number of independent responses: consequently, considering too many dependent responses will lead to poor precision of CIRCÉ results.

B.3.3 An improvement of CIRCÉ: "Iterative CIRCÉ"

A simple improvement of CIRCÉ makes it possible to use it, even if the code response-parameter dependence is not linear in the $[0; b]$ domain of variation of the α parameter vector, 0 being the nominal value of α (corresponding with values of the p_i multipliers equal to 1) and b the bias vector found by CIRCÉ. It is "iterative CIRCÉ". The referred iterations are related to the number of times for which CIRCÉ is used and are not those of the E-M algorithm. The principle is explained below:

1) A first CIRCÉ calculation is performed by considering:

$$R_j^{exp},\ R_j^{code}(\boldsymbol{\alpha}=\mathbf{0}),\frac{\boldsymbol{\partial R_j^{code}}(\boldsymbol{\alpha}=\mathbf{0})}{\boldsymbol{\partial \alpha}}$$

that is to say the responses and the derivatives at the nominal point, resulting from a standard use of the system code and of CIRCÉ, so-called "nominal CIRCÉ". A first bias and a first covariance matrix are obtained. They are denoted as $b_{(0)}$ and $C_{(0)}$.*

2) A second CIRCÉ calculation is carried out, by considering this time :

$$R_j^{exp},\ R_j^{code}\left(\boldsymbol{\alpha}=\boldsymbol{b_{(0)}}\right),\frac{\boldsymbol{\partial R_j^{code}}\left(\boldsymbol{\alpha}=\boldsymbol{b_{(0)}}\right)}{\boldsymbol{\partial \alpha}}$$

An increment of the bias, denoted as $\delta b_{(1)}$, and a new $\mathrm{C}_{(1)}$ covariance matrix are obtained. If the process is convergent, the following inequality holds: $\left|\delta b_{(1)}\right| < \left|b_{(0)}\right|$. Let us denote as $b_{(1)}$ the sum $b_{(0)} + \delta b_{(1)}$.

3) The iterative process is continued, by considering:

$$R_j^{exp},\ R_j^{code}\left(\boldsymbol{\alpha}=\boldsymbol{b_{(1)}}\right),\frac{\boldsymbol{\partial R_j^{code}}\left(\boldsymbol{\alpha}=\boldsymbol{b_{(1)}}\right)}{\boldsymbol{\partial \alpha}}$$

A new $\delta b_{(2)}$ increment and a new $C_{(2)}$ covariance matrix are obtained. One must check that $\left|\delta b_{(2)}\right| < \left|\delta b_{(1)}\right|$.

This iterative use of CIRCÉ is stopped when the absolute value of the last bias increment is very low. Generally 3 or 4 iterations are sufficient. Let us denote as *N* the iteration for which the process converges. The final bias is $b_{(N)} = b_{(0)} + \delta b_{(1)} + \cdots \delta b_{(N)}$ and the final covariance matrix is $C_{(N)}$.

With this iterative approach, there is still a hypothesis of linearity, but which is less strong than the hypothesis made with "nominal CIRCÉ". Indeed, instead of assuming that the following relationship, coming from the equation 3, is right, one writes:

$$R_j^{real} - R_j^{code} = R_j^{code}\left(\boldsymbol{\alpha_j}\right) - R_j^{code}(\mathbf{0}) = \frac{\boldsymbol{\partial R_j}(\mathbf{0})^T}{\boldsymbol{\partial \alpha}} \times \boldsymbol{\alpha_j}$$

$$R_j^{code}\left(\boldsymbol{\alpha_j}\right) - R_j^{code}\left(\boldsymbol{b_{(N)}}\right) = \frac{\boldsymbol{\partial R_j}(\boldsymbol{b_{(N)}})^T}{\boldsymbol{\partial \alpha}} \times \left(\boldsymbol{\alpha_j} - \boldsymbol{b_{(N)}}\right)$$

This means that the hypothesis of linearity is made around $\mathrm{b}_{(\mathrm{N})}$ instead of being made around 0.

B.3.4 Detailed description of the user guidelines of CIRCÉ

B.3.4.1 Introduction

A first rapid description of the most important items of these user guidelines can be found in §B.2.3. In the following chapters, the different steps of the guidelines are more deeply explained, and illustrated with the example of §B.2.2, the COTURNE study, as far as possible. Indeed, according to the considered study, some steps may be not addressed: for example, "iterative CIRCÉ" is not used for the COTURNE study. Nevertheless these steps will be mentioned, but without reference to the COTURNE case.

B.3.4.2 Before using CIRCÉ

* The number of an iteration of "iterative CIRCÉ" is denoted with an index, unlike the (m) number of the iteration of the E-M algorithm which is denoted with an exponent (cf. §B.0).

Representativeness of the considered experiment

This step is aimed at checking if the experiment used for the CIRCÉ study is representative of the reactor case for which uncertainty analysis will be performed. The results of the study of the example will be used for small- or intermediate-break LOCA. In COTURNE, the considered experiment, the incondensable gas is nitrogen or helium, gas flow is upward or downward, pressures range from 0.2 to 7 MPa, mean heat flux from 3.5 to 13.5 kW/m^2 and the incondensable mass fraction from 0.0015 to 0.45. These conditions are similar to those of the small- or intermediate-break LOCA provided by Areva to the CATHARE team. It is quite normal since COTURNE was designed to be representative of such reactor transients.

Besides, all the COTURNE tests are kept in the CIRCÉ study, since no test corresponds with conditions not met in the reactor case.

Choice of the responses and the parameters

Generally, the choice of the experimental responses does not pose problem since the user simply considers the measures at his/her disposal. Nevertheless, as written in §B.3.2, the responses must be significantly different. In the case of steady states, one must avoid considering the same quantity at two close locations. This issue is also relevant for transients: one must avoid selecting two responses measured at the same location and at two close times. Considering two responses not really independent is useless: both responses will give the same information. This issue is not relevant for COTURNE: All the tests are steady-state and both considered responses by test are independent since they are considered at two very different locations: gas inlet and middle length of the U-tube.

Besides, the couples responses-parameters must be convenient: each response must be sensitive to, at least, one out of the parameters. More precisely:

- For the responses: A R_j response with the absolute value of all its derivatives, i.e. the $\left|\frac{\partial R_j}{\partial \alpha_i}\right|$ values for i = 1, I, which are close to 0, must be eliminated. Such responses are *a priori* sensitive to parameters not considered in the study and keeping them would result in artificially high σ_i standard deviations.
- For the parameters: The considered parameters must be influential on the retained responses. In this case too, it can be checked via the examination of the absolute value of the derivatives: $\left|\frac{\partial R_j}{\partial \alpha_i}\right|$. A α_i parameter such that, for all the responses (i.e. for j = 1, J), $\left|\frac{\partial R_j}{\partial \alpha_i}\right|$, are close to 0, must be eliminated. Like for the responses, keeping such a parameter would generally result in artificially high σ_i standard deviations.

In the next §B.3.4.3, one will show that CIRCÉ gives other indications in case of not sensitive responses or not influential parameters.

Distribution of the derivative vectors

One reminds that two parameters are considered in this study. The first one, α_1, is related to the heat transfer through the liquid film, the second one, α_2, is related to the Sherwood number describing the steam diffusion through the gas layer rich in incondensable gas. There are 164 responses and consequently 164 derivatives vectors: $\frac{\partial \mathrm{R_j}}{\partial \alpha} = \begin{pmatrix} \frac{\partial \mathrm{R_j}}{\partial \alpha_1} \\ \frac{\partial \mathrm{R_j}}{\partial \alpha_2} \end{pmatrix}$. The extremities of the $\frac{\partial \mathrm{R_j}}{\partial \alpha}$ vectors are plotted below in Figure B.3.

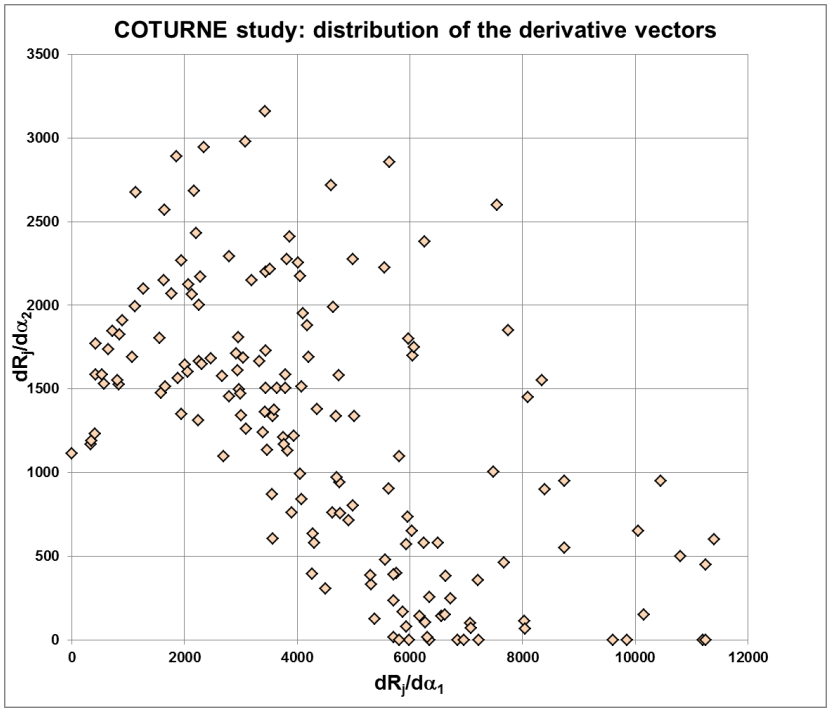

Figure B.3: COTURNE study: distribution of the derivative vectors

The vectors are well distributed in the $\left(\frac{\partial R_j}{\partial \alpha_1}; \frac{\partial R_j}{\partial \alpha_2}\right)$ plane: they are not at all collinear. The problem solved by CIRCÉ is well conditioned. If, in another CIRCÉ study, 3 parameters were for instance considered, this check should be done in the 3 planes: $\left(\frac{\partial R_j}{\partial \alpha_1}; \frac{\partial R_j}{\partial \alpha_2}\right)$, $\left(\frac{\partial R_j}{\partial \alpha_2}; \frac{\partial R_j}{\partial \alpha_3}\right)$ and $\left(\frac{\partial R_j}{\partial \alpha_3}; \frac{\partial R_j}{\partial \alpha_1}\right)$.

One notes also that all the derivatives are in the part of the plane defined by: $\left(\frac{\partial \mathrm{R_j}}{\partial \alpha_1} > 0; \frac{\partial \mathrm{R_j}}{\partial \alpha_2} > 0\right)$. Finding positive derivatives is logical due to the nature of the responses (overall heat transfer coefficients) with respect to that of the parameters. Generally, in a CIRCÉ study, the derivatives have always the same sign for a given α_i parameter, when considering all the R_j^{code} responses.

B.3.4.3 Checks with the first CIRCÉ results ("nominal CIRCÉ")

Choice of the responses and of the parameters

Some guidelines for the choice of the responses and the parameters are already given in §B.3.4.2. The first CIRCÉ results, i.e. without the use of "iterative CIRCÉ", provide complementary indications for this choice.

For the responses: detecting abnormal responses is possible via the observations of the r_j residuals. One recalls that each $(R_j^{exp} - R_j^{code})$ follows a scalar normal law with the following statistical parameters:

- mean value: $\frac{\partial \boldsymbol{R_j}^{\boldsymbol{T}}}{\partial \boldsymbol{\alpha}} \boldsymbol{b}$;
- variance: $\frac{\partial \boldsymbol{R_j}^{\boldsymbol{T}}}{\partial \boldsymbol{\alpha}} \boldsymbol{C} \frac{\partial \boldsymbol{R_j}}{\partial \boldsymbol{\alpha}} + \left(\sigma_j^{exp}\right)^2$.

Consequently the residuals defined by:

$$r_j = \frac{\left(R_j^{exp} - R_j^{code}\right) - \frac{\partial R_j}{\partial \alpha}^T \boldsymbol{b}}{\frac{\partial R_j}{\partial \alpha}^T \boldsymbol{C} \frac{\partial R_j}{\partial \alpha} + \left(\sigma_j^{exp}\right)^2}$$ **Equation 17**

obey a standardized normal law $N(0,1)$. A high absolute value of a given r_j residual, for example more than 2.5 or 3, indicates that the corresponding R_j response should not be retained. Generally, two reasons can explain this behaviour:

- The denominator of the residual is very low; it happens when all the derivatives of this response are also very low: the response is not sensitive to the parameters, for which the CIRCÉ study is performed; the physical reason for that must be found and the response can be eliminated;
- The numerator of the residual is very high. It happens when the $(R_j^{exp} - R_j^{code})$ difference is very high in absolute value, in other words when the code is very bad. In this case too, the reason for that must be found. It can stem from a problem with the experimental sensor. Or there is a bifurcation in the calculation which does not exist in the experiment. In any case, the response can be eliminated only if the high value of the $(R_j^{exp} - R_j^{code})$ difference is explained.

If there are no objective reasons to eliminate a response with a high residual, the response must be kept. The drawback is that such responses result in high σ_i standard deviations: the final variation range of the α_i parameters will be large.

In the COTURNE study, all the residuals are less than 2.5 in absolute value. There is no abnormal response and all of them are considered. That is not the case of all the CIRCÉ studies: looking at the residuals is an important step, which can avoid obtaining no meaningful results.

For the parameters: Really not influential parameters are easily detectable since the derivatives of all the responses with respect to them are close to 0, what can be checked before using CIRCÉ (cf. §B.3.4.2). But in some cases, the consideration of the derivatives shows that one (or more) parameters are significantly less influential than the other ones, but without being really negligible. The question to consider them or not is posed. To answer this question, two CIRCÉ calculations are carried out (a CIRCÉ calculation takes hardly one minute): a calculation with all the parameters and another one without the doubtful parameter(s). CIRCÉ results are compared for the remaining parameters: if the results are close, the doubtful parameters may be eliminated. Decreasing the number of considered parameters has the advantage to result in a better precision of the CIRCÉ results for the remaining parameters.

This issue is not relevant for the COTURNE study, since both parameters are clearly influential, even if the derivatives with respect to α_2 are globally smaller than the derivatives with respect to α_1(cf. Figure B.3). Nevertheless, it can be illustrated via another example. In an experiment studying the heat transfers in the dry zone, four parameters were considered at the beginning of the CIRCÉ study:

- Heat transfer coefficient in film boiling: α_1
- Heat transfer coefficient in vapour forced convection: α_2
- Heat transfer coefficient between interface and vapour phase: α_3
- Interfacial friction for annular flows: α_4

When looking at the derivatives, both first parameters α_1 and α_2 are clearly dominant, but α_3 and α_4 are not negligible. In Table B.1, CIRCÉ results are compared when considering the 4 parameters and when considering only α_1 and α_2:

Table B.1: comparison of CIRCÉ results with all the parameters and with only the two dominant parameters

Parameter	4 parameters		Without α_3 and α_4	
	Bias	Standard deviation	Bias	Standard deviation
Film boiling: α_1	-1.4167	0.0030	-1.2514	0.0024
Forced convection: α_2	-0.0853	0.1383	-0.0865	0.1594
Vapour-interface heat transfer: α_3	0.4558	0.0244	******	******
Interfacial friction: α_4	-0.7708	0.0219	******	******

The bias and the standard deviation of α_1 and α_2 are hardly modified in both cases. Consequently the CIRCÉ study can be done without α_3 and α_4.

The results are quite different if one out of both dominant parameters, $\alpha_1$or α_2, is eliminated (cf. Table B.2). One can note that the bias and the standard deviation of α_3 and α_4 are very different from the case with all the parameters and are abnormally high. The reason for these high values is that CIRCÉ tries to explain the $\left(R_j^{exp} - R_j^{code}\right)$ differences with not really influential parameters.

Table B.2: comparison of CIRCÉ results with all the parameters and with three parameters, not including a dominant parameter

Parameter	4 parameters		Without α_1		Without α_2	
	Bias	Standard deviation	Bias	Standard deviation	Bias	Standard deviation
Film boiling: α_1	-1.4167	0.0030	******	******	-1.6299	0.0036
Forced convection: α_2	-0.0853	0.1383	-0.2552	0.2067	******	******
Vapour-interface heat transfer: α_3	0.4558	0.0244	2.0357	0.044	5.8455	12.8982
Interfacial friction: α_4	-0.7708	0.0219	7.4250	5.8339	16.1122	25.0725

Starting from different $C^{(0)}$ initial matrices

One reminds that the CIRCÉ algorithm converges towards a local maximum of the likelihood (cf. §B.3.1.2). The $C^{(0)}$ initial matrix considered by default by CIRCÉ is the identity matrix. If the CIRCÉ results seem a little bit doubtful, it is advisable to try different initial matrices, what is very easy with the CIRCÉ software. But, up to now, in the CIRCÉ studies made for CATHARE, this precaution always turned out to be useless.

Experimental uncertainties

CIRCÉ can take them into account (see the algorithm in §B.3.1), but not in a conservative way. Indeed, one out of the hypotheses made by CIRCÉ is that the variance of $\left(R_j^{exp} - R_j^{code}\right)$ is the sum of two variances: $\mathrm{var}\left(R_j^{exp} - R_j^{real}\right)$ and $\mathrm{var}\left(R_j^{real} - R_j^{code}\right)$: that is the equation 4. This equation leads to equation 5, reminded below:

$$var(R_j^{exp} - R_j^{code}) = var(e_j) + var\left(\frac{\partial \boldsymbol{R_j}^{\boldsymbol{T}}}{\partial \boldsymbol{\alpha}} \boldsymbol{\alpha_j}\right) = \left(\sigma_j^{exp}\right)^2 + \frac{\partial \boldsymbol{R_j}^{\boldsymbol{T}}}{\partial \boldsymbol{\alpha}} \boldsymbol{C} \frac{\partial \boldsymbol{R_j}}{\partial \boldsymbol{\alpha}} \qquad \textbf{Equation 5}$$

It is apparent in this equation that a part of the variance of $\left(R_j^{exp} - R_j^{code}\right)$ is explained by the experimental uncertainties and the other part by the uncertainty of the α_i parameters, in the form of their C covariance matrix. Consequently, taking into account the experimental uncertainties leads to decrease the terms of C, i.e. the σ_i standard deviations for given $\left(R_j^{exp} - R_j^{code}\right)$ differences. In other words, the higher the experimental uncertainties are, the lower the σ_i standard deviations are.

Consequently, it is advisable to consider a minoring value of the experimental uncertainties, in order to be conservative. If they are badly known, it is even preferable not to consider them at all. Generally, in the CIRCÉ studies performed for CATHARE, considering or not the experimental uncertainties gives quite similar results since the $\left(R_j^{exp} - R_j^{code}\right)$ differences are significantly higher than the experimental uncertainties.

But that was not entirely the case of the COTURNE study. Considering that a minoring value of the experimental uncertainties is roughly 10% of the experimental responses seems plausible. 10% corresponding with two σ_j^{exp} standard deviations, one can write: $\sigma_j^{exp} = 0.05 \times R_j^{exp}$. CIRCÉ results with or without these experimental uncertainties are, C' being the matrix of the standard deviations, deduced from the C matrix:

- with experimental uncertainties: $\boldsymbol{b} = \begin{pmatrix} -0.046 \\ -0.152 \end{pmatrix}, \boldsymbol{C'} = \begin{pmatrix} 0.350 & 0 \\ 0 & 0.290 \end{pmatrix}$ (cf. §B.2.2);
- without experimental uncertainties: $\boldsymbol{b} = \begin{pmatrix} -0.046 \\ -0.129 \end{pmatrix}, \boldsymbol{C'} = \begin{pmatrix} 0.353 & 0 \\ 0 & 0.383 \end{pmatrix}$.

Only the second σ_2 standard deviation is significantly decreased when considering experimental uncertainties, moving from 0.383 to 0.290. But its precision, calculated with the bootstrap, is not excellent and can explain alone the difference between 0.383 and 0.290. Therefore, the finally considered results are with the experimental uncertainties equal to 10% of the experimental responses.

Checking the hypothesis of linearity

One reminds that a hypothesis of linearity between the code responses and the α_i parameters is made by the CIRCÉ algorithm. The CIRCÉ methodology assumes that these α_i parameters depend on the p_i multipliers by two possible formulations: $p_i = 1 + \alpha_i$ and $p_i = exp(\alpha_i)$.

For each α_i parameter, the formulation allowing the best respect of the linearity hypothesis is retained.

More precisely, each α_i parameter is regularly varied in its 95% variation interval found by CIRCÉ, i.e. $[b_i - 2\sigma_i;\ b_i + 2\sigma_i]$. For a given α_i value, both values of the R_j^{code} code responses are calculated with both formulations: they are different since the physical models are multiplied by $1 + \alpha_i$ in a case, by

$exp(\alpha_i)$ in the other case. Consequently the R_j^{code} vs α_i dependence is not the same according to the considered formulation. One out of these two formulations makes it possible to verify the best the hypothesis of linearity and is consequently retained. This check is performed independently for each α_i parameter and for all the responses.

This check can be illustrated with the COTURNE example. The α_1 parameter is firstly considered. Its range of variation $[b_1 - 2\sigma_1;\ b_1 + 2\sigma_1]$ is equal to [-0.75; 0.65] since b_1 = -0.046 and σ_1 = 0.350. The Figure B.4 shows the relationship between some responses and α_1, with the $p_1 = 1 + \alpha_1$ formulation on the left and with the $p_1 = exp(\alpha_1)$ formulation on the right. From both figures, it is apparent that the $p_1 = 1 + \alpha_1$ formulation makes it possible to respect better the linearity between the code responses and the α_1 parameter. This means that the response-p_1 dependence is of linear type, like the response-$\alpha_1$dependence.

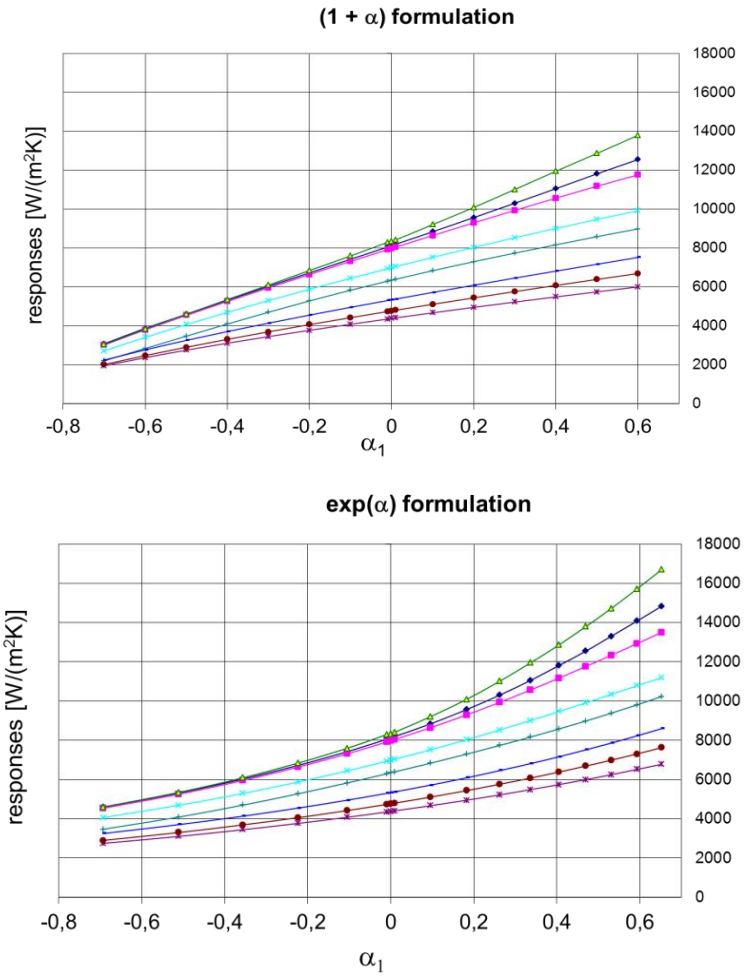

Figure B.4: COTURNE, study of the dependence responses - α_1 parameter

The same check is performed for the α_2 parameter. The range of variation considered for α_2 is $[b_2 - 2\sigma_2;\ b_2 + 2\sigma_2]$ = [-0.73; 0.43] since b_2 = -0.152 and σ_2 = 0.290. Figure B.5 shows the dependence of some typical responses (different from those of Figure B.4) with respect to α_2 with both formulations. This time, the $p_2 = exp(\alpha_2)$ formulation is slightly better than the $p_2 = 1 + \alpha_2$ formulation. It means that the response-p_2 dependence is of logarithmic type

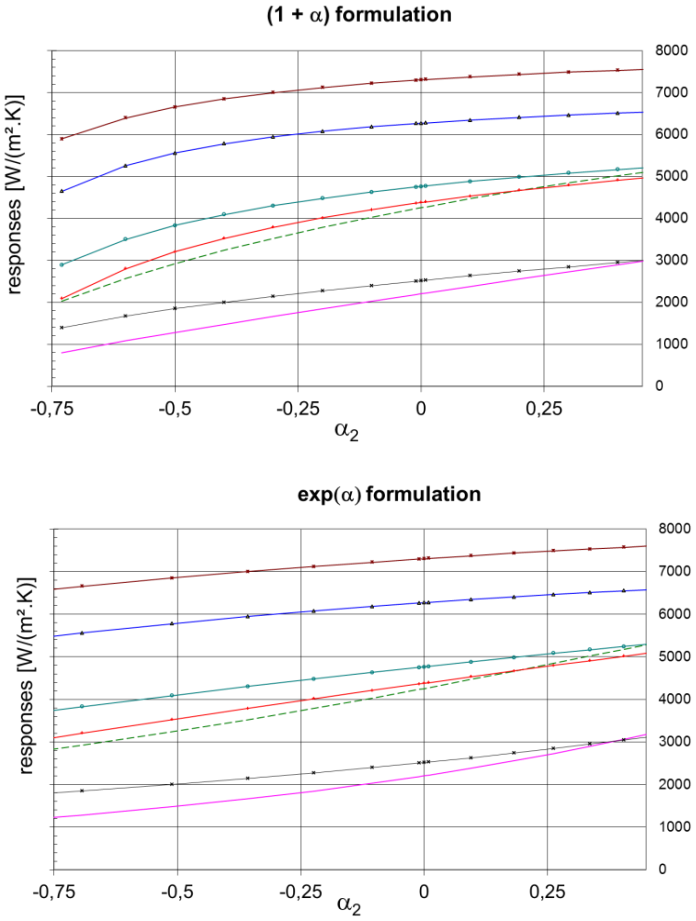

Figure B.5: COTURNE, study of the dependence responses - α_2 parameter

One can note that, in the COTURNE case, with the adequate changes of variable $p_1 = 1 + \alpha_1$ and $p_2 = \exp(\alpha_2)$, the hypothesis of linearity made by CIRCÉ is well verified. This observation is quite general for the CIRCÉ studies performed for CATHARE: there is always one out of both formulations, of linear or exponential type, which makes it possible to respect correctly the hypothesis of linearity. Therefore, this hypothesis is less restrictive that one can think at first sight.

The selection of the better formulation has important consequences for the statistical features of the p_i multiplicative parameters, which are those finally considered. Used alone, the CIRCÉ algorithm provides results only for the α_i parameters. They are converted into results for the p_i parameters with the adequate change of variable $p_i = 1 + \alpha_i$ or $p_i = exp(\alpha_i)$, as shown in Table B.3 for the COTURNE case. As the α_i parameters are assumed to obey a normal law by CIRCÉ, the p_i parameter obeys also a normal law if the $p_i = 1 + \alpha_i$ formulation is retained. If the $p_i = exp(\alpha_i)$ formulation is the best one, the p_i parameter obeys a log-normal law. That is why, in Table B.3, p_1 follows a normal law whereas p_2 follows a log-normal law.

Table B.3: COTURNE: final results resulting from the study of the linearity

	α_i parameters considered by CIRCÉ			p_i multipliers of physical models					
Physical models	b_i	σ_i	95% variation interval	Type of formulation	Type of law	Bias	Explanations for bias	95% variation interval	Explanations for the variation interval
h_{film}	-0.046	0.350	[-0.75; 0.65]	$p_1 = 1 + \alpha_1$	Normal	0.95	$0.95 = 1 - 0.046$	[0.25; 1.65]	0.25=1-0.75 1.65=1+0.65
Sherwood	-0.152	0.290	[-0.73; 0.43]	$p_2 = exp(\alpha_2)$	Log-normal	0.86	$0.86 = exp(-0.152)$	[0.48; 1.53]	$0.48 = exp(-0.73)$ $1.53 = exp(0.43)$

Nevertheless, the choice among both formulations is not always possible and there are cases where the $p_i = ex\,p(\alpha_i)$ formulation is the only one possible, independently of any consideration of linearity. Indeed, one must check that, even if the $p_i = 1 + \alpha_i$ formulation seems the best one, its use does not lead to possible negative values of the p_i multiplier. For that, the lower bound of the 95% variation interval $[b_i - 2\sigma_i;\ b_i + 2\sigma_i]$ of each α_i parameter is compared to -1. If this lower bound, $(b_i - 2\sigma_i)$ *is* less than -1, or even if it is rather close to -1, the $(p_i = 1 + \alpha_i)$ formulation must be strictly rejected. This case occurs with a low or negative bias value or/and a high standard deviation value. If the $(p_i = 1 + \alpha_i)$ formulation was kept, the lowest values of α_i, sampled from the $[b_i - 2\sigma_i;\ b_i + 2\sigma_i]$ interval would correspond with negative values of the p_i multiplier. This result is not physical, since the sign of a physical model cannot change.

Fortunately, it is not the case of α_1 in the COTURNE study, for which the $p_1 = 1 + \alpha_1$ formulation is the best one. This problem was rarely met in the CIRCÉ studies made for CATHARE.

Checking the hypothesis of normality

The normality of the α_i parameters is the second important hypothesis made by CIRCÉ. The individual realizations of the α vector corresponding with each R_j value (i.e. the α_j defined by $R_j^{code}(\alpha_j) = R_j^{real}$, cf. §B.3.1.2) are not known, consequently it is impossible to plot the α distribution. But the hypothesis of normality can be checked with the observation of the r_j residuals (defined in the equation 17, at the beginning of §B.3.4.3). Indeed, if each α_i parameter obeys a normal law, the residuals obey a standardized normal law $N(0,1)$.

Consequently, the empirical distribution of the residuals is plotted and compared with that of $N(0,1)$, as is done in Figure B.6 for the COTURNE study. This distribution is not perfectly that of a normal law, but it is very probably due to the rather low number of residuals (164, as many as responses) and to the choice of the classes of the histogram. Anyway and that is the most important point, other distributions such as the uniform one or the log-normal one would seem even less plausible.

Besides, the mean value of the residuals is 0.024 and their standard deviation is 1.023, therefore close to the 0 and 1 expected values of the theoretical law $N(0,1)$.

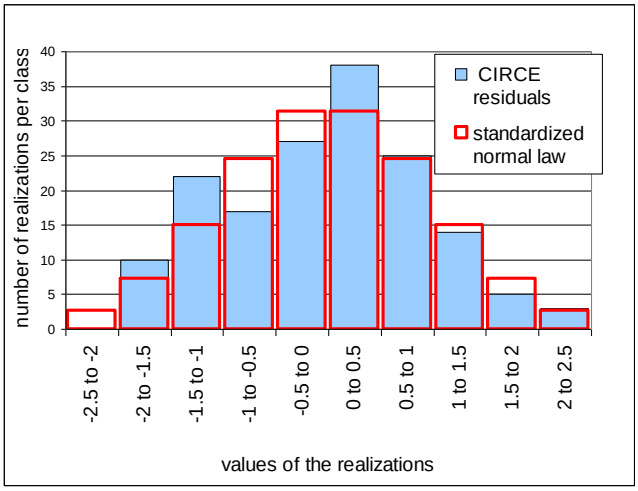

Figure B.6: COTURNE, empirical distribution of the residuals compared with that of the standardized normal law.

Another means to control the normality of the residuals is to plot a quantile-quantile (Q-Q) plot. Explanations for that can be found in any book of statistics. With a Q-Q plot, the definition of the classes, necessary for a histogram and rather arbitrary is no more needed. But a Q-Q plot is less meaningful than a histogram. Classical tests of fitness with $N(0,1)$, such as the Kolmogorov test, are generally too severe due to the limited number of responses.

A last comment is that, in fact, two conditions are needed so that the residuals obey $N(0,1)$: each α_i follows a normal law, but also the R_j^{code} dependence with respect to α_i is linear, since derivatives are a part of the expression of the residuals. Consequently both checks, linearity and normality, are highly connected.

Using or not "iterative CIRCÉ", consequences

"Iterative CIRCÉ" (cf. §B.3.3) must be used if the biases found with "nominal CIRCÉ" are high in absolute value. That is not the case in the COTURNE study because b_1 equals -0.046 and b_2 -0.152. But in the other study mentioned for the choice of parameters, devoted to quantification of the uncertainty of the physical models describing dry-zone heat transfers, the bias on the film-boiling heat transfer coefficient is quite high in absolute value being equal to -1.25 (cf. Table B.1). In this case, "iterative CIRCÉ" is used.

For the first iteration of "iterative CIRCÉ", the R_j^{code} code responses and the $\frac{\partial R_j}{\partial \alpha}$ derivative vectors must be calculated for $\alpha = b_{(0)}$, $b_{(0)}$ being the bias vector found by "nominal CIRCÉ". To this end, the physical models of CATHARE considered by CIRCÉ must be modified. It is done by shifting the value of their p_i multiplicative parameters, equal to 1 for "nominal CIRCÉ". For that, the results of the linearity study must be considered. For example, if, for a given p_i multiplier, the best formulation is $p_i = 1 + \alpha_i$, the physical model will be multiplied by $1 + b_i$ for "iterative CIRCÉ".

During the successive iterations of "iterative CIRCÉ", one cannot change the type of retained formulation for each parameter.

A precaution must be taken in case of $p_i = exp(\alpha_i)$ formulation. Indeed, the derivatives estimated by ASM or finite differences are the $\frac{\partial R_j^{code}}{\partial p_i}$ derivatives, whereas CIRCÉ considers only derivatives with respect to the α_i parameters: $\frac{\partial R_j^{code}}{\partial \alpha_i}$. One can write:

$$\frac{\partial R_j^{code}}{\partial \alpha_i} = \frac{\partial R_j^{code}}{\partial p_i} \times \frac{\partial p_i}{\partial \alpha_i} = \frac{\partial R_j^{code}}{\partial p_i} \times \frac{\partial [\exp(\alpha_i)]}{\partial \alpha_i} = \frac{\partial R_j^{code}}{\partial p_i} \times \exp(\alpha_i)$$

As in "iterative CIRCÉ", α_i is no more equal to 0, but is equal to the b_i bias, $\frac{\partial R_j^{code}}{\partial p_i}$ must be multiplied by $\exp(b_i)$ in order to obtain $\frac{\partial R_j^{code}}{\partial \alpha_i}$.

B.3.4.4 Checks with the final CIRCÉ results

Introduction

The final CIRCÉ results are those of "nominal CIRCÉ", if all the biases calculated with this version of CIRCÉ are low in absolute value. That is the case of the COTURNE study. Otherwise, they are those of "iterative CIRCÉ", after convergence of the bias values.

In both cases, linearity and normality must be checked as explained in the former §B.3.4.3.

In the case of "iterative CIRCÉ", one must check that the formulations $p_i = 1 + \alpha_i$ or $p_i = \exp(\alpha_i)$ (one formulation for each α_i parameter) chosen for the iterations of "iterative CIRCÉ" are always valid: of course, it is impossible to modify them. At the convergence of "iterative CIRCÉ", the values of b_i and σ_i have changed with respect to those found by "nominal CIRCÉ". Consequently, the final $[b_i - 2\sigma_i;\ b_i + 2\sigma_i]$ range of variation to be considered for this check is also modified. In all the CIRCÉ studies performed for CATHARE, the choice of formulation made for each parameter was always confirmed at the convergence of "iterative CIRCÉ".

Some comments on "iterative CIRCÉ"

The following observations can be made for the successive iterations of "iterative CIRCÉ":

The CIRCÉ results are often significantly modified between "nominal CIRCÉ" and the first iteration of "iterative CIRCÉ". After that, they become more stable. A very good convergence is generally obtained after 2, 3 or 4 iterations of "iterative CIRCÉ".

The CIRCÉ algorithm is based on the maximum of likelihood. The logarithm of this likelihood ln(L) is given by the CIRCÉ software at each iteration of "iterative CIRCÉ". One can check that, generally, ln(L) slightly increases during these iterations. Be careful that it can decrease in absolute value, since it is very often negative.

With the $b_{(n)}$ bias value estimated at each (n) iteration of "iterative CIRCÉ", one can calculate:

- The Mean Error defined by $ME = \frac{1}{J}\sum_{j=1}^{J}\left(R_j^{exp} - R_j^{code}\left(\boldsymbol{b}_{(n)}\right)\right)$
- The Mean Square Error defined by $MSE = \frac{1}{J}\sum_{j=1}^{J}\left(R_j^{exp} - R_j^{code}\left(\boldsymbol{b}_{(n)}\right)\right)^2$

Both quantities significantly decrease between "nominal CIRCÉ" and the first iteration of "iterative CIRCÉ". This decrease is less obvious for the other iterations, but generally, at the convergence of "iterative CIRCÉ", one obtains their lowest value: it is an additional criterion to decide that "iterative CIRCÉ" has converged.

Uncertainty analysis using CIRCÉ results: the so-called "bounding" calculations

An uncertainty analysis of the experiment used by CIRCÉ is performed. The outputs are all the responses considered in the CIRCÉ study. The input uncertain parameters are the p_i multipliers, the probability density function (PDF) of which has been estimated by CIRCÉ. This verification is aimed at checking that, with the p_i sampled according to the CIRCÉ results, the experimental responses are inside the ranges of variation found by the uncertainty analysis for the code responses, therefore the name of bounding calculations sometimes used for this uncertainty analysis.

More precisely, *N* code runs of the experiment are performed (typically 100, sometimes more, up to 1000) by varying the values of the p_i parameters according to their PDF. Consequently *N* values of each R_j^{code} response are obtained, and ranked by increasing order:

$$R_j(1) < R_j(2) < \cdots < R_j(N-1) < R_j(N)$$

Order statistics are used to obtain estimations of, for example, the 2.5% and 97.5% percentiles of each R_j^{code} response, respectively denoted as $R_j^{0.025}$ and $R_j^{0.975}$.

In the ideal case where:

- A very high number of responses would be considered, in order to avoid a sampling effect,
- *N*, the number of code runs would be also very high, so that the estimations $R_j^{0.025}$ and $R_j^{0.975}$ would be very precise,

the CIRCÉ results would be validated if both following inequalities were strictly verified:

$R_j^{exp} \leq R_j^{0,025}$ for 2.5% of the responses and $R_j^{exp} \geq R_j^{0,975}$ also for 2.5% of the responses

Practically, as both above conditions (number of responses and of code runs) are not met, one checks that both inequalities are roughly respected.

In the COTURNE case, 93 code runs of the experiment are carried out, for the 164 considered responses. For each R_j response, $R_j(2)$ is an estimation of the 2.5% percentile and $R_j(92)$ an estimation of the 97.5% percentile. The results are:

- There is 1 response such as $R_j^{exp} \leq R_j^{0,025}$, i.e. 0.6% out of the responses.
- There are 7 responses such as $R_j^{exp} \geq R_j^{0,975}$, i.e. 4.3% out of the responses.

The results of the bounding calculations are not perfect, but they can be considered as satisfactory. The situation to be avoided is to have significantly too narrow or too broad $\left[R_j^{0.025}; R_j^{0.975}\right]$ intervals with respect to the R_j^{exp}responses. In addition, the number of responses such as $R_j^{0.025} \leq R_j^{exp} \leq R_j^{0.975}$ is almost perfect, since it equals 95.1%, very close to the theoretical 95%.

The results of the bounding calculations can be presented in the form of Figure B.7. The points $\left(R_j^{exp}; R_j^{0.025}\right)$ and $\left(R_j^{exp}; R_j^{0.975}\right)$ are plotted with respect to the first bisector. Theoretically, 2.5% out of the $\left(R_j^{exp}; R_j^{0.025}\right)$ points must be located under this first bisector, and, in the same way, 2.5% out of the $\left(R_j^{exp}; R_j^{0.975}\right)$ points must be located above it. The 7 responses such as $R_j^{exp} \geq R_j^{0,975}$ are clearly

apparent in this figure, and in a less extent the response such as $R_j^{exp} \leq R_j^{0,025}$. One can note that the 2.5% percentile of rather numerous responses is close to the first bisector.

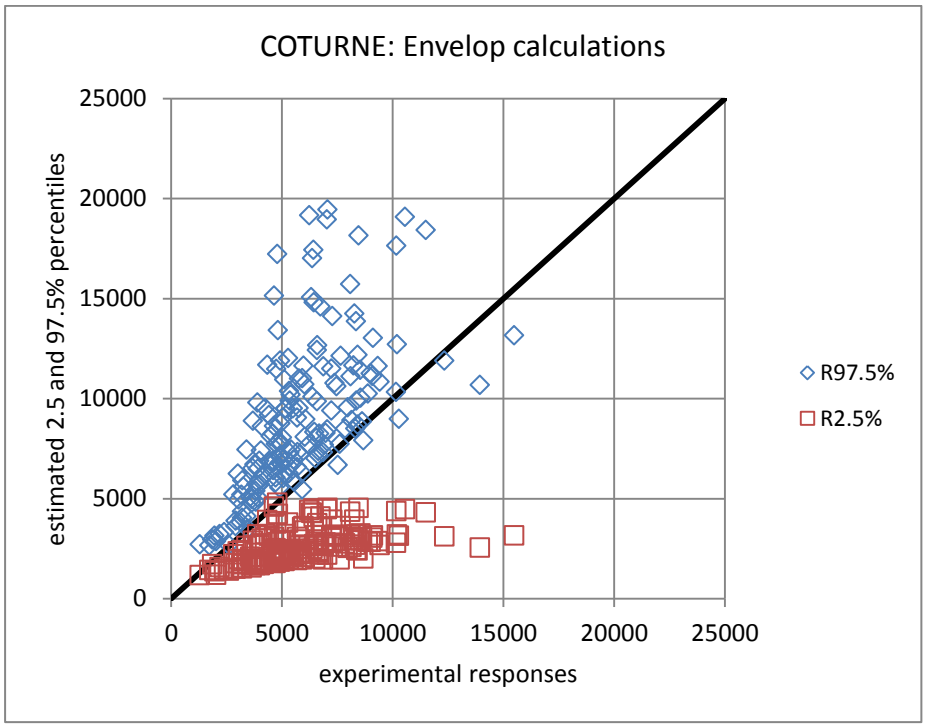

Figure B.7: bounding calculations of the COTURNE experiment

It is important to note that obtaining such good uncertainty-analysis results is not obvious. Bounding analyses were performed with uncertainties given by expert judgment and uncertainties found by CIRCÉ for another experiment than COTURNE. The CIRCÉ results were very satisfactory whereas the code-response ranges of variation coming from expert judgment did not properly bound experimental responses.

These bounding calculations gave always good results for all the CIRCÉ studies performed up to now for CATHARE. They give confidence in the quality of the CIRCÉ algorithm to process data of a given experiment. But they do not give indications on the quality of the CIRCÉ results when applied to another experiment, at another scale, or to the reactor case.

Bounding calculations for PREMIUM must be performed with the experiment used in Phase III, e.g., FEBA: these should theoretically give good results. It is not sure that performing the same kind of bounding calculations will give such good results for Phase IV which uses the PERICLES 2-D reflooding experiment.

Accuracy of the CIRCÉ results thanks to the bootstrap technique

Bootstrap techniques are very usual in statistics to know estimator accuracies. In the CIRCÉ case, the use of such a technique gives the accuracy of both the biases, b_i, and standard deviations, σ_i, of the α_i parameters.

The bootstrap as applied in CIRCÉ lies on the following property: each $(R_j^{exp} - R_j^{code})$ follows a scalar normal law with the following statistical parameters:

- Mean value: $\frac{\partial R_j}{\partial \alpha}^T \boldsymbol{b}$
- Variance: $\frac{\partial R_j}{\partial \alpha}^T \boldsymbol{C} \frac{\partial R_j}{\partial \alpha} + \left(\sigma_j^{exp}\right)^2$ (cf. §B.3.1.3)

Quite a large number of resamples (e.g., 100, denoted as K) of the input data deck of CIRCÉ are generated. Each resample is a fictitious input data deck, with the same derivatives as in the initial CIRCÉ input data deck, but each $(R_j^{exp} - R_j^{code})$ difference being replaced by a realization of $N\left(\frac{\partial R_j}{\partial \alpha}^T b\,;\, \frac{\partial R_j}{\partial \alpha}^T C \frac{\partial R_j}{\partial \alpha} + \left(\sigma_j^{exp}\right)^2\right)$, b and C being the CIRCÉ results.

CIRCÉ is used for each k resample with $k = 1, K$: it provides K values of the b bias vector and of the C covariance matrix, denoted as b^k and C^k.

Finally, statistical features of the b^k and C^k are calculated while considering all the resamples. The mean values of each b_i bias and each σ_i standard deviation can be considered: they must be very close to the b_i and σ_i values found by CIRCÉ with the real input data deck; otherwise the results would be really questionable (which never happened with the CIRCÉ studies for CATHARE. The check of the standard deviations coming from the K b^k and C^k provides more information: the more these standard deviations are low, the better the precision of the b_i and σ_i values found by CIRCÉ with the real input data deck is.

The bootstrap technique was applied to the COTURNE study. Table B.4 shows the standard deviation found by the bootstrap for the biases and standard deviations found by CIRCÉ.

Physical model	h_{film}		Sherwood	
Quantities estimated by CIRCÉ	b_1	σ_1	b_2	σ_2
Value found by CIRCÉ	-0.046	0.350	-0.152	0.290
Corresponding standard deviation found by the bootstrap	0.040	0.025	0.073	0.057

Table B.1: COTURNE, bootstrap results

It is apparent that the accuracy of b_1 and $\sigma_1$related to hfilm is the best one, since the bootstrap gives low standard deviations for both quantities: respectively 0.040 and 0.025. Nevertheless, the accuracy of b_2 and σ_2, for the second parameter, the Sh number, is acceptable. For example, with the bootstrap results, one can affirm that, with the considered responses, σ_2 found for the Sh ranges in the $[0.290 - 2 \times 0.057; 0.290 + 2 \times 0.057 = [0.176\,;\, 0.404]]$ interval. The magnitude of σ_2 is kept. This interval includes also the value of 0.383 found for without taking into account the experimental uncertainties (cf. §B.3.4.3)

The accuracy of the CIRCÉ results, given by the bootstrap is directly connected to the configuration of the derivatives, but again more to the number of considered responses. The higher this number the better the CIRCÉ results accuracy. The indications given by the bootstrap are local, around the b and C estimators found by CIRCÉ. In any case, the bootstrap indicates if these b and C estimators are completely false.

B.4 CIRCÉ FROM A PRACTICAL POINT OF VIEW

B.4.1 Calculation of the derivatives

B.4.1.1 Introduction: $\frac{\partial R}{\partial \alpha}$ and $\frac{\partial R}{\partial p}$ derivatives

CIRCÉ uses first order derivatives of the code responses with respect to the α_i parameters: $\frac{\partial R_j^{code}}{\partial \alpha_i}$. The calculation of these derivatives must be rather precise, especially when using "iterative CIRCÉ": otherwise, the convergence of "iterative CIRCÉ" can be difficult to obtain, due to a too imprecise calculation of the different bias increments $\delta b_{(1)}, \delta b_{(2)}$, etc.

Practically, the calculated derivatives are the $\frac{\partial R_j^{code}}{\partial p_i}$ derivatives, with respect to the p_i multipliers of the physical models. The $\frac{\partial R_j^{code}}{\partial \alpha_i}$ derivatives which are those considered by CIRCÉ, are deduced from $\frac{\partial R_j^{code}}{\partial p_i}$ by considering the retained change of variable $p_i = f(\alpha_i)$ with $f(\alpha_i) = 1 + \alpha_i$ or $f(\alpha_i) = \exp(\alpha_i)$. With both forms of the f function, the following relationship holds: $f'(0) = 1$. It means that, with the simplified notations: p for p_i, α for α_i and R for R_j^{code}, one can write:

$$\frac{\partial R}{\partial \alpha}(\alpha = 0) \quad = \quad \frac{\partial R}{\partial p}(p = 1) \times \frac{\partial p}{\partial \alpha}(\alpha = 0) \quad = \quad \frac{\partial R}{\partial p}(p = 1) \times f'(0) \quad = \quad \frac{\partial R}{\partial p}(p = 1)$$

Consequently, for $\alpha = 0$, i.e. for "nominal CIRCÉ", the $\frac{\partial R_j^{code}}{\partial p_i}$ derivatives are equal to the $\frac{\partial R_j^{code}}{\partial \alpha_i}$ derivatives, and can be directly be used by CIRCÉ.

The problem is different for "iterative CIRCÉ". CIRCÉ needs $\frac{\partial R}{\partial \alpha}$ derivatives for a value of α equal to the b bias found with the previous iterations of "iterative CIRCÉ". One can write:

$$\frac{\partial R}{\partial \alpha}(\alpha = b) \quad = \quad \frac{\partial R}{\partial p}(p = f(b)) \times \frac{\partial p}{\partial \alpha}(\alpha = b) \quad = \quad \frac{\partial R}{\partial p}(p = f(b)) \times f'(b)$$

If the $f(\alpha) = 1 + \alpha$ formulation is chosen, $f'(\alpha) = 1$ for all the α values, including $\alpha = b$, and $\frac{\partial R}{\partial p}$ can be directly used for $\frac{\partial R}{\partial \alpha}$. But with the $f(\alpha) = \exp(\alpha)$ formulation, $f'(b) = \exp(b)$: consequently the $\frac{\partial R}{\partial p}$ derivatives must be multiplied by $\exp(b)$ in order to obtain $\frac{\partial R}{\partial \alpha}$.

B.4.1.2 Adjoint sensitivity method and finite differences

In the CIRCÉ studies performed for CATHARE, the ASM (Adjoint Sensitivity Method) provides the $\frac{\partial R}{\partial p}$ derivatives for simple cases, that is to say if the CATHARE input data deck contains only 1-D modules without reflood or fuel rods with a pressurized gap, which is not the case of the experiments considered for PREMIUM. The main advantage of the ASM is that it calculates the exact derivatives of the code, by combination of different derivatives including those of the Jacobian matrix. A second advantage is that only one ASM calculation is needed whatever the number of considered parameters is.

When using the ASM is not possible, the only solution which does not require specific developments is the approximation of the derivatives by finite differences. It has been the case for numerous CIRCÉ studies

performed for CATHARE. The principle of finite differences is very simple and well-known and requires two calculations for each p parameter, for example, a nominal calculation with $p = p_{nom}$ (= 1 for "nominal CIRCÉ") and a "perturbed" calculation with a value of $p = p_{pert} = p_{nom} + \delta p$, slightly different from $p = p_{nom}$.

An obvious drawback of the finite differences is that numerous calculations are needed if several p_i parameters are considered: at least as many calculations as the number of p_i parameters, plus the nominal calculation. One will even show that, in order to have no doubtful values of each $\frac{\partial R}{\partial p_i}$ derivative, more numerous calculations must be performed. The other drawback is that only approximations of the derivatives are given with this method. Consequently some precautions must be taken in order to have reliable derivatives. They are explained in the next §B.4.1.3. It is important to note that these explanations are only based on the experience gained from CIRCÉ studies performed for CATHARE: in any case they can be considered as universal.

B.4.1.3 General precautions for finite differences

Choice of the δp increment

The first obvious question is the choice of the increment. The first idea coming to one's mind is to take very low increments since $\frac{\partial R}{\partial p} = lim_{\delta p \to 0} \frac{R(p_{nom}+\delta p)-R(p_{nom})}{\delta p}$. But such increments, for example 10-7 or 10-8 for a p multiplier (the nominal value of which is equal to 1) result in a very weak perturbation of the R response, which is of the same magnitude as the noise on R coming from numerical reasons. As a consequence, higher increments, such as ±10-4 or ±10-5, are more advisable, or even ±10-2 if the dependence response-linear is close to a linear dependence.

In any case, it is strongly advisable to estimate $\frac{\partial R}{\partial p}$ with several increments, for example ±10-4 and ±10-5: in order to check that the 4 estimations of $\frac{\partial R}{\partial p}$ are very close, or at least 3 out from 4, for example.

Sequence of the time steps in the nominal and the perturbed calculations

Another difficulty comes from the fact that the sequence of the time steps is not necessarily the same between the nominal calculation and the perturbed calculation. Consequently, the times of the perturbed calculation are different from the times of the nominal calculation. That is not really a difficulty if the tests of the experiment considered by CIRCÉ are of steady-state type, resulting from the stabilization of transients: the time where the responses are considered, at the end of the experiment, is not really relevant. It was for instance the case of the COTURNE study.

But this difficulty must be taken into account in transients such as those encountered in reflood experiments. Let us denote as t_{exp} the time of the experimental response corresponding to R_j^{code}. In both calculations, nominal and perturbed, there is little chance to find a time rigorously equal to this experimental time. But $R(p_{nom}, t_{exp})$ as well as $R(p_{pert}, t_{exp})$ can be estimated by linear interpolation of two adjacent times. $\frac{\partial R}{\partial p}$ is then estimated by $\frac{R(p_{pert},t_{exp})-R(p_{nom},t_{exp})}{p_{pert}-p_{nom}}$.

However this interpolation to t_{exp} is less compulsory if the dependence response-parameter is quasi-linear. Let us denote as t_{nom} the time of the nominal calculation which is the closest one to t_{exp}, and in the same way t_{pert} the time of the perturbed calculation the closest one to t_{exp}. $\frac{R(p_{pert},t_{pert})-R(p_{nom},t_{nom})}{p_{pert}-p_{nom}}$ is an

acceptable approximation of $\frac{\partial \mathrm{R}}{\partial \mathrm{p}}$ because, in a quasi-linear case, rather high values of the increment of the parameter, such as 10-2, or even 10-1 can be used. Consequently $R(p_{pert}, t_{pert})$ is different from $R(p_{nom}, t_{nom})$ especially because both values of the parameter, $\mathrm{p_{pert}}$ and $\mathrm{p_{nom}}$ are significantly different. Comparatively, having different times t_{pert} and t_{nom} has a low influence on the responses.

In other cases, nonlinear, when low increments of the parameter, such as 10-4 or 10-5 must be used, the interpolation to t_{exp} is highly advisable. In addition and if possible, another issue must be considered. The problem is not only that t_{nom} and t_{pert} are different from t_{exp}. More generally, without specific precautions, all the sequence of the time steps is different in the nominal and the perturbed calculations. This difference can affect the value of $R(p_{pert}, t_{pert})$ as much as the difference between $\mathrm{p_{pert}}$ and $\mathrm{p_{nom}}$. The solution chosen for the CIRCÉ studies performed to CATHARE is to impose the sequence of the time steps of the nominal calculation to the perturbed calculation. More precisely, all the time steps of the nominal calculation are saved in a specific file. This file is read for the perturbed calculation in order to impose the time steps of the nominal calculation. This solution is certainly the best one, but it requires specific developments. In addition, imposing the sequence of time steps of the nominal calculation to the perturbed calculation is possible only if both values of the parameter, $\mathrm{p_{pert}}$ and $\mathrm{p_{nom}}$ are very close. In case of high increments, problems of convergence of the perturbed calculation occur when imposing the sequence of time steps of the nominal calculation. But in such a case, as explained above, $\frac{\partial R}{\partial p}$ can be simply approximated by $\frac{R(p_{pert},t_{pert})-R(p_{nom},t_{nom})}{p_{pert}-p_{nom}}$, even if t_{pert} and t_{nom} are different.

Case of a transient with oscillations

Another problem can occur in case of transients, if the response is located on a time trend with oscillations. Such a case was observed in CIRCÉ studies performed for reflood experiments. Figure B.8 illustrates this.

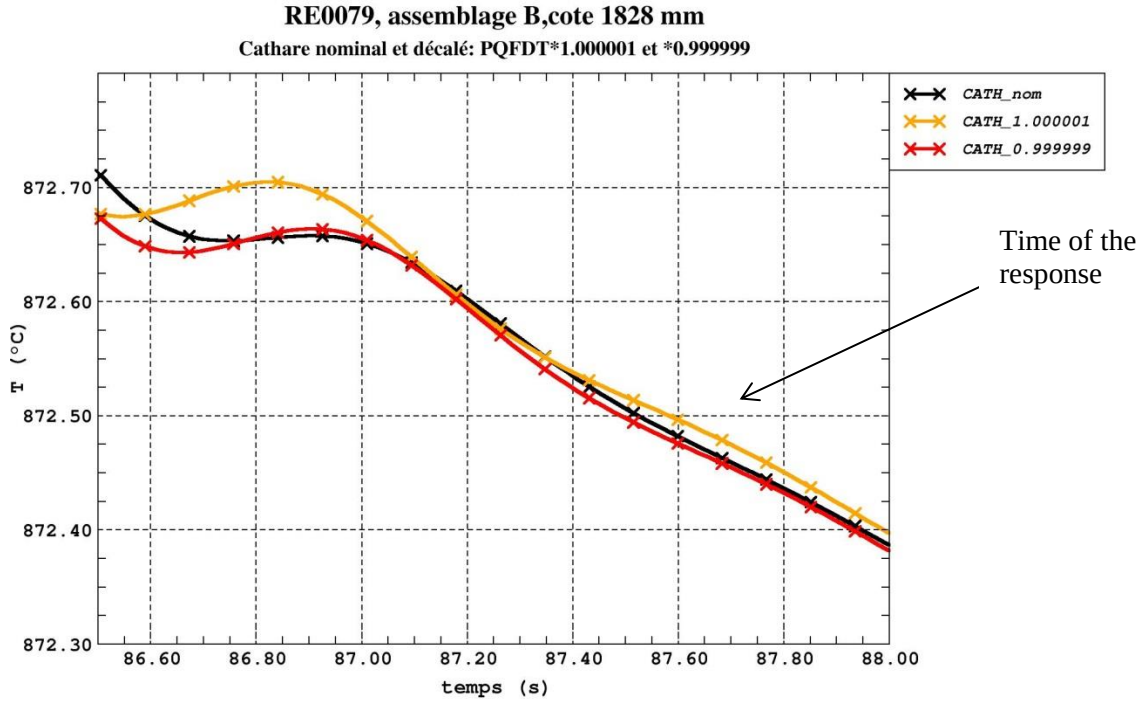

Figure B.8: Nominal and perturbed calculations in a case with oscillations: case of low increments

This figure shows a zoom of the time trend "clad temperature". The nominal calculation is plotted in black. Two perturbed calculations are performed, the sequence of the time steps of the nominal calculation being imposed on both perturbed calculations, as advised above. Both perturbed calculations are carried out with very low increments: an increment equal to $+10^{-6}$ (yellow curve) and another one equal to -10^{-6} (red curve). Finite differences calculated with both increments for a response considered at t_{exp} = 87.6s are strongly different. It is apparent in Figure B.8, since at this time, the difference between the nominal calculation and the calculation performed with $\delta p = +10^{-6}$ is higher than the difference between the nominal calculation and the calculation performed with $\delta p = -10^{-6}$. This difference would be even very much more important if the response was considered before, for instance at 86.8s. This problem comes from the fact that the oscillation of the nominal calculation is duplicated with a shift in the perturbed calculations.

The solution is to consider high increments, even if the problem is not linear. In such a way, the difference between the nominal and the perturbed calculations will mainly come from the increment and not from the shift of the oscillations. In the case presented in Figure B.8, the increments are modified: $\pm 10^{-2}$ values are considered instead of $\pm 10^{-6}$ values. One obtains Figure B.9, plotted for the same case as that of Figure B.8, but with a larger range of variation of the time.

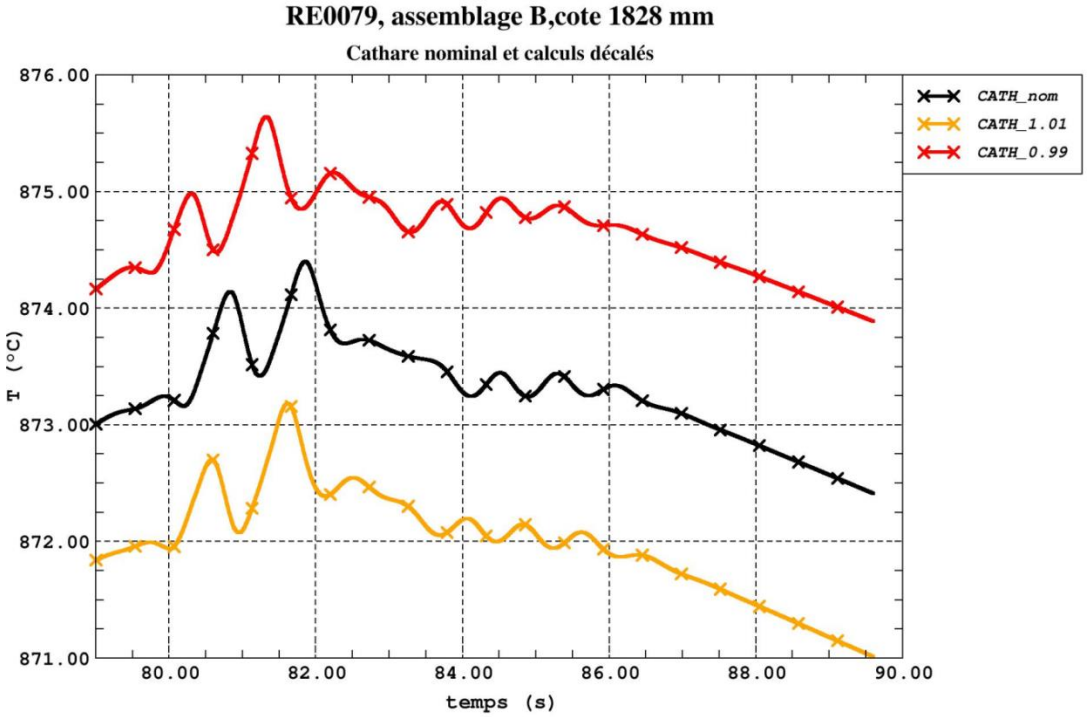

Figure B.9: nominal and perturbed calculations in a case with oscillations: case of high increments

One can note in Figure B.9 that, this time, the difference between the nominal calculation and the calculation performed with $\delta p = +10^{-2}$ has the same magnitude as the difference between the nominal calculation and the calculation performed with $\delta p = -10^{-2}$, at least for the time when the response is considered, i.e., at 87.6s. Consequently both finite differences have the same magnitude. It would be nevertheless less true between 80 and 82s, in the area of the strongest oscillations. If the response was located in this area, it would be advisable to consider still higher increments, for example $\pm 10^{-1}$.

A last comment is that, with such high increments, it is impossible to impose the sequence of time steps of the nominal calculation to the perturbed calculations. Consequently, the only precaution to be taken is to interpolate the code response of all the calculations, nominal and perturbed, at the experimental time, for the calculation of the finite differences.

B.4.2 The CIRCÉ software

It is described only in the case where the C covariance matrix of the α_i parameters is diagonal, i.e. when it is defined by:

$$\boldsymbol{C} = \begin{pmatrix} \sigma_1^2 & \cdots & 0 \\ \vdots & \ddots & \vdots \\ 0 & \cdots & \sigma_I^2 \end{pmatrix}$$

Three programs written in Fortran77 are useful. They are:

- biaisbloc.f for a standard use of CIRCÉ. One reminds that CIRCÉ uses an iterative algorithm which starts from an initial $\boldsymbol{C}$ covariance matrix. In biaisbloc.f, this initial matrix is the identity matrix.
- biaisbloccinitalea.f. In this program, several initial $\boldsymbol{C}$ covariance matrices are automatically generated and CIRCÉ is run for each $\boldsymbol{C}$ initial matrix. For each CIRCÉ run, the software indicates the likelihood of the J $\left(R_j^{exp} - R_j^{code}\right)$ differences, depending on the $\boldsymbol{b}$ and $\boldsymbol{C}$ estimations. At the end of the output file, CIRCÉ indicates what the initial matrix is leading to the maximum likelihood and recalls the $\boldsymbol{b}$ and $\boldsymbol{C}$ estimations found with this initial matrix. Such a program can be useful because the $\boldsymbol{b}$ and $\boldsymbol{C}$ estimations made by CIRCÉ correspond to a local maximum of the likelihood (cf. §B.3.1.2. and §B.3.4.3). If the CIRCÉ results obtained with the standard program biaisbloc.f are odd, it is advisable to use biaisbloccinitalea.f.
- biaisblocbootstrap.f. This program corresponds with the bootstrap which gives the accuracy of each component of the $\boldsymbol{b}$ and $\boldsymbol{C}$ estimations (cf. §B.2.3.5 and the end of §B.3.4.4). The number of resamples is chosen by the user, as well as the number of $\boldsymbol{C}$ initial matrices per resample. Indeed, it is advisable to consider several initial matrices for each resample for the reasons given for the use of biaisbloccinitalea.f.

CIRCÉ works in the Unix environment. Running one out of the three quoted above programs is very simple. It is described for example for biaisbloc.f:

- Compilation: f77 –o biaisbloc biaisbloc.f
- Running : biaisbloc <name_input_data_deck > name_output_file.

B.4.3 The CIRCÉ input data deck

The main feature of a CIRCÉ input data deck is that it is entirely independent of the system code for which CIRCÉ is used. In other words, CIRCÉ works in a stand-alone way.

In this chapter, the CIRCÉ input data deck is rather precisely described. Nevertheless, in its present version, rather numerous keywords are required, whereas they are not really useful. If participants in PREMIUM are interested in using CIRCÉ, CEA will simplify the input data deck by suppressing the useless keywords and will provide an updated description of the CIRCÉ input data deck.

The CIRCÉ input data deck consists in two parts. The first part contains general information, such as the number of considered responses, of parameters, if experimental uncertainties of the responses are taken into account, etc. Its structure depends on the used program: biaisbloc.f, biaisbloccinitalea.f or biaisblocbootstrap.f (cf. previous §B.4.2). For example, in biaisbloccinitalea.f, several initial C matrices are used. Consequently, the number of these initial matrices must be indicated. Or in biaisblocbootstrap.f, the bootstrap is used: the number of resamples must be given in the input data deck.

The second part contains the data really useful for the CIRCÉ algorithm, as shown in Figure B.1 (§B.2.1.2). Consequently, for each R_j response, one will find:

- The R_j^{code} code value;
- The R_j^{exp} corresponding experimental value, measured in the considered experiment;
- The standard deviation of the experimental uncertainty of R_j^{exp}, i.e. σ_j^{exp} with the notations used for the explanation of the CIRCÉ algorithm (cf. §B.3.1.2); if the user prefers not to consider the experimental uncertainties, he/she must enter 0.0 for this σ_j^{exp} standard deviation;
- The derivatives of R_j^{code} with respect to the I parameters, i.e. the I components of the $\frac{\partial R_j^{code}}{\partial \alpha}$ vector.

More precisely, here is an example of a block related to a R_j response:

```
TEMPERAT WALLAX  CRAYONS  41.02000  17  785.17787    772.50000     1.0
   PQFDT   WALLAX  CRAYON      -15.38670
   P1K2FDT WALLAX CRAYON       9.62614
   TOZFDT  THREED  PERC3D      6.67776
```

First line:

- The TEMPERAT keyword indicates the type of response: in the example, it is a temperature.
- The WALLAX and CRAYONS keywords are useless and will be suppressed.
- The 41.0200 value indicates the time when the response is considered.
- The 17 number is the number of the mesh where the response is considered.
- The 785.17787 value is R_j^{code}.
- The 772.50000 value is R_j^{exp} .
- The 1.0 value is σ_j^{exp}.

Following lines:

In this example, three parameters are considered, the names of which, corresponding to the CATHARE syntax, are PQFDT, P1K2FDT and TOZFDT. For each parameter, one finds:

- The name of the parameter, e.g. PQFDT for the first parameter;
- Two useless keywords, e.g. WALLAX and CRAYON for the first parameter, which will be suppressed;
- The value of the derivative of R_j^{code} with respect to the considered parameter, e.g. -15.38670 for the first parameter.

B.4.4 The CIRCÉ output files

The present version of the output files provided by CIRCÉ is in French and will be translated into English if participants in PREMIUM are interested in using CIRCÉ. The information given in this output file is firstly described for the standard module of CIRCÉ, biaisbloc.f. This is:

- Summary of the features of the CIRCÉ input data deck: number of responses for example;
- Number of iterations of the CIRCÉ algorithm;
- The $\boldsymbol{C}$ covariance matrix, i.e. the variances of the α_i parameters;
- The $\boldsymbol{C}'$ matrix of the standard deviations of the α_i parameters, simply deduced from $\boldsymbol{C}$ by calculating the square root of the variances;
- The $\boldsymbol{b}$ bias vector;
- The logarithm of the likelihood of the J $\left(R_j^{exp} - R_j^{code}\right)$ differences;
- For each R_j response, the value of the r_j residuals as defined in equation 17.

For biaisbloccinitalea.f, the same information as that provided by biaisbloc.f, except for the residuals, is given for each CIRCÉ run, performed with a different initial C matrix. At the end of the output file, the results corresponding with the highest value of the likelihood of the J $\left(\mathrm{R_j^{exp}} - \mathrm{R_j^{code}}\right)$ differences are recalled.

The principle of the output file of biaisblocbootstrap.f is the same as that of biaisbloccinitalea.f: CIRCÉ results are given for each C initial matrix of each resample. At the end of the results of each resample, the results corresponding with the highest value of the likelihood of the J $\left(\mathrm{R_j^{exp}} - \mathrm{R_j^{code}}\right)$ differences are recalled. At the end of the output file, the mean value and the standard deviation of each component of the b and C estimations are given.

B.5 CONCLUSION

CIRCÉ is a powerful tool, developed by CEA and devoted to the inverse quantification of the uncertainties of the physical models. It is particularly adapted to intermediate experiments where a limited number of physical models are influential, such as the reflood experiments FEBA or PERICLES considered for the PREMIUM benchmark. The description of the uncertainty of the physical models is of probabilistic type, with the estimation of the mean value and the standard deviation of dimensionless parameters associated with the considered physical models.

CIRCÉ is based on the E-M algorithm, which is very classical in statistics and applied in other fields than thermo-hydraulics. CIRCÉ works in a stand-alone way and can be used for any code, especially a thermo-hydraulic system code such as CATHARE.

All the CIRCÉ studies performed for CATHARE - and they are rather numerous, more than 15 - were successful. Both main hypotheses: linearity and normality, are systematically controlled, and their check gives always satisfactory results. bounding calculations are also performed for each study, and confirm always the CIRCÉ results.

But each CIRCÉ study is rather long, whereas the use of the CIRCÉ software is immediate. The methodology for a correct use of CIRCÉ has been defined during these studies and can partly explain the rather long duration of each study. That is why the part "User's guidelines", described in §B.3.4 must be carefully applied.

But an issue which will always take a long time is the definition of the data to be given in the CIRCÉ input data deck. The choice of the experimental responses can be difficult for transients: they must be sensitive to the studied parameters and independent, while being numerous enough. The estimation of the derivatives by finite differences is another difficulty, still more important. The precautions for estimating

these derivatives are described as precisely as possible in the §B.4.1 and taking these precautions should facilitate the work of a future user. What stays compulsory is the high number of code runs necessary for the estimation of these derivatives, especially if "iterative CIRCÉ" is used.

Improvements of CIRCÉ are possible. A first attempt was carried out by CEA answering an IRSN request: it was aimed at suppressing the hypothesis of linearity. It was possible but by replacing the system code by a meta-model. In any case, quite numerous runs of the system code were necessary. This work was given up because, in the experiments considered for CATHARE, the hypothesis of linearity was generally correctly verified. The issue of the hypothesis of normality was not tackled. Indeed the type of PDF considered in uncertainty analysis, different from normal or log-normal, is often the uniform one, and in this case, the principle of the maximum of likelihood used by the E-M algorithm does no more apply.

In fact, the CIRCÉ results are highly dependent on the choice of the experimental responses: this choice has certainly more influence on the CIRCÉ results than the not rigorous verification of both hypotheses: linearity and normality. It is the main user's effect in the CIRCÉ applications. Another relevant problem is the extrapolability of the CIRCÉ results when considering another experiment or a reactor case, because CIRCÉ is only (inverse) data processing. That is why the confirmation step planned in the PREMIUM benchmark with the reflood 2-D PERICLES tests in addition to the quantification step performed with the FEBA experiment is a true challenge for CIRCÉ.

B.6 ACKNOWLEDGEMENTS

The author, Agnès de Crécy, deeply thanks Didier Girard, statistician from CNRS (Centre National de la Recherche Scientifique), LMC-IMAG, University of Grenoble, for having found that the E-M algorithm solved the problem of inverse quantification of uncertainties considered by CIRCÉ and more generally for his help at the beginning of the CIRCÉ studies.

The author thanks also the different engineers having performed CIRCÉ studies: Thomas Mieusset, Philippe Germain, Vladimir Kalitvianski and especially Pascal Bazin: because he has performed the COTURNE study quoted in this document, but especially for his valuable advice during all the CIRCÉ studies.

ADDENDUM B1: THE PRINCIPLE OF MAXIMUM LIKELIHOOD

The principle of maximum likelihood may be explained in the following way. Let us consider a random variable. It follows a law, the type of which is assumed to be known, but the mean vector and/or the covariance matrix are unknown: the maximum of likelihood gives an estimation of these unknown statistical parameters. In the case of this document, the random variable is the α vector of the parameters associated with the physical models, the law is the multivariate normal one and the unknowns are the b mean vector and the C covariance matrix. As the law is known, it is possible to express the probability density function (PDF) of α as a function of b and C. For example:

$$f(\alpha) = \frac{1}{\sigma\sqrt{2\pi}} \exp - \frac{(\alpha - b)^2}{2\sigma^2}$$, at one dimension ($\boldsymbol{C}$ = one scalar σ^2).

The principle of maximum likelihood provides an estimation of the b and C parameters of the law, by using a sample of the J α_j realizations of the random variable. The likelihood of this sample, denoted as L, is the value of the probability density for the J α_j observed data. Let us denote as $f(\alpha_j)$ the probability associated with α_j. The L likelihood is equal to $\prod_{j=1}^{J} f(\alpha_j)$. It is an explicit function of the b and C unknown

parameters of the law. Their estimation corresponds with the value of b and C which maximizes the L likelihood: they are so that $\frac{\partial \mathrm{L}}{\partial \mathrm{m}}$ and $\frac{\partial \mathrm{L}}{\partial \mathrm{C}}$ are equal to 0.

For example, in the simple case of the normal law with $b = 0$, for which only C has to be to calculated, the equation $\frac{\partial L}{\partial C} = 0$ leads to $\hat{C} = \frac{1}{J}\sum_{j=1}^{J} \alpha_j \, \alpha_j^T$, which is the equation 2 of this document, used by the CIRCÉ algorithm.

ADDENDUM B2: CASE WITH BIAS CALCULATION: COMPARISON OF CIRCÉ ALGORITHM WITH E-M ALGORITHM

The equations for CIRCÉ are extensively presented in §B.3.1.3. One can note that, for the estimation of $C^{(m)}$, CIRCÉ algorithm is simply deduced from the E-M algorithm without bias, thanks to the change of variable $\alpha_j' = \alpha_j - b^{(m-1)}$. But CIRCÉ, which maximizes the likelihood of $(R_j^{exp} - R_j^{code})$ to obtain $\mathrm{b}^{(\mathrm{m})}$, is an approach different from the E-M algorithm. Indeed, in the E-M algorithm, the $b^{(m)}$ value is firstly calculated with the equation 18:

$$\boldsymbol{b^{(m)} = \frac{1}{J}\sum_{j=1}^{J} \overline{\alpha}_j = b^{(m-1)} + \frac{1}{J}\sum_{j=1}^{J} C^{(m-1)} \times \frac{\partial R_j}{\partial \alpha} \times \frac{R_j^{exp} - R_j^{code} - \frac{\partial R_j}{\partial \alpha}^T b^{(m-1)}}{\frac{\partial R_j}{\partial \alpha}^T C^{(m-1)} \frac{\partial R_j}{\partial \alpha} + \left(\sigma_j^{exp}\right)^2}} \qquad \textbf{Equation 18}$$

$\boldsymbol{C^{(m)}}$ is calculated after $\boldsymbol{b^{(m)}}$ thanks to the equation 19:

$$\boldsymbol{C^{(m)} = \frac{1}{J}\sum_{j=1}^{J}\left(\overline{\alpha}_j \overline{\alpha}_j^T + C_j\right) - b^{(m)} b^{(m)T}} \qquad \textbf{Equation 19}$$

With respect to the E-M algorithm, each iteration of the CIRCÉ algorithm can be divided into two steps as described below.

First step, denoted as $(m - 0.5)$. This is aimed at the estimation of $\boldsymbol{b}$ and is the following one:

- $\boldsymbol{C^{(m-0.5)} = C^{(m-1)}}$;
- $\boldsymbol{b^{(m-0.5)}}$ is obtained by exact maximization of the likelihood of the $\left(R_j^{exp} - R_j^{code}\right)$ for the bias calculation. The equations to be considered are those of CIRCÉ (equation 16), but where $\left(\boldsymbol{b^{(m)}; C^{(m)}}\right)$ is replaced by $\left(\boldsymbol{b^{(m-0.5)}; C^{(m-0.5)}}\right)$.

Second step This is aimed at the estimation of $\boldsymbol{C}$. It is exactly an E-M iteration, but defined in $\left(\boldsymbol{b^{(m-0.5)}; C^{(m-0.5)}}\right)$. In other words, for this second step, the considered equations are:
The equations of Bayes' theorem:

- the equation 11 for the $(\overline{\alpha}_j = \overline{\alpha'}_j + \boldsymbol{b^{(m-0.5)}})$ term, with $\left(\boldsymbol{b^{(m-0.5)}; C^{(m-0.5)}}\right)$ instead of $\left(\boldsymbol{b^{(m-1)}; C^{(m-1)}}\right)$;
- the equation 7 for the $\boldsymbol{C_j}$ term, with $\boldsymbol{C^{(m-0.5)}}$ instead of $\boldsymbol{C^{(m-1)}}$;

The equations of the E-M algorithm coming from the maximization of the likelihood:

- equation 18, with $\left(\boldsymbol{b^{(m-0.5)}; C^{(m-0.5)}}\right)$ instead of $\left(\boldsymbol{b^{(m-1)}; C^{(m-1)}}\right)$ in the term on the right;
- equation 19, with $\boldsymbol{b^{(m-0.5)}}$ instead of $\boldsymbol{b^{(m)}}$ in the term on the right.

This assertion can be demonstrated as follows. The bias calculation, corresponding with the first step, is firstly considered.

The linear system (equation 16) solved by CIRCÉ to find the bias can be written in the form of the equation 20, where $\mathrm{b}^{(\mathrm{m})}$ is replaced by $\mathrm{b}^{(\mathrm{m}-0.5)}$ and $\mathrm{C}^{(\mathrm{m})}$ by $\mathrm{C}^{(\mathrm{m}-0.5)}$:

$$\sum_{j=1}^{J} \frac{\frac{\partial R_j}{\partial \alpha} \times \left(R_j^{exp} - R_j^{code} - \frac{\partial R_j}{\partial \alpha}^T \boldsymbol{b}^{(\boldsymbol{m}-\mathbf{0.5})} \right)}{\frac{\partial R_j}{\partial \alpha}^T \boldsymbol{C}^{(\boldsymbol{m}-\mathbf{0.5})} \frac{\partial R_j}{\partial \alpha} + \left(\sigma_j^{exp} \right)^2} = 0 \qquad \textbf{Equation 20}$$

The equation 21 is obtained by multiplying the equation 20 by $\frac{1}{J}\boldsymbol{C}^{(\boldsymbol{m}-\mathbf{0.5})}$:

$$\frac{1}{J}\sum_{j=1}^{J} \boldsymbol{C}^{(\boldsymbol{m}-\mathbf{0.5})} \frac{\frac{\partial R_j}{\partial \alpha} \times \left(R_j^{exp} - R_j^{code} - \frac{\partial R_j}{\partial \alpha}^T \boldsymbol{b}^{(\boldsymbol{m}-\mathbf{0.5})} \right)}{\frac{\partial R_j}{\partial \alpha}^T \boldsymbol{C}^{(\boldsymbol{m}-\mathbf{0.5})} \frac{\partial R_j}{\partial \alpha} + \left(\sigma_j^{exp} \right)^2} = 0 \qquad \textbf{Equation 21}$$

The term on the left of the equation 21 is exactly the same as the $\left(\mathrm{b}^{(\mathrm{m})} - \mathrm{b}^{(\mathrm{m}-0.5)}\right)$ increment of the equation 18 of the E-M algorithm written in $\left(\mathrm{b}^{(\mathrm{m}-0.5)}; \mathrm{C}^{(\mathrm{m}-0.5)}\right)$ instead of $\left(\mathrm{b}^{(\mathrm{m}-1)}; \mathrm{C}^{(\mathrm{m}-1)}\right)$. As the bias is calculated at the first step by its $\mathrm{b}^{(\mathrm{m}-0.5)}$ value, the $\left(\mathrm{b}^{(\mathrm{m})} - \mathrm{b}^{(\mathrm{m}-0.5)}\right)$ increment is equal to 0, what is written by the equation 21.

Let us move to the calculation of the matrix of covariance, corresponding to the second step. Its expression for the E-M algorithm is given by equation 19, where $\mathrm{b}^{(\mathrm{m})}$ is replaced by $\mathrm{b}^{(\mathrm{m}-0.5)}$ since both values of the bias are the same. Consequently, equation 19 is written in the form of equation 22:

$$\boldsymbol{C}^{(\boldsymbol{m})} = \frac{1}{J}\sum_{j=1}^{J}\left(\overline{\boldsymbol{\alpha}}_{\boldsymbol{j}}\overline{\boldsymbol{\alpha}}_{\boldsymbol{j}}^{\boldsymbol{T}} + \boldsymbol{C}_{\boldsymbol{j}}\right) - \boldsymbol{b}^{(\boldsymbol{m}-\mathbf{0.5})}\boldsymbol{b}^{(\boldsymbol{m}-\mathbf{0.5})\boldsymbol{T}} \qquad \textbf{Equation 22}$$

The $\overline{\boldsymbol{\alpha}}_{\boldsymbol{j}}$ mean value of $\boldsymbol{\alpha}_{\boldsymbol{j}}$ is given by the equation 11 written for $\left(\boldsymbol{b}^{(\boldsymbol{m}-\mathbf{0.5})}; \boldsymbol{C}^{(\boldsymbol{m}-\mathbf{0.5})}\right)$:

$$\overline{\boldsymbol{\alpha}}_{\boldsymbol{j}} = \boldsymbol{b}^{(\boldsymbol{m}-\mathbf{0.5})} + \overline{\boldsymbol{\alpha}}_{\boldsymbol{j}}' = \boldsymbol{b}^{(\boldsymbol{m}-\mathbf{0.5})} + \boldsymbol{C}^{(\boldsymbol{m}-\mathbf{0.5})} \times \frac{\partial \boldsymbol{R}_{\boldsymbol{j}}}{\partial \boldsymbol{\alpha}} \times \frac{R_j^{exp} - R_j^{code} - \frac{\partial R_j}{\partial \alpha}^T \boldsymbol{b}^{(\boldsymbol{m}-\mathbf{0.5})}}{\frac{\partial R_j}{\partial \alpha}^T \boldsymbol{C}^{(\boldsymbol{m}-\mathbf{0.5})} \frac{\partial R_j}{\partial \alpha} + \left(\sigma_j^{exp} \right)^2} \qquad \textbf{Equation 23}$$

Let us denote as $\boldsymbol{\delta}_{\boldsymbol{j}}$ the term:

$$\boldsymbol{\delta}_{\boldsymbol{j}} = \boldsymbol{C}^{(\boldsymbol{m}-\mathbf{0.5})} \times \frac{\partial \boldsymbol{R}_{\boldsymbol{j}}}{\partial \boldsymbol{\alpha}} \times \frac{R_j^{exp} - R_j^{code} - \frac{\partial R_j}{\partial \alpha}^T \boldsymbol{b}^{(\boldsymbol{m}-\mathbf{0.5})}}{\frac{\partial R_j}{\partial \alpha}^T \boldsymbol{C}^{(\boldsymbol{m}-\mathbf{0.5})} \frac{\partial R_j}{\partial \alpha} + \left(\sigma_j^{exp} \right)^2} \qquad \textbf{Equation 24}$$

of the equation 23. One can write:

$$\overline{\boldsymbol{\alpha}}_{\boldsymbol{j}} = \boldsymbol{b}^{(\boldsymbol{m}-\mathbf{0.5})} + \boldsymbol{\delta}_{\boldsymbol{j}}$$

with, from the equation 21:

$$\frac{1}{J}\sum_{j=1}^{J} \boldsymbol{\delta}_{\boldsymbol{j}} = \mathbf{0}$$

The equation 22 becomes, by introducing the $\boldsymbol{\delta}_{\boldsymbol{j}}$ increment:

$$\boldsymbol{C}^{(\boldsymbol{m})} = \frac{1}{J}\sum_{j=1}^{J}\left(\boldsymbol{b}^{(\boldsymbol{m}-\mathbf{0.5})} + \boldsymbol{\delta}_{\boldsymbol{j}}\right)\left(\boldsymbol{b}^{(\boldsymbol{m}-\mathbf{0.5})} + \boldsymbol{\delta}_{\boldsymbol{j}}\right)^T + \frac{1}{J}\sum_{j=1}^{J}\boldsymbol{C}_{\boldsymbol{j}} - \boldsymbol{b}^{(\boldsymbol{m}-\mathbf{0.5})}\boldsymbol{b}^{(\boldsymbol{m}-\mathbf{0.5})\boldsymbol{T}} \qquad \textbf{Equation 25}$$

By expanding equation 25, the term:

$$\boldsymbol{b}^{(\boldsymbol{m}-\mathbf{0.5})}\frac{1}{J}\sum_{j=1}^{J}\boldsymbol{\delta}_{\boldsymbol{j}}^{\boldsymbol{T}}$$

and the term:

$$\boldsymbol{b}^{(\boldsymbol{m-0.5})\boldsymbol{T}} \frac{1}{J} \sum_{j=1}^{J} \boldsymbol{\delta_j}$$

appears. These are equal to $\mathbf{0}$, since:

$$\frac{1}{J} \sum_{j=1}^{J} \boldsymbol{\delta_j} = \mathbf{0}$$

Finally, equation 25 becomes the simple equation 26:

$$\boldsymbol{C}^{(\boldsymbol{m})} = \frac{1}{J} \sum_{j=1}^{J} \left(\boldsymbol{\delta_j} \boldsymbol{\delta_j^T} + \boldsymbol{C_j} \right) \qquad \textbf{Equation 26}$$

By replacing δ_j by its value defined in equation 24 and C_j by its value defined in equation 7 written for $C^{(m-0.5)}$, one finds equation 13 of CIRCÉ for $C^{(m)}$. Consequently for the C calculation, each iteration of the E-M algorithm applied to $\left(b^{(m-0.5)}; C^{(m-0.5)}\right)$, is equivalent to a CIRCÉ iteration.

Finally, it is apparent that the only difference between the CIRCÉ and E-M algorithms is the order with which the b bias vector and the C covariance matrix are updated at each iteration. One can check that, at each iteration, the values found for b and C by both algorithms are very close, leading to the same results at convergence.

APPENDIX C: METHODOLOGY FOR THE QUANTIFICATION OF THE INPUT UNCERTAIN PARAMETERS BY THE USE OF THE FFTBM

C.1 OVERVIEW

In the last years various methodologies were proposed to evaluate the uncertainty of Best Estimate (BE) code predictions. The most used method at the industrial level is based upon the selection of input uncertain parameters, on assigning related ranges of variations and Probability Distribution Functions (PDFs) and on performing a suitable number of code runs to get the combined effect of the variations on the results.

The objective of the Post-BEMUSE Reflood Model Input Uncertainty Methods (PREMIUM) benchmark is to progress on the issue of the quantification of the uncertainty of the physical models in system thermal-hydraulic codes, by considering a concrete case: the physical models involved in the prediction of core reflooding.

A methodology to characterize the variation ranges of the input uncertain parameters is proposed in the document in place of the usual approach based (mostly) on engineering judgment. The procedure is based on the use of the Fast Fourier Transform Based Method (FFTBM), already part of the Uncertainty Method based on the Accuracy Extrapolation (UMAE) method and extensively used in several international frameworks.

C.2 GENERAL DETAILS

A methodology to characterize the variation ranges of the input uncertain parameters is proposed in the document in place of the usual approach based (mostly) on engineering judgment. The procedure is based on the use of the Fast Fourier Transform Based Method (FFTBM), already part of the Uncertainty Method based on the Accuracy Extrapolation (UMAE) method and extensively used in several international frameworks.

The general details of the developed methodology are presented hereafter.

C.2.1 Name of the methodology

Methodology for characterizing the range of input uncertainty parameters by the use of the FFTBM.

C.2.2 Involved institutions

The methodology has been developed by San Piero a Grado Nuclear Research Group of University of Pisa (GRNSPG-UNIPI).

C.2.3 Current availability

The methodology is currently available for the application within the framework of "PREMIUM" benchmark. The documentation of the methodology and the associated software must not be disclosed to third parties without written consensus received by GRNSPG.

C.2.4 Brief description of methodology

The proposed methodology is originating from the UMAE methodology [C.4], which focuses not on the evaluation of individual parameter uncertainties but on the propagation of errors by extrapolating the accuracy from relevant experiments to another experiment or a full scale NPP. Within the UMAE, the quantification of the accuracy of code calculations is performed, using the amplitude of the Fourier Transform of the experimental signal and of the difference between this one and the calculated trend. The accuracy of a code calculation can be evaluated through these values, by representing the discrepancies of the addressed calculation with respect to the experimental data with a dimensionless Average Amplitude (AA) which represents the relative magnitude of these discrepancies [C.5][C.6].

The quantification of variation ranges of input parameters for physical models is achieved through running the calculations of reference case of a physical model and "sensitivity" cases, constituted by a single-parameter variation, application of the Fast Fourier Transform Based Method (FFTBM) for quantification of the accuracy of calculated responses respect to experimental data and further comparison of differences between AA values obtained from sensitivity cases and an AA of the reference case. The variation range of an input parameter is derived from the established criteria for maximum allowed deviation of an AA from the reference one [C.7]. A detailed description of the methodology is provided in Section 0.

C.2.5 Advantages and drawbacks

The present methodology proposes a FFTBM-based procedure to characterize the ranges of variation of the input uncertain parameters in place of the usual approach based (mostly) on engineering judgment for the uncertainty methods based on the propagation of input error. The FFTBM tool itself has been validated and applied in the numerous international benchmarks [[C.8], [C.9]. The proposed methodology is independent of an applied thermal-hydraulic system code, as well as of the type of investigated input parameter and analysed responses. The necessary FFTBM software is already developed and ready-to-use.

It should be mentioned that the proposed methodology is based on rather engineering considerations and previous experience from the application of FFTBM than on statistical methods. It worth be noted though, that considering the general poor knowledge of the true nature of statistical distribution of input parameters and coefficients of the physical models, and taking into account the current status of the proposed methodology, a Uniform distribution is assigned to the quantified range of variation of an input parameter.

C.2.6 Details on the possible validation

The FFTBM-based tool for quantification of code calculation accuracy has been previously developed and validated in various applications for thermal-hydraulic calculations including international benchmarks [C.8], [C.9], [C.10], [C.11].

The proposed procedure for quantification of quantification of variation ranges of input uncertainty parameters for physical models has been developed and validated on calculation of two experimental tests performed at Separate Effect Test Facilities Marviken [C.12] and Edward's Pipe [C.13] and an experimental test performed at Integral Test Facility LOBI. The results were presented at the BEMUSE Follow-up meeting and OECD/CSNI Workshop on Best Estimate Methods and Uncertainty Evaluations at

Barcelona, 2011 [C.7] [C.14] . The validation process is currently continuing for a series of SETF and ITF experimental tests.

C.2.7 Overview of code and general/specific software use

The FFTBM is a software package written with FORTRAN 77 Standard. Within the framework of "PREMIUM" benchmark the tool will be available as a standalone executable running under Microsoft Windows environment.

The program capabilities can be summarized as follows:

- Research and extraction of the addressed variables from data files;
- Analysis of several time windows in a same execution, where each time window can identify whatever phase in the transient (optional);
- Time shifting of data trends to analyse separately the effects of delayed or anticipated code predictions concerning some particular phenomena or systems interventions (optional);
- Interpolation of data points to a "power of 2" number of points, coherent with sampling frequency and minimum analysis frequency;
- FFT evaluation of the signals to be processed;
- Evaluation of the *AA* and *WF* quantities;
- Output files generation, including information to be processed by standard software in order to trace any desired graphic concerning data curves, error curves, interpolated curves, FFT signals transforms, FFT data spectra, *AA* - *WF* data (optional).
- Evaluation of the global Average Amplitude (AA_{tot} and WF_{tot} values, see Eq. (10) and (11)) in all the previously considered time windows for the analysed code calculation.

C.3 DESCRIPTION OF METHODOLOGY

C.3.1 The FFTBM tool

The simplest formulation about the accuracy of a given code calculation, with reference to the experimental measured trend, is obtained by the difference function:

$$\Delta F(t) = F_{calc}(t) - F_{\exp}(t) \tag{1}$$

The information contained in this time dependent function, continuously varying, should be condensed to give a limited number of values which could be taken as indexes for quantifying accuracy. This is allowed because the complete set of instantaneous values of ΔF(t) is not necessary to draw an overall judgment about accuracy.

Integral approaches satisfy this requirement, since they produce a single value on the basis of the instantaneous trend of a given function of time. On the other hand, searching for functions expressing all the information through a single value, some interesting details could be lost. Therefore, it would be preferable to define methodologies leading to more than one value in order to characterize the code calculation accuracy.

Information that comes from the time trend of a certain parameter, be it a physical or a derivate one, may be not sufficient for a deep comprehension of a concerned phenomenon; in such a case, it may be useful to

study the same phenomenon from other points of view, free of its time dependence. In this context, the complete behaviour of a system in periodic regime conditions (periodic conditions due to instability phenomena are explicitly excluded), can be shown by the harmonic response function that describes it in the frequency domain.

Furthermore, the harmonic analysis of a phenomenon can point out the presence of perturbations otherwise hidden in the time domain.

C.3.1.1 The FFT algorithm

It is well known that the Fourier transform is essentially a powerful problem solving technique. Its importance is based on the fundamental property that one can analyse any relationship from a completely different viewpoint, with no lack of information with respect to the original one. The Fourier transform can translate a given time function g(t), in a corresponding complex function defined, in the frequency domain, by the relationship:

$$\tilde{g}(f) = \int_{-\infty}^{+\infty} g(t) \cdot e^{-j \cdot 2\pi \cdot f \cdot t} dt \tag{2}$$

Afterwards, it is assumed that the experimental and calculated trends, to which the Fourier transform is applied, verify the analytical conditions required by its application theory; i.e., it is assumed that they are continuous (or generally continuous) in the considered time intervals with their first derivatives, and absolutely integratable in the interval $(-\infty, +\infty)$.

This last requirement can be easily satisfied in our case, since the addressed functions assume values different from zero only in the interval (0, T). Therefore:

$$\tilde{g}(f) = \int_{0}^{T} g(t) \cdot e^{-j \cdot 2\pi \cdot f \cdot t} dt \tag{3}$$

The Fourier integral is not suitable for machine computation, because an infinity of samples of g(t) is required. Thus, it is necessary to truncate the sampled function g(t) so that only a finite number of points are considered, or in other words, the discrete Fourier transform is evaluated. Truncation introduces a modification of the original Fourier transform (the Fourier transform of the truncated g(t) has a rippling); this effect can be reduced choosing the length of the truncation function as long as possible.

When using functions sampled in digital form, the Fast Fourier Transform (FFT) can be used. The FFT is an algorithm that can compute more rapidly the discrete Fourier transform. To apply the FFT algorithm, functions must be identified in digital form by a number of values which is a power of 2. Thus, if the number of points defining the function in the time domain is:

$$N = 2^{m+1} \tag{4}$$

the algorithm gives the transformed function defined in the frequency domain by 2m+1 values corresponding to the frequencies f_n, in which T is the time duration of the sampled signal:

$$f_n = \frac{n}{T} \text{ , where } n = 0, 1, \ldots, 2^m \tag{5}$$

Taking into account the fact that the adopted subroutine packages evaluate the FFT normalized to the time duration T, from Eq. (3) and (5) it can be seen that $|\tilde{g}(0)|$ represents the mean value of the function g(t) in the interval (0,T), while $|\tilde{g}(f_i)|$ represents the amplitude of the i-th term of the Fourier polynomial expansion for the function g(t). Generally, the Fourier transform is a complex quantity described by the following relationship:

$$\tilde{g}(f) = \mathrm{Re}(f) + j \cdot \mathrm{Im}(f) = |\tilde{g}(f)| \cdot e^{j\theta(f)} \tag{6}$$

where:

- Re(f) is the real component of the Fourier transform
- Im(f) is the imaginary component of the Fourier transform
- $|\tilde{g}(f)|$ is the amplitude or Fourier spectrum of g(t)
- θ(f) is the phase angle or phase spectrum of Fourier transform.

It is well known that:

$$|\tilde{g}(f)| = \sqrt{(\mathrm{Re}(f))^2 + (\mathrm{Im}(f))^2}$$
$$\theta(\mathrm{f}) = \mathrm{tg}^{-1}\frac{\mathrm{Im}(\mathrm{f})}{\mathrm{Re}(\mathrm{f})} \tag{7}$$

C.3.1.2 The FFTBM algorithm

The method developed to quantify the accuracy of code calculations is based on the amplitude of the FFT of the experimental signal and of the difference between this one and the calculated trend. In particular, with reference to the error function ΔF(t), defined by the Eq. (1), the method defines two values characterizing each calculation:

- the dimensionless ***Average Amplitude, AA***:

$$\mathrm{AA} = \frac{\sum_{n=0}^{2^m} |\tilde{\Delta}\mathrm{F}(\mathrm{f_n})|}{\sum_{n=0}^{2^m} |\tilde{\mathrm{F}}_{\mathrm{exp}}(\mathrm{f_n})|} \tag{8}$$

- the ***Weighted Frequency, WF***:

$$\mathrm{WF} = \frac{\sum_{n=0}^{2^m} |\tilde{\Delta}\mathrm{F}(\mathrm{f_n})| \cdot \mathrm{f_n}}{\sum_{n=0}^{2^m} |\tilde{\Delta}\mathrm{F}(\mathrm{f_n})|} \tag{9}$$

The AA factor can be considered a sort of "average fractional error" of the addressed calculation, whereas the weighted frequency WF gives an idea of the frequencies related with the inaccuracy.

The accuracy of a code calculation can be evaluated through these values, by representing the discrepancies of the addressed calculation with respect to the experimental data with a point in the WF-AA plane. The most significant information is given by AA, which represents the relative magnitude of these discrepancies; WF supplies different information allowing better identification of the character of

accuracy. In fact, depending on the transient and on the parameter considered, low frequency errors can be more important than high frequency ones, or vice versa.

Trying to give an overall picture of the accuracy of a given calculation, it is required to combine the information obtained for the single parameters into average indexes of performance. This is obtained by defining the following quantities:

$$(\mathrm{AA})_{\mathrm{tot}} = \sum_{\mathrm{i}=1}^{\mathrm{N_{var}}} (\mathrm{AA})_{\mathrm{i}} (\mathrm{w_f})_{\mathrm{i}} \tag{10}$$

$$(\mathrm{WF})_{\mathrm{tot}} = \sum_{\mathrm{i}=1}^{\mathrm{N_{var}}} (\mathrm{WF})_{\mathrm{i}} (\mathrm{w_f})_{\mathrm{i}} \tag{11}$$

With $\sum_{i=1}^{N_{var}} (w_f)_i = 1$ where

- N_{var} is the number of parameters selected (to which the method has been applied)
- $(w_f)_i$ are weighting factors introduced for each parameter, to take into account their importance from the viewpoint of safety analyses.

The need of (wf)i definition derives from the fact that the addressed parameters are characterized among other things by different importance and reliability of measurement. Thus, each (wf)i takes into account of:

- *"experimental accuracy"*: experimental measures of thermal-hydraulic parameters are characterized by a more or less sensible uncertainty due to:
    - intrinsic characteristics of the instrumentation;
    - assumptions formulated in getting the measurement;
    - unavoidable discrepancies existing between experimental measures and the code calculated ones (mean values evaluated in cross-sections, volume centres, or across junctions, etc.);

- *"safety relevance"*: particular importance is given to the accuracy quantification of calculations concerned with those parameters (e.g., clad temperature, from which PCT values are derived) which are relevant for safety and design.

Last, a further contribution is included in the weighting factors definition; this is a component aiming at accounting for the physical correlations governing most of the thermal-hydraulic quantities. Taking as reference parameter the primary pressure (its measurement can be considered highly reliable), a normalization of the AA values calculated for other parameters with respect to the AA value calculated for the primary side pressure is carried out. Doing thusly, the weighting factor for the generic j-th parameter, is defined as:

$$(\mathrm{w_f})_j = \frac{(\mathrm{w_{exp}})_{\mathrm{j}} \cdot (\mathrm{w_{saf}})_{\mathrm{j}} \cdot (\mathrm{w_{norm}})_{\mathrm{j}}}{\sum_{\mathrm{j}=1}^{\mathrm{N_{var}}} (\mathrm{w_{exp}})_{\mathrm{j}} \cdot (\mathrm{w_{saf}})_{\mathrm{j}} \cdot (\mathrm{w_{norm}})_{\mathrm{j}}} \tag{12}$$

and:

$$\sum_{\mathrm{j}=1}^{\mathrm{N_{var}}} (\mathrm{w_f})_{\mathrm{j}} = 1 \tag{13}$$

where:

- N_{var} is the number of parameters to which the method is applied;
- $(w_{exp})_j$ is the contribution related to the experimental accuracy;
- $(w_{saf})_j$ is the contribution expressing the safety relevance of the addressed parameter;
- $(w_{norm})_j$ is component of normalization with reference to the average amplitude evaluated for the primary side pressure.

This introduces a degree of engineering judgment that has been fixed by a proper and unique definition of the weighting factors (see Table C.)). It should be noted that this set of weighting factors has been validated for the application of FFTBM for ITF simulations. The most suitable factor for the definition of an acceptability criterion, therefore, for using the method, is the average amplitude AA. With reference to the accuracy of a given calculation, it has been defined the following acceptability criterion:

$$(AA)_{tot} < K \tag{14}$$

where K is an acceptability factor valid for the whole transient. The lower the $(AA)_{tot}$ value is, the better the accuracy of the analysed calculation (i.e., the code prediction capability and acceptability is higher). On the other hand, $(AA)_{tot}$ should not exceed unity in any part of the transient ($AA = 1$ means a calculation affected by a 100% error). Because of this requirement, the accuracy evaluation should be performed at different steps during the transient.

With reference to the experience gathered from previous application of this methodology, K = 0.4 has been chosen as the reference threshold value identifying good accuracy of a code calculation. In addition, in the case of upper plenum pressure, the acceptable threshold is given by K = 0.1.

Table C.1: selected weighting factors in ITF applications for typical thermal-hydraulic parameters

Parameter	ID	w_{exp}	w_{saf}	w_{norm}
Primary pressure	PP	1.0	1.0	1.0
Secondary pressure	SP	1.0	0.6	1.1
Pressure drops	PD	0.7	0.7	0.5
Mass inventories	MS	0.8	0.9	0.9
Flow rates	FR	0.5	0.8	0.5
Fluid temperatures	FT	0.8	0.8	2.4
Clad temperatures	CT	0.9	1.0	1.2
Collapsed levels	LV	0.8	0.9	0.6
Core power	PW	0.8	0.8	0.5

C.3.2 Quantification of the Ranges of Variation of the Input Uncertain Parameters by FFTBM

A procedure to characterize the boundaries of the input uncertain parameters shall give emphasis to the connection between the ‘objective sources’ of uncertainty [C.9] and the list of input uncertain parameters.

It is worth noting that 'objective sources' of uncertainty and 'suitable lists' of input uncertain parameters should be considered for uncertainty method design and application, respectively. Moreover, both sets of parameters (i.e., 'objective sources' of uncertainty and 'suitable lists') are part of recognized international documents. Namely, reference is made for the sources of uncertainty to an OECD/CSNI (Organization for Economic Cooperation and Development / Committee on the Safety of Nuclear Installations) document issued in 1998 and to a more recent IAEA (International Atomic Energy Agency) document, issued in 2008. The lists of input uncertain parameters are derived from the application of various uncertainty methods in the UMS [C.8] and BEMUSE projects [C.10] completed or nearly completed under the umbrella of OECD/CSNI.

The proposed procedure is based on the use of the FFTBM plus series of considerations as the one here below:

- One single input parameter shall not be 'responsible' for the entire error |exp-calc|, unless exceptional situations to be evaluated case by case;
- Initial guess for Max and Min for variation ranges have to be based on the usual (adopted) expertise;
- More than one experiment can be used per each NPP and each scenario. Highly influential parameters are expected to be the same. The bounding ranges should be considered for the NPP uncertainty analysis;
- A data base of suitable uncertainty input parameters can be created per each NPP and each transient scenario.

Once the facility and the experiment has been chosen based on the selected NPP transient, the main steps of the procedure proposed in Figure C.10 are:

- To run the Reference Case (RC),
- To select the Responses (R),
- To derive the AA_R^{REF} for each selected response by FFTBM,
- To select a set of Input Uncertainty Parameters (IP),
- To run sensitivity cases for which identified input parameter,
- To apply FFTBM to the sensitivity cases to obtain $AA_R^{*,IP}$,
- To apply the criteria for identifying the range [Min, Max],
- To discard not relevant Input Uncertainty Parameters.

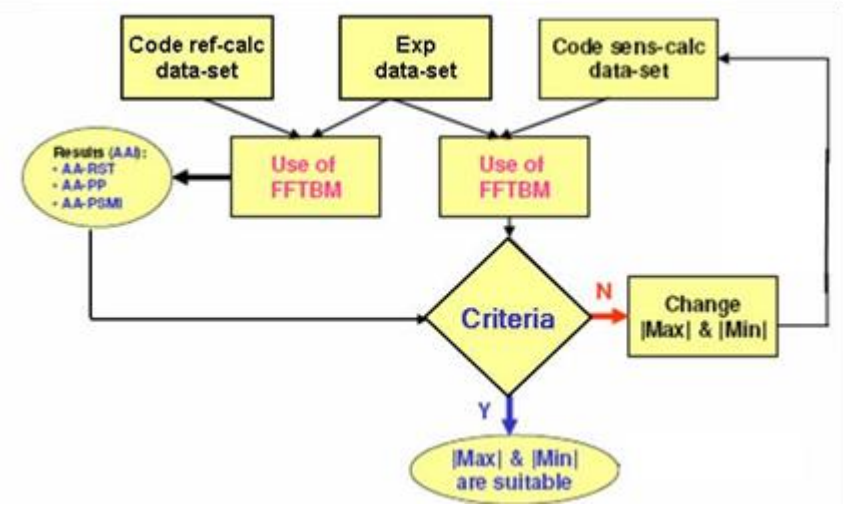

Figure C.10: FFTBM procedure for quantifying the range of variation of input uncertain parameters.

The criteria to be applied for the quantification of the range of the input parameters are presented by Eq. (15), (16) and (17). Each criterion includes a set of statements to be satisfied.

$$\mathrm{AA}_{\mathrm{p}}^{*,\mathrm{IP}} < 0.1 \tag{15}$$

$$\mathrm{AA}_{\mathrm{G}}^{*,\mathrm{IP}} - 1 < \mathrm{T1} \tag{16}$$

$$AA_G^{*,IP} = \sqrt{\frac{\sum_{i=1}^{N}\left(AA_{R_i}^{*,IP}\cdot w_{f_i}\right)^2}{\sum_{i=1}^{N}\left(AA_{R_i}^{REF}\cdot w_{f_i}\right)^2}} \tag{17}$$

where

- w_{f_i} are FFTBM weighting factors;
- *T1* is the acceptability threshold.

The criterion defined by Eq. (15) constitutes the acceptability of code prediction of the pressure in the facility. While the Eq. (16) defines the calculation acceptability based on the global AA, defined by Eq. (17). By specifying the acceptability threshold T1, user defines the range of allowable $AA_G^{*,IP}$ and, therefore, the allowable range of variation of input uncertain parameter. It should be noted that weighting factors w_{f_i} in Eq. (17) are not the same as provided in Table C., which are used for FFTBM application to ITF simulations. Weighting factors w_{f_i} in Eq. (17) are defined and validated at the stage of development of methodology for quantification of the ranges of variation of the input uncertain parameters by FFTBM against a series of experimental tests at SETF.

An example of application of methodology for the Edwards' Pipe standard problem is provided in an Addendum.

C.4 DESCRIPTION OF FFTBM SOFTWARE

The FFTBM is a software package written with FORTRAN 77 Standard. Within the framework of "PREMIUM" benchmark the tool will be available as a standalone executable running under Microsoft Windows environment.

The program capabilities can be summarized as follows:

- Research and extraction of the addressed variables from data files;
- Analysis of several time windows in a same execution, where each time window can identify whatever phase in the transient (optional);
- Time shifting of data trends to analyse separately the effects of delayed or anticipated code predictions concerning some particular phenomena or systems interventions (optional);
- Interpolation of data points to a "power of 2" number of points, coherent with sampling frequency and minimum analysis frequency;
- FFT evaluation of the signals to be processed;
- Evaluation of the *AA* and *WF* quantities;
- Output files generation, including information to be processed by standard software in order to trace any desired graphic concerning data curves, error curves, interpolated curves, FFT signals transforms, FFT data spectra, *AA* - *WF* data (optional).
- Evaluation of the global Average Amplitude (AA_{tot} and WF_{tot} values, see Eq. (10) and (11)) in all the previously considered time windows for the analysed code calculation.

Figure C.2 provides a typical control input deck for FFTBM. FFTBM requires three text files to run:

1. A file containing the experimental data to be analysed. This file shall have the same name specified in the card EXP in the control input deck (file named 'exp.txt' in Figure C.11). An example of this file is given in Figure C.12. The first column shall be the time vectors of the considered parameters, whereas the remaining columns are the addressed experimental quantities for which the FFTBM will calculate the *AA* and *WF*;
2. A file containing the calculated data to be analysed. This file shall have the same name specified in the card *CALC* in the control input deck (file named 'calc.txt' in Figure C.11). This file is similar to the one given for the experimental data in Figure C.12. The first column shall be the time vectors of the considered parameters, whereas the remaining columns are the addressed calculated quantities for which the FFTBM will calculate the *AA* and *WF*;
3. A control input file which specifies how to read the data files and the options selected for evaluating the *AA* and *WF* for each parameter and the AA_{tot} and WF_{tot} for the global calculation. The file name of the input deck shall be 'FFT_(name).txt' where <(name)> can be user defined.

The control input file may consist with 8 types of input cards. Each type of card leads with a unique key word. The keywords are show in

Table C**.2**. The key words shall be written in upper cases.

```
ID          SAMPLE
CALC        C:\FFT\calc.txt
OPTC        1           0
EXP         C:\FFT\exp.txt
OPTE        1           0
FREQ        0.5         0.4
TIME        0           8350
GLOB        1
!
exp01       0.7         0.7         0.5
exp02       0.7         0.7         0.5
exp03       0.7         0.7         0.5
exp04       0.7         0.7         0.5
exp05       0.7         0.7         0.5
exp06       0.7         0.7         0.5
exp07       0.7         0.7         0.5
exp08       0.7         0.7         0.5
exp09       0.7         0.7         0.5
exp10       0.5         0.8         0.5
exp11       0.8         0.9         0.9
exp12       0.8         0.9         0.9
exp13       0.8         0.9         0.9
exp14       0.8         0.9         0.9
exp15       0.8         0.9         0.9
exp16       1.0         1.0         1.0
exp17       1.0         1.0         1.0
exp18       0.5         0.8         0.5
exp19       0.8         0.8         2.4
exp20       0.8         0.8         2.6
exp21       0.8         0.8         2.6
exp22       0.8         0.8         2.6
exp23       0.9         1.0         1.2
exp24       0.9         1.0         1.2
exp25       0.9         1.0         1.2
!
```

Figure C.11: example of the FFTBM control input deck file.

All cards can be written in any order. The exclamation mark, '!', is used as leading of comments. All fields should be put in the line after the key word. The control input file ends with a blank line or EOF. Some cards are mandatory and shall be present in any input deck.

To run FFTBM, user has to prepare the control input file 'FFT_(name).txt' and write 'FFTBM' under DOS window. 'FFT_(name).txt' shall be in the same directory of the 'FFTBM' executable file.

Time	EXP01	EXP02	EXP03	EXP04	EXP05	EXP06	EXP07	EXP08	EXP09	EXP10	EXP11
0.0000	137.8910	22.9386	17.8164	22.9384	17.8167	-157.6476	167.8348	-157.6534	167.8368	0.0000	779.0652
20.3869	135.7021	22.7659	17.8139	22.8202	17.8261	-159.1646	168.3170	-158.8222	168.2850	41.0285	776.4101
42.4513	135.4288	22.6994	17.7491	22.7488	17.7611	-158.4424	167.6662	-158.1380	167.6269	86.3459	771.6105
62.8382	135.1026	22.5124	17.5676	22.5738	17.6178	-155.7657	165.2524	-156.0958	165.6916	121.6904	764.3773
82.9671	133.6754	22.1258	17.2787	22.3979	17.4726	-158.7996	164.9413	-155.3987	164.8729	146.5452	757.5460
103.0960	132.2086	21.2706	16.7911	22.1137	17.3920	-159.3018	162.0400	-157.0495	164.7693	165.4576	759.0745
125.0313	130.1404	20.6943	16.5535	21.4896	17.0766	-160.4408	160.8007	-158.3531	162.7562	185.1451	761.8048
145.4183	128.3211	20.4617	16.5099	20.9648	16.8164	-161.2718	160.5181	-160.7632	161.5618	204.5742	765.2749
165.4181	127.3991	20.4265	16.5270	20.6728	16.6703	-162.1830	160.8967	-161.9476	161.3623	223.5900	768.9066
186.7083	126.8580	20.4133	16.5343	20.5225	16.5936	-162.9829	161.1300	-162.8469	161.3468	244.4142	773.0564
206.7081	125.9606	20.2499	16.4639	20.3135	16.4922	-163.8734	160.7826	-163.7954	160.9659	262.8616	776.9584
226.7080	125.1556	20.0789	16.3834	20.1391	16.4082	-164.8156	160.3677	-164.8009	160.6084	281.7223	781.1909
246.7078	124.5938	19.9436	16.3194	20.0261	16.3536	-165.3593	160.0125	-165.5240	160.3623	300.5313	785.5811
266.7077	124.4071	19.9040	16.2990	19.9941	16.3379	-165.6854	159.9296	-165.8661	160.3286	319.3404	790.1178
286.7075	124.3600	19.9062	16.2981	19.9909	16.3361	-165.9288	159.9114	-166.0345	160.2742	338.0978	794.8123
306.7074	124.4524	19.9425	16.3157	20.0182	16.3488	-165.9831	159.9762	-166.0501	160.2794	356.8551	799.6832
326.7072	124.2242	19.8864	16.2953	19.9431	16.3163	-166.1177	159.1207	-166.0734	159.4684	375.6125	804.7231
346.7071	122.6632	19.5048	16.1026	19.6117	16.1527	-167.7020	158.1432	-167.9860	158.6394	394.2665	809.9583
368.3843	58.4940	25.7186	12.8604	26.1769	13.0634	-36.0842	86.8929	-36.0537	87.7624	414.4708	815.7006
388.5132	46.9275	26.4857	12.6486	27.0882	12.8645	-15.9962	74.1678	-15.7849	75.1632	434.2616	821.5554
409.6744	43.5792	26.6199	12.7529	27.5447	12.8944	-9.9879	69.5087	-10.0238	71.1941	452.4506	827.1812
430.1903	42.1803	28.1691	12.9201	27.8772	12.9487	-7.1430	67.0768	-7.2223	69.3184	471.3113	833.2990
450.3192	41.6524	28.1542	12.9891	28.0490	12.9900	-5.4215	66.2186	-6.2220	68.5048	489.0352	838.9098
470.3191	41.2037	28.4001	13.0442	28.1557	13.0320	-4.5077	65.6274	-5.6777	67.5229	507.3792	844.6746
490.7060	40.8926	28.3764	13.0438	28.1719	13.0376	-4.0366	64.4685	-5.3979	66.2120	526.2399	850.5782
510.7059	40.5796	28.4160	13.0516	28.1499	13.0234	-3.8373	63.0347	-5.1568	65.0513	544.4805	856.3467
531.4799	40.2120	28.3522	13.0335	28.4840	13.0943	-3.6302	61.3961	-4.7474	64.0046	564.3231	862.6861
553.4152	39.9499	28.3797	13.0147	28.5354	13.1149	-3.4645	60.3435	-4.0243	62.7299	582.7704	868.6612
573.6731	39.8292	28.3313	13.0442	28.5685	13.1219	-3.3040	60.7272	-3.3427	61.1081	600.9077	874.5273
594.8343	39.4220	28.2120	13.0685	27.1707	13.0407	-3.0503	62.2258	-2.3139	59.1598	620.3368	880.8629
615.7373	38.8621	27.9425	13.0529	25.2907	13.0707	-3.0814	60.9528	-1.8215	57.8281	638.7325	886.6990
636.3823	38.3907	26.1915	13.0314	25.5013	13.0812	-2.8614	57.6367	-2.7700	57.7037	656.3530	891.2320
656.6403	37.9854	24.5114	12.5322	26.0534	13.0993	-2.7604	55.0543	-3.6304	57.1415	673.9736	[illegible]
677.8014	37.2350	21.8844	12.9669	24.3814	13.1063	-1.1244	53.2757	-3.0032	54.5818	691.9042	[illegible]
698.1883	35.6740	27.8314	13.1574	[illegible]	[illegible]	[illegible]	50.2034	-4.1876	52.2293	703.1172	[illegible]
718.5753	37.0578	28.2395	13.0907				[illegible]	-4.0140	45.5968	718.7226	[illegible]
738.7042	35.0066	25.7691	[illegible]					-13.0664	39.7157	736.1881	[illegible]
759.7363	35.4930	23.3467						[illegible]	41.0784	754.9455	[illegible]
780.6393	34.6879	[illegible]							33.1143	773.1862	[illegible]
800.6392	[illegible]	[illegible]							30.0960	791.5818	[illegible]
[illegible]									[illegible]	802.7432	
										[illegible]	

Figure C.12: example of the file containing the experimental (or calculated) quantities.

Table C.2: keywords of FFTBM control input and their meaning.

INDEX	KEYWORD	MEANING	DEFAULT VALUES
1	ID	Provides the file name of the output file	Mandatory
2	CALC	Specifies the path of calculated data file	Mandatory
3	OPTC	Specifies the number of lines to skip at begin and the numbers of the columns to analyse for the calculated data file	[0 - 0*]
4	EXP	Specifies the path of experimental data file	Mandatory
5	OPTE	Specifies the number of lines to skip at begin and the numbers of the columns to analyse for the experimental data file	[0 - 0*]
6	FREQ	Specifies the minimum frequency of analysis (ffix) and the cut frequency (fcut)	Mandatory
7	TIME	Specifies the starting and ending time of the window	[0 - 0**]
8	GLOB	Specifies the option for the global calculation	0***

* All columns shall be analysed.
** The analysis shall be performed for all transient.
*** No global calculation shall be performed.

The output file consists with 2 blocks: the first contains the echo of the control input file (N_{val} is the number of points used in the interpolation process), the second contains the results of the calculation (i.e., the AA and the WF values for each parameter and the AAtot and WFtot for the global calculation). Figure C.13 shows a typical output file of FFTBM.

The software produces also three plots that are saved in files which names begin with the name contained in the ID card of the input deck and have the following suffixes:

- '_AA.jpg': Figure containing the average accuracy values *AA* for each parameter (Figure C.14);
- '_WF.jpg': Figure containing the weighted frequency values *WF* for each parameter (Figure C.15);
- Figure containing the average accuracy values *AA* as function of the weighted frequency values *WF* (Figure C.16).

```
**************** ECHO OF THE INPUT (15/ 3/2005   17:26) ****************

ID         SAMPLE
FFIX       0.5 Hz
FCUT       0.4 Hz
T_start    0 s
T_end      8350 s
NVAL       4096
File calc  C:\FFT\calc.txt
File exp   C:\FFT\exp.txt

*****************************************************************************

VARIABLES ID           AA           WF      ( wfi    - wexp    wsaf    wnor)

       exp01       1.9351       0.0361     (0.0139 - 0.70    0.70    0.50)
       exp02       0.7369       0.0276     (0.0139 - 0.70    0.70    0.50)
       exp03       0.8516       0.0435     (0.0139 - 0.70    0.70    0.50)
       exp04       0.7291       0.0333     (0.0139 - 0.70    0.70    0.50)
       exp05       0.7918       0.0404     (0.0139 - 0.70    0.70    0.50)
       exp06       0.3256       0.0391     (0.0139 - 0.70    0.70    0.50)
       exp07       1.3854       0.0329     (0.0139 - 0.70    0.70    0.50)
       exp08       0.3307       0.0383     (0.0139 - 0.70    0.70    0.50)
       exp09       1.6172       0.0352     (0.0139 - 0.70    0.70    0.50)
       exp10       0.0353       0.0081     (0.0114 - 0.50    0.80    0.50)
       exp11       0.1755       0.0447     (0.0368 - 0.80    0.90    0.90)
       exp12       0.1829       0.0429     (0.0368 - 0.80    0.90    0.90)
       exp13       0.2026       0.0352     (0.0368 - 0.80    0.90    0.90)
       exp14       0.1562       0.0442     (0.0368 - 0.80    0.90    0.90)
       exp15       0.1115       0.0233     (0.0368 - 0.80    0.90    0.90)
       exp16       0.0749       0.0335     (0.0568 - 1.00    1.00    1.00)
       exp17       0.0582       0.0236     (0.0568 - 1.00    1.00    1.00)
       exp18       0.2815       0.0632     (0.0114 - 0.50    0.80    0.50)
       exp19       0.2121       0.0297     (0.0872 - 0.80    0.80    2.40)
       exp20       0.4587       0.0601     (0.0945 - 0.80    0.80    2.60)
       exp21       0.2651       0.0525     (0.0945 - 0.80    0.80    2.60)
       exp22       0.0550       0.0259     (0.0945 - 0.80    0.80    2.60)
       exp23       0.6095       0.0196     (0.0613 - 0.90    1.00    1.20)
       exp24       0.7799       0.0103     (0.0613 - 0.90    1.00    1.20)
       exp25       0.6040       0.0155     (0.0613 - 0.90    1.00    1.20)

GLOBAL FACTORS     0.3770       0.0340
```

Figure C.13: example of the FFTBM output file.

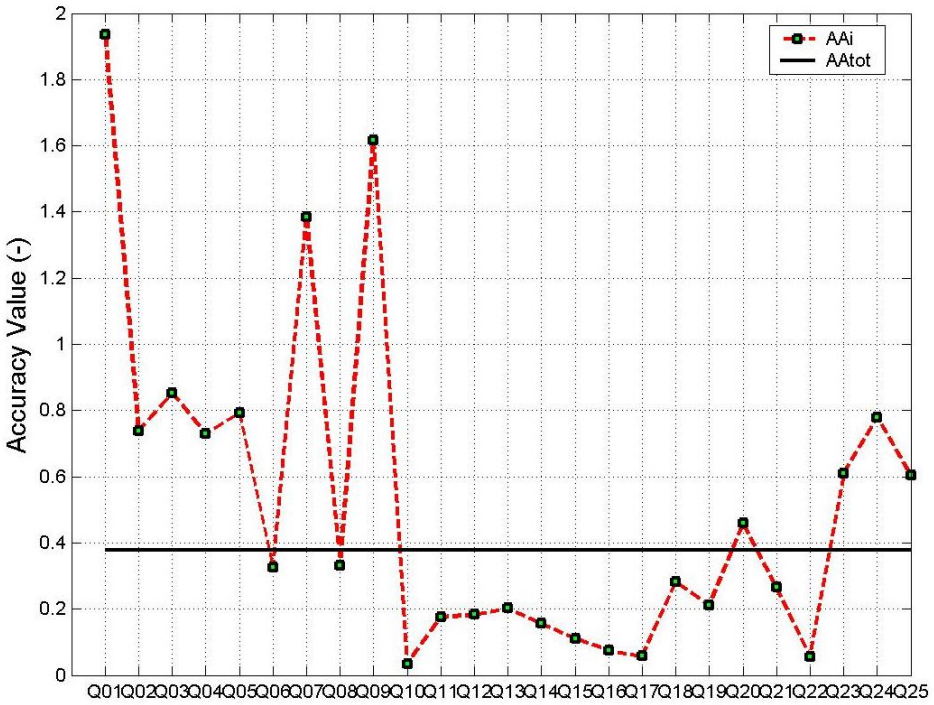

Figure C.14: example of average-accuracy values, AA, for each parameter.

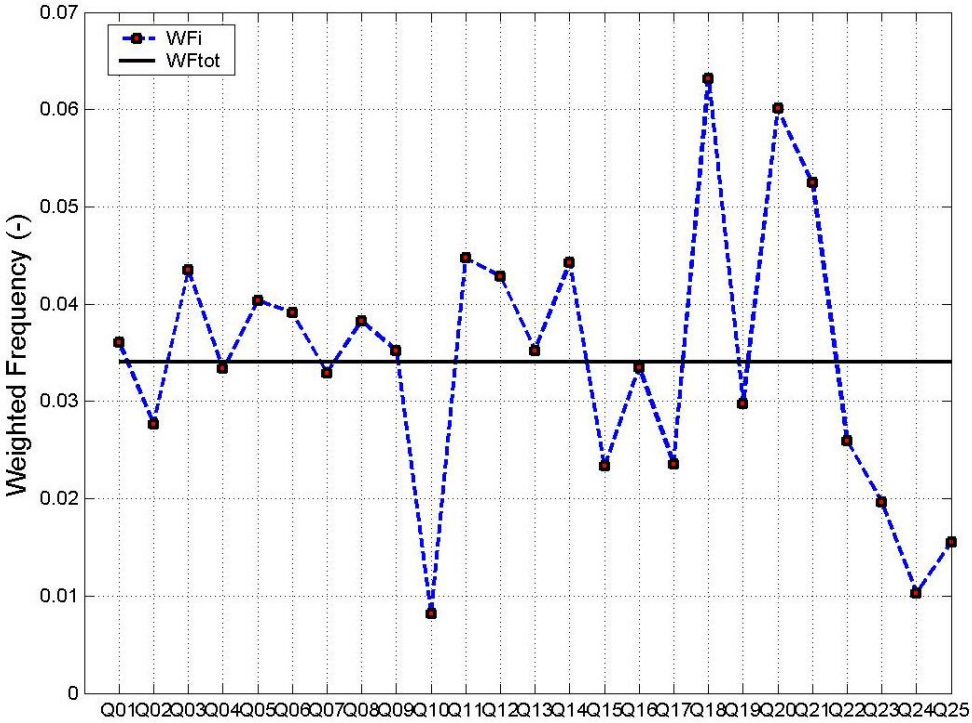

Figure C.15: example of weighted-frequency values, WF, for each parameter.

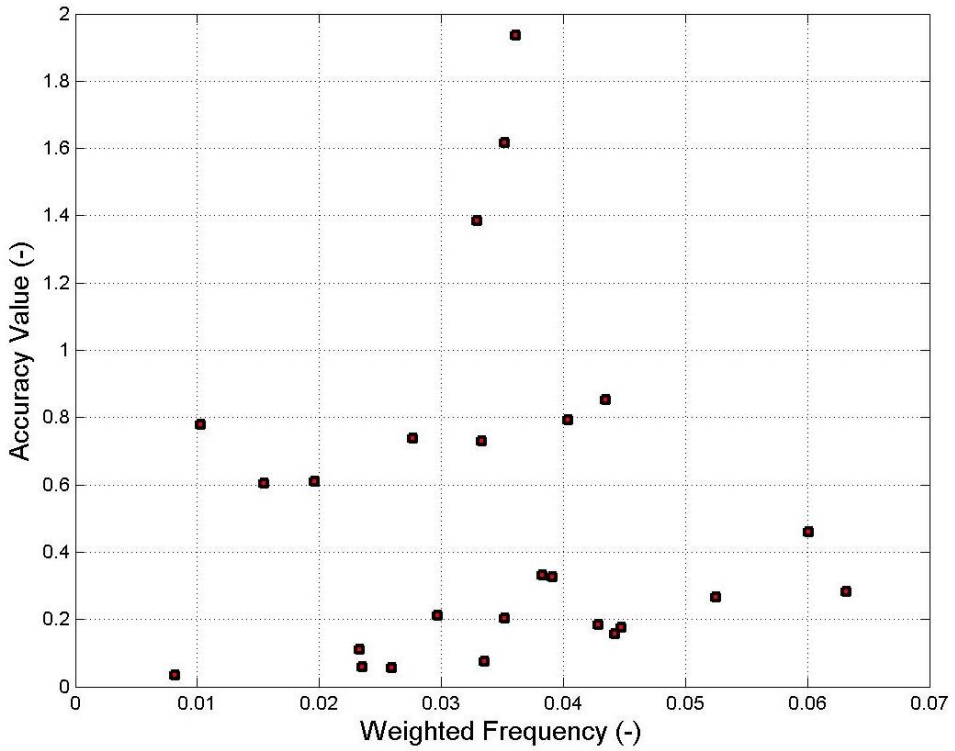

Figure C.16: example of average-accuracy values, AA, as a function of the weighted-frequency values, WF.

C.5 REFERENCES

[C.1] N. Aksan, R. Pochard, H. Glaeser, F. D'Auria, A. Sjöberg, C. Richards, *CSNI Separate Effecst Test Matrix for Thermal-Hydraulic Code Validation,* NEA/CSNI/R(93)14, September 1993.

[C.2] Annunziato A., H. Glaeser, J. Lillington, P. Marsili, C. Renault, A. Sjöberg, *CSNI Integral Test Facility Validation Matrix for the Assessment of Thermal-Hydraulic Codes for LWR LOCA and Transients*, NEA/CSNI/R(96)17, July 1996.

[C.3] A. Kovtonyuk, A. Petruzzi, F. D'Auria, *Details of the FFTBM method for PREMIUM Phase – III*, PREMIUM Coordination Meeting, Pisa, Italy, October 2011.

[C.4] D'Auria F., Debrecin N., Galassi G. M., *Outline of the Uncertainty Methodology based on Accuracy Extrapolation (UMAE*), J. Nuclear Technology, 109, No 1, pp 21-38 (1995).

[C.5] Leonardi M., D'Auria F., Pochard R., *The FFT based method in the frame of the UMAE*, Spec. Workshop on Uncertainty Analysis Methods, London, March 1994.

[C.6] Ambrosini W., Bovalini R., D'Auria F., *Evaluation of accuracy of thermalhydraulic code calculations*, J. Energia Nucleare,vol. 2, 1990.

[C.7] A. Petruzzi, A. Kovtonyuk, M. Raucci, D. De Luca, F. Veronese and F. D'Auria, *A procedure for characterizing the range of input uncertainty parameters by the use of the FFTBM*, OECD/CSNI Workshop on Best Estimate Methods and Uncertainty Evaluations, Barcelona, Spain, 16-18 November 2011.

[C.8] Wickett T., D'Auria F., Glaeser H. et al, *Report of the Uncertainty Method Study for Advanced Best Estimate Thermalhydraulic Code Applications*" OECD/NEA/CSNI R (97) 35, I and II, June 1998.

[C.9] Petruzzi A., D'Auria F., *Thermal-Hydraulic System Codes in Nuclear Reactor safety and Qualification procedures*, Science and Technology of Nuclear Installations, ID 460795, 2008.

[C.10] OECD/NEA/CSNI*, BEMUSE Programme. Phase 3 report "Uncertainty and Sensitivity Analysis*

of the LOFT L2-5 experiment", OECD/CSNI Report NEA/CSNI/R(2007)4.
[C.11] A. Del Nevo, E. Coscarelli, A. Kovtonyuk, F. D'Auria, *Analytical Exercise On OECD/NEA/CSNI PKL-2 Project Test G3.1: Main Steam Line Break Transient In PKL-III Facility Phase 2: Post-Test Calculations,* TH/PKL-2/02(10) Rev. 1, Universita di Pisa, Pisa, March 2011.
[C.12] C. Queral, J. Mulas, C.G. de la Rua, *Analysis of the RELAP5/MOD3.2.2beta Critical Flow Models and Assessment Against Critical Flow Data from the Marviken Tests,* NUREG/IA-0186, US NRC, Washington DC, July, 2000.
[C.13] OECD/NEA/CSNI, *International Standard Problems (ISP),* OECD/CSNI Report NEA/CSNI/R(97)3.
[C.14] *A. Kovtonyuk, A. Vanni, A. Petruzzi, F. D'Auria et al., Use of FFTBM for Characterizing Input Uncertainty Parameter Ranges, OECD/NEA/CSNI meeting to address BEMUSE Follow-up, Barcelona, April 2011.*

ADDENDUM C1: Sample of Application of the Methodology

In this Addendum the summary of the results achieved for the "Edwards' pipe" standard problem is provided. This problem contains many features of the depressurization and blowdown of an initially subcooled liquid that occur in a reactor system postulated loss of coolant accident. The water in the pipe has an initial pressure of 7.0 MPa and a temperature of 502 K which corresponds to an initial subcooling of 56.8 K. The transient is initiated by the rupture of a bursting disk allowing the rapid discharge to the environment at atmospheric pressure. The pressure of the environment was atmospheric pressure (0.1 MPa).

This experiment cover a wide spectrum of physical phenomena involved at different geometrical scales. The two principal phenomena which are observed are: 1. depressurization; 2. flashing.

The first 10ms of the transient are characterized by the propagation of a rarefaction wave from the opening end into the pipe and the reflection of the wave at the closed end of the pipe where a distinct undershoot of the pressure occurs. During the later phase of the blowdown the depressurization is controlled by the strong evaporation (flashing) of the liquid phase.

A nodalization for the RELAP5/Mod3.3 system thermal-hydraulic code has been developed. The sketch of the nodalization and the boundary conditions of the experiment are given in Figure C.17. The responses of interest are the pressure and the void fraction measured at about middle length of the pipe. The results of reference case calculation are provided on Figure C.18 and Figure C.19.

The input parameters that have been initially investigated were about 10. Through the use of the FFTBM, the input parameters that determine a little variation of AA values in correspondence of large variations of those parameters were discharged (e.g., the pipe roughness and the thermal non-equilibrium constant in the Henry-Fauske critical flow model). Finally the analysis was reduced to investigate the following input parameters:

- Form loss coefficient (Kloss) at the break,
- Initial fluid temperature,
- Break area,
- "Henry‑Fauske" choked-flow model, discharge coefficient.

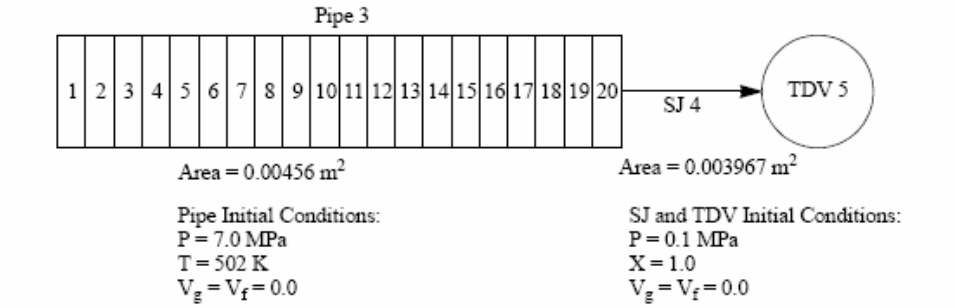

Figure C.17: nodalization and boundary condition of the Edwards' pipe model.

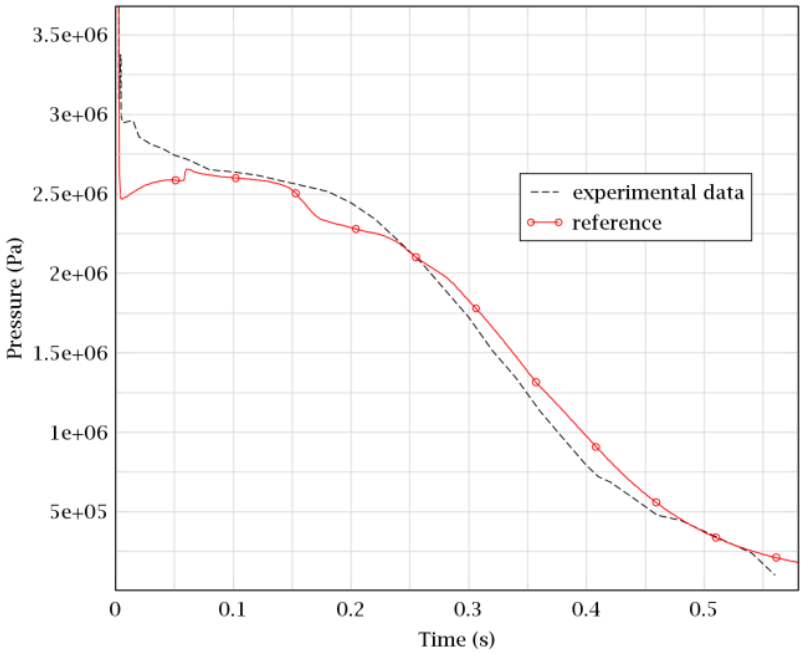

Figure C.18: Edwards' pipe pressure predicted by reference case model.

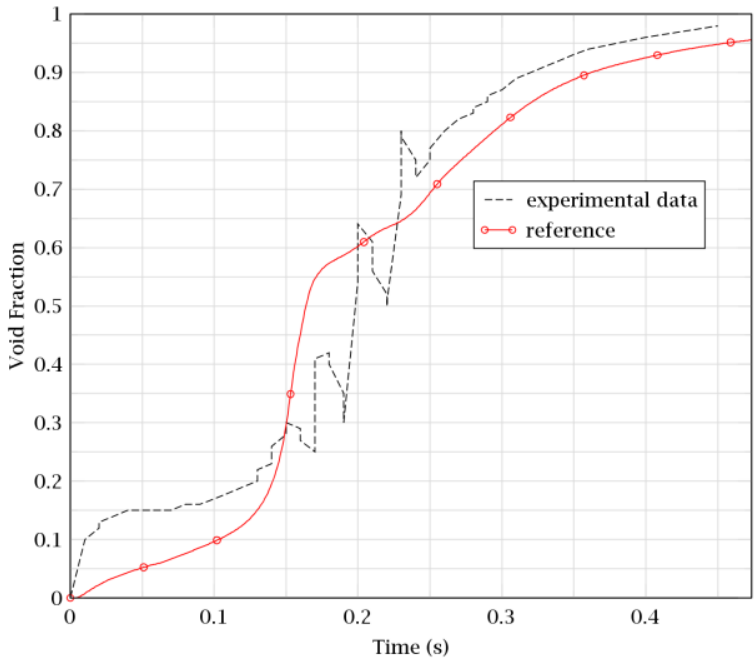

Figure C.19: Edwards' pipe void fraction predicted by reference case model.

Figure C.20 shows the results of the application of the FFTBM procedure in relation with the acceptability criterion defined by Eq. (15) (i.e., $AA_p^{*,IP} < 0.1$) for the four selected input parameters. The attention shall be focused on the AA value for the pressure (AAP) and its limit equal to 0.1. The corresponding ranges of variation [Min(IP), Max(IP)]a for each of the four input parameters satisfying the criterion defined by Eq.(15) are then identified.

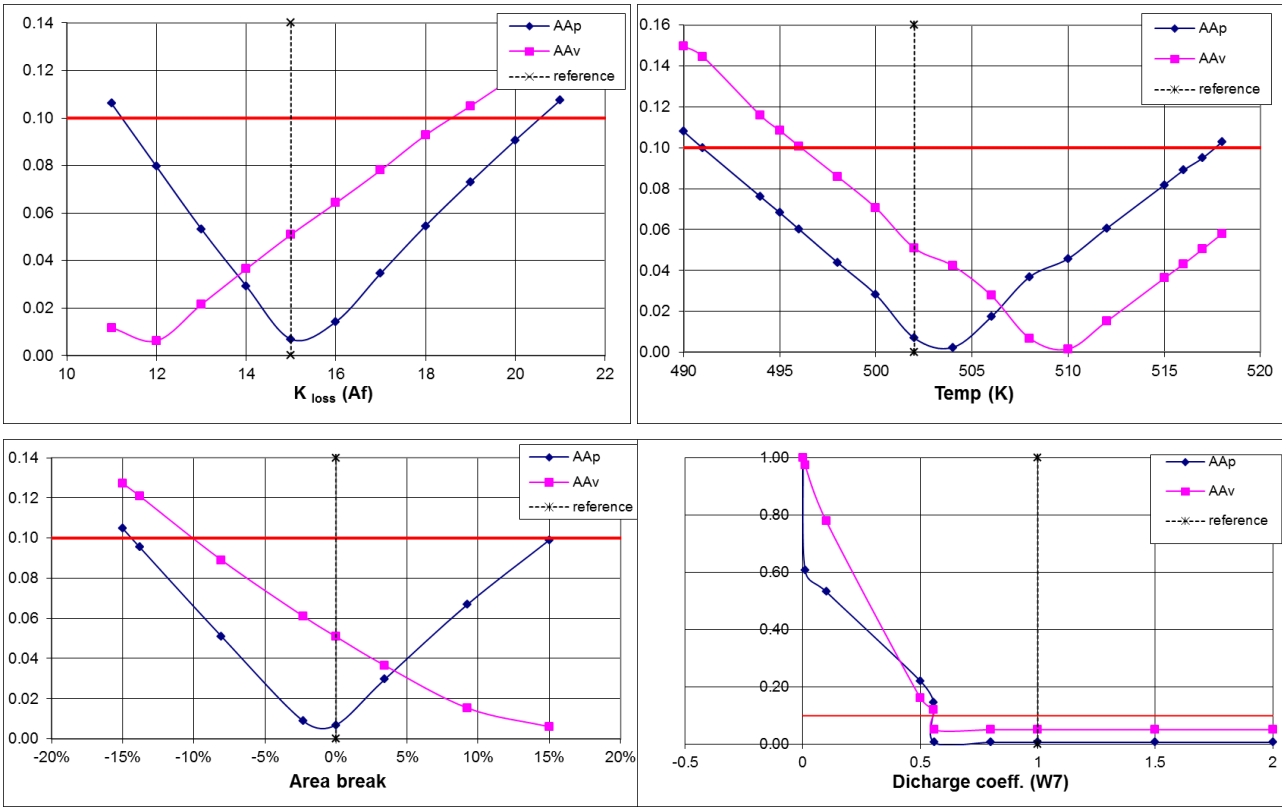

Figure C.20: values of AA_P and AA_V and ranges of variation of input parameters.

The further step is the calculation of the global AAG and application of the acceptability criterion. In the case of the considered experiment and responses of interest (pressure and void fraction), the Eq. (17) can be rewritten as:

$$AA_G^{(*)} := \sqrt{\frac{\left(AA_p^{(*)} \cdot \left(w_f\right)_p\right)^2 + \left(AA_v^{(*)} \cdot \left(w_f\right)_v\right)^2}{\left(AA_p^{(ref)} \cdot \left(w_f\right)_p\right)^2 + \left(AA_v^{(ref)} \cdot \left(w_f\right)_v\right)^2}} \qquad (18)$$

The calculated according to the Eq. (16) values $(AA_G^{*,IP} - 1)$ for three input parameters of interest are shown on Figure C.21 through Figure C.23 together with different threshold limits T1. The discharge coefficient for Henry-Fauske has been discarded from the analysis since there are no significant variations of AAP and AAV in the reasonable limits of variation of the coefficient (see Figure C.20).

Specifying the threshold limit as T1=2, the range of variation of each input uncertain parameter is obtained and provided in Table C.3.

Table C.3: quantified ranges of variation of input parameters for Edwards' pipe problem

Parameter	Variation range
Break area	± 3%
Kloss at the break	± 7%
Initial fluid temperature	± 3K

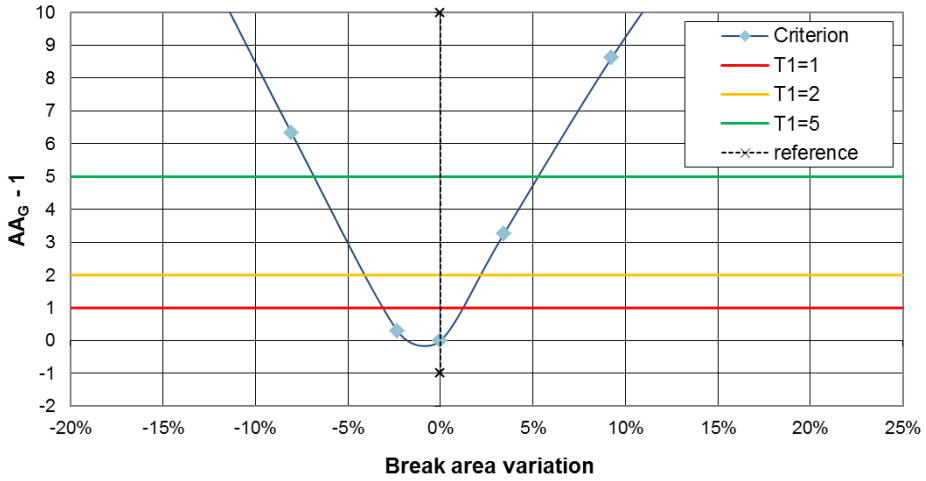

Figure C.21: calculated AA_G for break area variation of Edwards' pipe model.

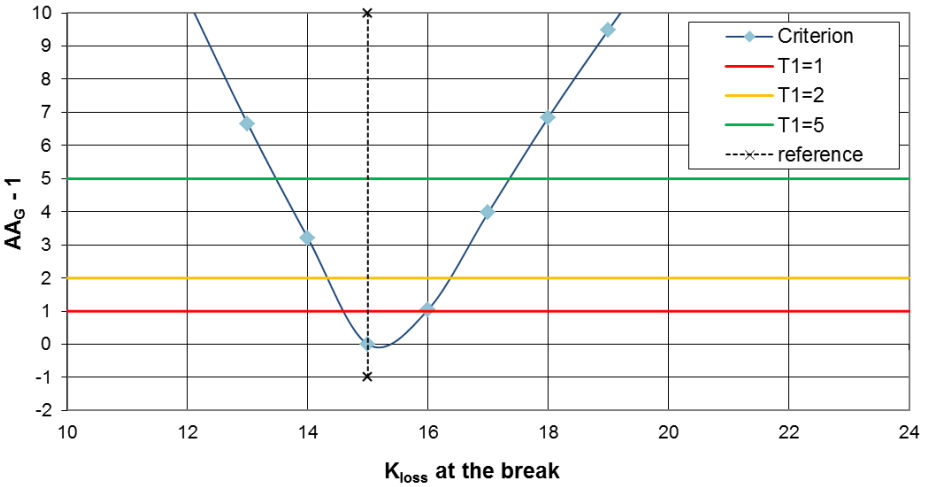

Figure C.22: calculated AA_G for K_{loss} at break variation of Edwards' pipe model.

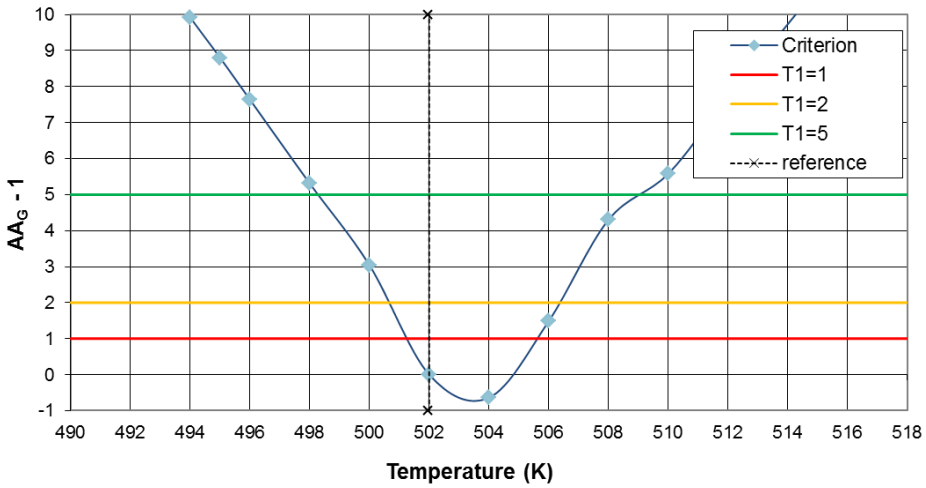

Figure C.23: calculated AA_G for initial fluid temperature variation of Edwards' pipe mode.

APPENDIX D: GENERAL REQUIREMENTS AND DESCRIPTION SPECIFICATION OF METHODOLOGIES AND EXPERIMENTAL DATA TO BE USED IN PREMIUM BENCHMARK

D.1 CONTEXT

PREMIUM (Post-BEMUSE REflood Models Input Uncertainty Methods) is an activity launched with the aim to push forward the methods of quantification of physical models uncertainties in thermal-hydraulic codes. It is endorsed by OECD/NEA/CSNI/WGAMA.

The benchmark is addressed to all who apply uncertainty quantification methods based on input uncertainties quantification and propagation. It is based on a selected case of uncertainty analysis application to a reflood scenario (including the simulation of quench front propagation) in an experimental test facility. The scope of the benchmark comprises a review of the existing methods, the identification of potentially important uncertain input parameters for selected case, a quantification of uncertainties using experimental data and, finally, a confirmation/validation of the performed quantification on the basis of blind calculation of a second experiment.

A more detailed description of the framework of the benchmark and proposed experiments can be found in the paper "PREMIUM-Benchmark on the quantification of the uncertainty of the physical models in the system thermal-hydraulic codes" presented in the Workshop on BEPU Methods in Barcelona, Nov. 2011 (attached to this specification).

This document is a specification of the benchmark and guideline to PREMIUM participants. In its main part, it describes the information that the organizing committee must compile in order to complete PREMIUM Phase I (Introduction and methodology review) document. However its goal is not only the description of methodologies but also reaching a consensus between participants on the different steps of an uncertainty quantification methodology.

That Phase I final document, addressed to all participants, will encompass an introduction, final specification and time schedule of PREMIUM, together with the description of the methodologies and experiments finally involved in the benchmark.

D.2 PARTICIPATION AND GUIDELINES

There are different ways to participate in PREMIUM. Four different types of participants can be distinguished:

1. Participants who have at their disposal methodologies for quantification of uncertainties of the physical models;
2. Participants willing to become users of one of the available methodologies;
3. Participants willing to use an expert-judgment based method improved thanks to methods of fitting of data;

4. Participants willing to develop their own method in parallel with PREMIUM participation.

In parallel, some of the participants will contribute with own experimental data to be used in the quantification step.

For the confirmation/validation step, as explained in the attached paper, PERICLES experiment has been chosen. However, for the quantification step, the list of facilities and tests involved in PREMIUM is not closed, though FEBA/SEFLEX experiment has been already proposed (see attached paper). Therefore, an optional contribution of experimental data to be used in the benchmark can be done by any participant having a connection with suitable facilities and tests.

Having this into consideration, this document is, in its main part, a guideline addressed to PREMIUM participants that will provide:

A. Methodologies for quantification of physical model uncertainties (type 1 participants);
B. The use of experimental data (PERICLES and FEBA responsible institutions, and all other possible contributors of experiments for quantification step).

Such participants will have to provide a description of their methodologies and/or detailed information of the involved experimental facilities and their data, according to the specifications.

All the participants willing to use their own methodology/experimental data must strictly make them available to the rest of participants. The conditions of the distribution and the proprietary questions will be clarified for each particular case.

D.3 STRUCTURE

This document is structured in order to include specifications for these three precise contributions to PREMIUM:

- Methodologies for quantification of physical model uncertainties (to be used in PREMIUM Phase III)
- Experimental data for the quantification step (to be used in PREMIUM Phase III)
- Experimental data for the confirmation/validation step (to be used in PREMIUM Phase IV, addressed only to PERICLES responsible institution)

For each of these, a specification of the contents and structure of the description that the contributing organization has to provide in order to be used in PREMIUM are given in Chapters D.4, D.5 and D.6, along with the general requirements that the methodologies/experimental data must fulfil.

Next, a general outline of the Kick-Off Meeting, addressed to all participants, is presented in Chapter D.7.

Finally, an updated schedule of Phase I, including deadlines of description handouts, is provided in Chapter D.8.

D.4 METHODOLOGIES FOR QUANTIFICATION OF PHYSICAL-MODEL UNCERTAINTIES

This particular guideline section is addressed to all the participants of PREMIUM willing to contribute with a methodology for quantification of physical model uncertainties during Phase III.

D.4.1 General requirements

The methodology to be used in PREMIUM Phase III has to fulfil the following requirements:

- It must address the quantification of physical model uncertainties according to probability theory, possibility theory, interval analysis, or other chosen type of representation (e.g., probability distribution function for selected influential parameters).
- It has to be suitable as a basis for quantification of uncertainties in a Reflood scenario.
- It must be validated as far as possible.
- The resources needed to use the methodology have to be reasonable.
- It has to be flexible enough to support different system codes.
- Methodology algorithm and software have to be completely available for the rest of PREMIUM participants.
- A very clear explanation is required in order to allow all participants to use it, and simplicity of use is advisable to avoid wasted resources and human error.

D.4.2 Description specification

If the previous requirements are met, in order to use a methodology in PREMIUM Phase III, it is compulsory that the contributing organization provides a complete description, user guidelines and details on used codes/software, as specified below.

First, very **general details** about the methodology should be given:

- Name of the methodology;
- Involved institutions;
- Current availability;
- Brief description of methodology (including type of uncertainty representation);
- Advantages and drawbacks;
- Details on the possible validation;
- Overview of code and general/specific software use;
- Technical literature and references.

Next, **user-oriented description/guidelines** should be given:

- Description of the methodology and explanation of the algorithm (step-by-step explanation is recommended);
- Simplifications made by the methodology;
- At least one example of application.

Finally, it is important to detail **code and software** use in the methodology application:

- Detail capabilities of being used with different system codes;
- Describe software specifically developed for methodology.

All the descriptions handed over will be included in Phase I final document and distributed along PREMIUM benchmark participants. Additionally, each methodology will have to be presented in PREMIUM Kick-Off Meeting (see Chapter D.7), through a summary of this information illustrating as good as possible the advantages and limitations of the methodology.

D.5 EXPERIMENTAL DATA FOR QUANTIFICATION STEP

This particular guideline section is addressed to all the participants of PREMIUM willing to contribute with experimental data to be used in the process of quantification of physical model uncertainties during Phase III.

D.5.1 General requirements

The experimental data to be used in PREMIUM Phase III have to fulfil the following requirements:

- experiment must consist of a reflooding test similar to FEBA/SEFLEX test;
- experiment results will have to be available for the rest of PREMIUM participants;
- experiment data must be sufficiently validated and suitable as a basis for quantification of uncertainties (qualified instrumentation, sufficient number of measuring points and test runs, etc.);
- in order to follow a typical sequence of uncertainty analysis, the approach of the experiment used in the quantification step should possibly be simpler than the one on the validation step experiment PERICLES, for example with a constant power radial distribution; blockage arrays must be avoided since there is no blockage in the confirmation phase with PERICLES;
- simplicity in the geometry is preferred also in order to minimize user effect (i.e., avoiding problems with input deck writing/editing).

D 5.2 Description specification

If the previous requirements are met, in order to use the data of an experiment in PREMIUM Phase III, it is compulsory for the contributing organization to provide a detailed description about the facility, test and experimental data, as specified below.

First, very **general details** about the facility should be given:

- Name of facility;
- Institutions involved;
- Brief description;
- Current availability of results;
- Reference plant and/or scaling criteria;
- Related technical documentation available and references.

Next, the explanation of the **test selection** should be more specifically described:

- Selection of data series to be used in PREMIUM Phase III, among all the data available for the given facility; precise justification is required;
- Objectives of the selected tests;
- Problems/errors/limitations detected during test or data analysis that might affect the quantification/evaluation of input uncertainties;
- Other special considerations.

In order to make a complete **description of the problem**, the contributing organization has to provide sufficient technical information to build up the input deck, which should include:

- A complete geometrical description of problem, preferably through drawings:
  - Rod/housing section and length;
  - Number of rods/bundles and geometrical disposition;
  - Presence of gap or grid spacers;
  - Location of measuring points;
  - Other important geometrical considerations;
- Information on materials description, which should be as complete as possible.

It is also important to detail the **boundary and initial conditions** in the selected tests with their experimental uncertainties. One can quote for each of the selected data series that will be used in PREMIUM Phase III:

- Experiments identification number
- Feedwater rates
- Pressures
- Feedwater temperatures (at least one measurement per experiment)
- Average power delivered by rod surface and/or power distribution
- Special conditions, if any (material change, grid disposition, etc.)
- Initial profiles:
  - Axial cladding temperature
  - Power radial/axial profile.

The owner of the experiment can also provide the input data decks of the considered tests.

In addition to the data necessary to write input data decks, the participant must give the **measured quantities**, to be used in the method of quantification of the input uncertainties. These quantities should be provided with their experimental uncertainties. One can quote for example:

- Time evolutions:
  - Cladding temperature at different axial levels,
  - Pressure drops in the segments of the test section channel,
  - Temperatures around hottest level (cladding, fluid, housing),
  - Coolant outlet conditions (water carry over, coolant temperature, coolant pressure);
- Axial level vs. quench time.

Optionally, time evolution of calculated quantities (e.g., heat transfer coefficient) can be provided, on condition that the calculation is very precisely defined.

In case of **additional phenomena** taken into consideration such as grids, radial power distribution, etc. adequate data to analyze separately their effects has to be presented.

Experimental uncertainties of these measured data must be provided if they are available.

All the descriptions handed over will be included in Phase I final document and distributed along PREMIUM benchmark participants. Additionally, each experiment will have to be presented in PREMIUM Kick-Off Meeting (see Chapter D.7), through a summary of this information.

D.6 EXPERIMENTAL DATA FOR VALIDATION STEP (BLIND TEST)

This particular guideline section is addressed to the responsible institution of PERICLES experiment. Its corresponding data will be used in the confirmation/validation step during PREMIUM Phase IV (a blind test of input uncertainties obtained in Phase III).

D.6.1 General requirements

The experimental data to be used in PREMIUM Phase IV fulfils the following requirements:

- Experiment consists of a reflooding test;
- Experiment data is unpublished so far, in order to perform the blind test. Only the coordinating institutions CEA and IRSN have this data at their disposition;
- Experiment data is sufficiently qualified and suitable as a basis for validation (e.g. sufficient number of measuring points and test runs);
- In order to follow a typical sequence of uncertainty analysis, the approach of PERICLES experiment, used in the confirmation/validation step, is more complex than the one on the quantification step reference experiment FEBA/SEFLEX; for example, a larger number of fuel rod simulators and power radial distribution are taken into consideration (and its effect can be separated); overly-complicated approaches are avoided (e.g. blockage arrays);
- Simplicity in the geometry is also maintained in order to minimize user effect (i.e., avoiding problems with input deck writing/editing).

D.6.2 Description specification

In order to use the data of an experiment in PREMIUM Phase IV, the contributing organization will have to provide a detailed description about the facility and test, as specified below.

First, very **general details** about the facility should be given:

- Name of facility;
- Institutions involved;
- Brief description;
- Detailed current availability of results;
- Reference plant and/or scaling criteria;
- Related technical documentation available and references.

Next, the explanation of the **test selection** should be more specifically described:

- Selection of data series to be used in PREMIUM Phase IV, among all the data available for the given facility; precise justification is required;
- Objectives of the selected tests;
- Other special considerations.

In order to make a complete **description of the problem**, the contributing organization has to provide sufficient technical information to build up the input deck, which should include:

- A complete geometrical description of problem, preferably through drawings:
    - Rod/housing section and length;
    - Number of rods/bundles and geometrical disposition;

  - Presence of gap or grid spacers;
  - Location of measuring points;
  - Other important geometrical considerations.
- Information on materials description, which should be as complete as possible.

It is also important to detail the **boundary and initial conditions** in the selected tests with their experimental uncertainties. One can quote for each of the selected data series that will be used in PREMIUM phase III:

- Experiments identification number
- Feedwater rates
- Pressures
- Feedwater temperatures (at least one measurement per experiment)
- Average power delivered by rod surface and/or power distribution
- Special conditions, if any (material change, grid disposition, etc.)
- Initial profiles:
  - Axial cladding temperature,
  - Power radial/axial profile.

The owner of the experiment can also provide the input data decks of the considered tests.

Experimental uncertainties of these measured data must be provided if they are available.

All the descriptions handed over will be included in Phase I final document and distributed along PREMIUM benchmark participants. Additionally, the experiment will have to be presented in PREMIUM Kick-Off Meeting (see Chapter D.7), through a summary of this information.

D.7 ORGANIZATION OF THE KICK-OFF MEETING

This Chapter is addressed to all the participants of PREMIUM benchmark and presents the foreseen activities within the Kick-Off Meeting, which will place at the end of February (see dates in Chapter D.8).

According to their involvement on the benchmark, these are the instructions to be followed by each participant during the kick-off meeting:

- **All participants:** Each participant will indicate his way to participate in PREMIUM (the four different types of participants distinguished by UPC and CSN, see Chapter D.1);
- **Participants having at their disposal a methodology:** Presentation of the methodology;
- **Participants using an own experiment for phase II:** Presentation of the experiment;
- **Coordinators:** Introduction to PREMIUM for new potential participants, presentations of Phases II, III and IV (including PERICLES experiment).

As mentioned, the presentations of the methodologies and experiments given in the Meeting should reasonably include the specifications given in the previous Chapters.

D.8 SCHEDULE

The participants willing to contribute with their methodology or experimental data have to deliver the requested information by the 6th February 2012 in order to be presented in the kick-off meeting (20-22 February 2012).

Participants who have not presented their own methodologies/experiment by then or have not accepted to use one of the ones proposed by other participants during the Kick-Off meeting must submit the requested specifications before 31 March 2012.

This is the complete schedule for Phase I:

- December 14th, 2011: preliminary specification of Phase I delivered to the PREMIUM CC;
- December 23rd, 2011: comments from the PREMIUM CC;
- January 11th, 2011: final specification delivered to the PREMIUM CC and distributed by NEA secretariat to potential participants;
- February 6th, 2012: participants will deliver their contributions for Phase I to the Coordinator of Phase I (see Chapter D.9);
- February 20th – 21st, 2012: kick-off meeting (possible extension to February 22nd, depending on the number of participants)
- March 31st, 2012: participants who have not presented their own methodology or have not accepted to use one of the methods proposed by other participants must submit the requested information about the method they want to use;
- April 30th, 2012: preliminary report on Phase I is delivered to the participants;
- May 31st, 2012: final report on Phase I (corrections and implementation of the review performed by the participants).

D.9 COORDINATION

The coordination of PREMIUM Phase I is in the charge of the Universitat Politècnica de Catalunya (UPC), Barcelona. All the descriptions of uncertainties methodologies or qualification experiments should be sent to:

Francesc Reventós (UPC) francesc.reventos@upc.edu
Elsa de Alfonso (UPC) elsa.de.alfonso@upc.edu

APPENDIX E: DESCRIPTION OF THE MODEL CALIBRATION THROUGH DATA ASSIMILATION (MCDA) METHOD

Data Assimilation: deterministic and probabilistic methodology for the quantification of the input-parameter uncertainties

E.1 INTRODUCTION

Thermal hydraulic system analysis must include uncertainties in predicting system performance, those uncertainties originating from the numerics and the parameters including initial conditions, boundary conditions, and physical models. To reduce the parameter uncertainties, and subsequently the response uncertainties, one can calibrate the target parameters by adjusting the parameter values to achieve better agreement between measured and predicted response values. This process is called data assimilation, and the calibrated parameter distribution is called the *a posteriori* distribution of the parameters. Data assimilation thus integrates experimental data and computational results, including their mean values and uncertainties, for the purpose of updating the parameters of the computational models.

Bayesian statistics initially proposed by Thomas Bayes [E.1] indicates how the degree of belief changes after utilizing the additional information. The probability density function (pdf) $f(x)$ that reflects the level of certainty about the value x before using any existing data about x is called the *a priori* distribution of x. After additional information has been gathered, the belief in the certainty of x can be improved by the impact of the information provided, e.g. empirical data. The pdf $f(x|Y)$ that reflects a new level of certainty about x given observed Y is the *a posteriori* distribution of x. The probability density function $f(Y|x)$, also called likelihood function, is the probability that Y will be observed given that x is known to be true. The *a posteriori* distribution of x is then calculated as follows:

$$f(x|Y) = \frac{f(Y|x)\, f(x)}{f(Y)} \tag{1}$$

where the probability density function $f(Y)$ is the probability that Y will be observed independent of x. The *a posteriori* distribution is thus proportional to the product of the likelihood function and the *a priori* distribution. The above forms of Bayes' theorem provide a statistical approach for data assimilation indicating how prior knowledge is updated by additional experimental data.

Following the Bayesian approach, the *a posteriori* distribution for parameter vector $\mathbf{p}$ is derived as [E.2]:

$$\rho(\mathbf{p}\,|\,\mathbf{r}_m) = c \cdot \exp\left[-\frac{1}{2}\left(\{\mathbf{r}_m - \mathbf{r}\}^{\mathrm{T}}\, \mathbf{C}_m^{-1}\, \{\mathbf{r}_m - \mathbf{r}\} + \{\mathbf{p} - \mathbf{p}_0\}^{\mathrm{T}}\, \mathbf{C}_p^{-1}\, \{\mathbf{p} - \mathbf{p}_0\} \right) \right] \tag{2}$$

where $\mathbf{r}_m$ denotes the experiment data vector, $\mathbf{r}$ the simulation response vector, $\mathbf{C}_m$ the measurement error covariance matrix, $\mathbf{p}_0$ the nominal values of the parameters, $\mathbf{C}_p$ the parameter covariance matrix, and c the normalization constant. The mathematical approach used to solve the above equation depends on the linearity of the system. After identifying uncertainties on the measured values and the parameters, linearity test will be conducted to determine whether the system responses are or are not linearly dependent upon the parameters. Deterministic approach will be used for a linear system to obtain the mean value and standard deviation of the parameters, and probabilistic method will be utilized for a nonlinear system to estimate the *a posteriori* distributions of the parameters. Uncertainty quantification will be followed determining the response distributions and the safety margins to complete the safety analysis.

E.2 DETERMINISTIC METHOD FOR THE LINEAR PROBLEMS

A discussion based upon the parameters and observables uncertainties being Gaussian and the system being linear is presented in this section. To determine the solution that maximizes the pdf of the a posteriori parameter vector, i.e., to determine the mean values of the *a posteriori* parameters, the parameter vector that minimizes θ is sought:

$$\theta = \left\{\mathbf{r}_m - \mathbf{r}\right\}^{\mathrm{T}} \mathbf{C}_m^{-1} \left\{\mathbf{r}_m - \mathbf{r}\right\} + \alpha^2 \left\{\mathbf{p} - \mathbf{p}_0\right\}^{\mathrm{T}} \mathbf{C}_p^{-1} \left\{\mathbf{p} - \mathbf{p}_0\right\} \tag{3}$$

where the regularization parameter α controls the amount of parameter adjustments allowed indicating the degree of weighting between the mismatch term, i.e. $\left\{\mathbf{r}_m - \mathbf{r}\right\}^{\mathrm{T}} \mathbf{C}_m^{-1} \left\{\mathbf{r}_m - \mathbf{r}\right\}$ and the regularization term, i.e. $\left\{\mathbf{p} - \mathbf{p}_0\right\}^{\mathrm{T}} \mathbf{C}_p^{-1} \left\{\mathbf{p} - \mathbf{p}_0\right\}$. The regularization parameter was selected based on the characteristic L-curve [E.3]. Plotting the mismatch term versus the regularization term as the regularization parameter value is varied produces the characteristic L curve. The value of the regularization parameter is chosen at a corner where the mismatch term increases rapidly without any significant change in the regularization term. If the system is linear, the system response can be approximated as follows:

$$\mathbf{r} \cong \mathbf{r}_0 + \mathbf{S}_{\mathbf{p}_0} \left(\mathbf{p} - \mathbf{p}_0\right) \tag{4}$$

where $\mathbf{S}_{\mathbf{p}_0}$ is the sensitivity matrix computed about the nominal values of the *a priori* parameter. The solution to the minimization problem is accomplished by substituting Equation (4) into Equation (3) and differentiating the equation with respect to $\mathbf{p}$ as follows [E.4]:

$$\mathbf{p}_0^{post} = \mathbf{p}_0 + \left[\mathbf{S}^{\mathrm{T}} \mathbf{C}_m^{-1} \mathbf{S} + \alpha^2 \mathbf{C}_p^{-1}\right]^{-1} \mathbf{S}^{\mathrm{T}} \mathbf{C}_m^{-1} \left[\mathbf{r}_m - \mathbf{r}_0\right] \tag{5}$$

A posteriori distributions of the parameters for the linear system are characterized by the mean values and the covariance matrix. The *a posteriori* parameter covariance matrix is computed by:

$$\mathbf{C}_p^{post} \equiv E\left(\left[\mathbf{p} - \mathbf{p}_0^{post}\right]\left[\mathbf{p} - \mathbf{p}_0^{post}\right]^{\mathrm{T}}\right) \tag{6}$$

Substituting Equation (5) for the posteriori parameters into Equation (6) produces the following expression for $\mathbf{C}_p^{post}$ [E.5], E.6]:

$$\mathbf{C}_p^{post} \cong \mathbf{C}_p^{prior} - \mathbf{C}_p^{prior}\mathbf{S}^{\mathrm{T}}\mathbf{K}^{\mathrm{T}} - \mathbf{K}\mathbf{S}\mathbf{C}_p^{prior} + \mathbf{K}\left[\mathbf{C}_m + \mathbf{S}\mathbf{C}_p^{prior}\mathbf{S}^{\mathrm{T}}\right]\mathbf{K}^{\mathrm{T}} \tag{7}$$

where $\mathbf{K} \equiv \left[\mathbf{S}^{\mathrm{T}}\mathbf{C}_m^{-1}\mathbf{S} + \alpha^2\mathbf{C}_p^{prior-1}\right]^{-1}\mathbf{S}^{\mathrm{T}}\mathbf{C}_m^{-1}$. An approximation is involved in the derivation of Equation (7) since the parameter-response covariance matrices, i.e. $\mathbf{C}_{pr}$ and $\mathbf{C}_{rp}$, which appear in the derivation are removed. Given *a posteriori* parameter uncertainties, one can propagate the uncertainties through the simulation model to predict *a posteriori* uncertainties on the responses. For the linear system, the *a posteriori* covariance matrix of the system response is given by:

$$\mathbf{C}_r^{post} = \mathbf{S}_{\mathbf{p}_0^{post}}\mathbf{C}_p^{post}\mathbf{S}_{\mathbf{p}_0^{post}}^{\mathrm{T}} \tag{8}$$

where $\mathbf{S}_{\mathbf{p}_0^{post}}$ is the sensitivity matrix obtained about the nominal values of the *a posteriori* parameters. Equation (8) is referred to as the sandwich rule and is used to propagate the *a posteriori* parameter uncertainties.

E.3 PROBABILISTIC METHOD FOR THE NONLINEAR PROBLEMS

The deterministic approach, based upon a first-order truncated Taylor series for the responses, is inappropriate to treat nonlinear behaviour of the system. To address the nonlinear responses in data assimilation, a sampling approach is employed by propagating the parameter uncertainties to predict the *a posteriori* distributions of the parameters. This is conducted using the Markov Chain Monte Carlo (MCMC) method [E.7], [E.8] which seeks to determine the steady-state Markov distribution by generating Markov chains that coincide with the target distribution, i.e., the *a posteriori* distribution of the parameters in our case. MCMC simulation searches the original target distribution by generating sequences of random samples from the target distribution, and subsequently visualizes the distribution utilizing all accepted chains obtained during the simulation.

To determine the *a posteriori* distribution for the parameter vector $\mathbf{p}$ given by Equation (2), the Metropolis algorithm was used for a MCMC implementation, which is presented as follows:

1. Initialize the parameter vector by guessing it at some value;
2. Given the current parameter vector is $\mathbf{p}^i$, generate a new parameter vector $\mathbf{p}^*$ by perturbing $\mathbf{p}^i$ in $\left[\mathbf{p}^i - \mathbf{m},\ \mathbf{p}^i + \mathbf{m}\right]$, where $\mathbf{m}$ is a trial space vector;
3. Compute the Metropolis acceptance probability using the following expression, $\alpha = \min\left\{1,\ \dfrac{\rho(\mathbf{p}^* \mid \mathbf{r}_m)}{\rho(\mathbf{p}^i \mid \mathbf{r}_m)}\right\}$;
4. Define $\mathbf{p}^{i+1} = \begin{cases}\mathbf{p}^* & \text{with probability } \alpha \\ \mathbf{p}^i & \text{with probability } 1-\alpha\end{cases}$ selecting which value to assign via a random number in [0,1];
5. Return to step 2.

The acceptance rate of the trial vector $\mathbf{p}^*$ is defined as the total number of accepted chains divided by the total number of chains generated. If the acceptance rate is much less or much more than 50%, one can alter the size of the perturbation by decreasing or increasing its trial space.

E.4 REFERENCES

[E.1] Thomas Bayes, "An Essay Towards Solving a Problem in the Doctrine of Chance," Philosophical Transactions of the Royal Society, 53, 370-418, 1763.

[E.2] A. Tarantola, *Inverse Problem Theory and Methods for Model Parameter Estimation*, Society for Industrial and Applied Mathematics, Philadelphia, 2005.

[E.3] H. W. Engl and W. Grever, "Using the L-Curve for Determining Optimal Regularization Parameters," Numerische Mathematik, 69, 25, 1994.

[E.4] J. W. Hines, B. R. Upadhyaya, J. M. Doster, R. M. Edwards, K. D. Lewis and P. J. Turinsky, "Advanced Instrumentation and Control Methods for Small and Medium Reactors with IRIS Demonstration," DE-FG07-07ID14895/UTNE/2009-1, 2009.

[E.5] Jaeseok Heo, "Optimization of Design for SMR via Data Assimilation and Uncertainty Quantification," Ph.D. Dissertation, North Carolina State University, 2011.

[E.6] D. G. Cacuci and M. Ionescu-Bujor, "Best-Estimate Model Calibration and Prediction Through Experimental Data Assimilation - I: Mathematical Framework," Nuclear Science and Engineering, 165, 18-44, 2010

[E.7] Nicholas Metropolis, Arianna W. Rosenbluth, Marshall N. Rosenbluth, Augusta H. Teller and Edward Teller, "Equation of State Calculation by Fast Computing Machines," Journal of Chemical Physics, vol. 21, No.2, pp. 1087-1092, 1953.

[E.8] D. Higdon, M. Kennedy, J. C. Cavendish, J. A. Cafeo and R. D. Ryne, "Combining Field Data and Computer Simulation for Calibration and Prediction," SIAM J. Sci. Comput. Vol. 26, No. 2, pp. 448-466, 2004.

APPENDIX F: DESCRIPTION OF THE DIPE METHOD

F.1 DESCRIPTION OF THE DIPE METHOD

The principle of the DIPE (Determination of Input Parameters Empirical properties) method is represented by the flowchart on Figure F.1 below.

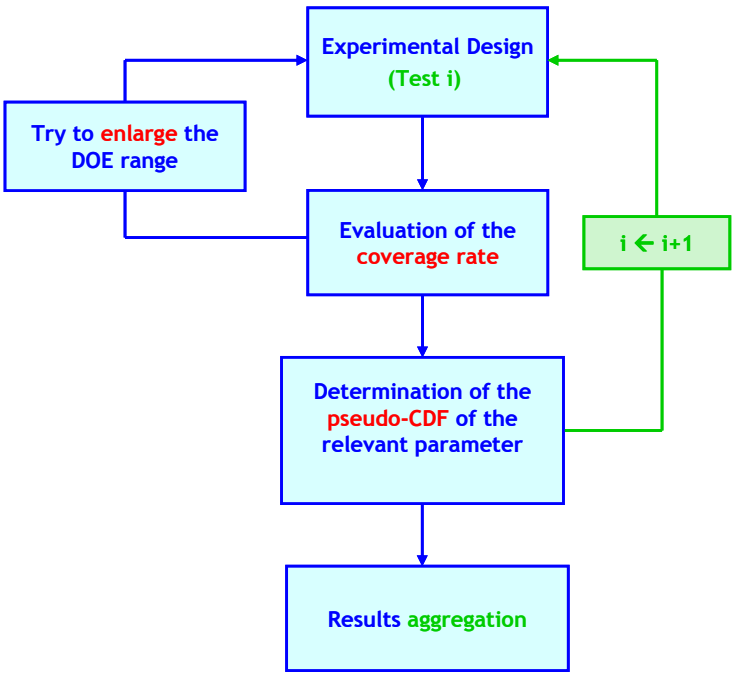

Figure F.1: principle of DIPE

F.1.1. Description of the 1D DIPE

The description of the method is illustrated by a simple separate effect test using only one input uncertain parameter noted X and one output parameter of interest.

Experimental Design: Several simulations are carried out by varying the parameter X on a chosen interval, and the time curves noted C(X) calculated by CATHARE are compared with the experimental data noted Cexp, as showed on Figure F.2.

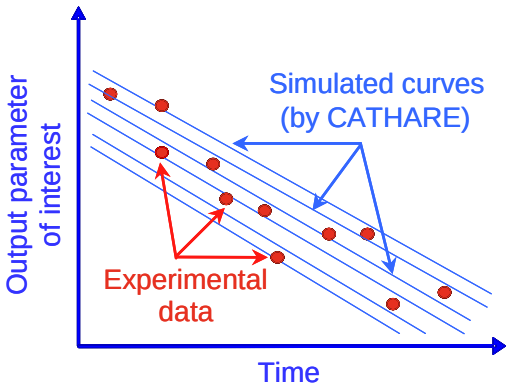

Figure F.2: experimental curve framed by simulated curves

Evaluation of the coverage rate: For each value of the uncertain parameter noted X_i (thus for each simulated curve calculated with X_i noted $C(X_i)$), the coverage rate is the ratio, noted $P(X_i)$, of the number of experimental points (circled on the figure 3) above the corresponding simulated curve $C(X_i)$ and the total number of experimental is calculated, as indicated on Figure F.3.

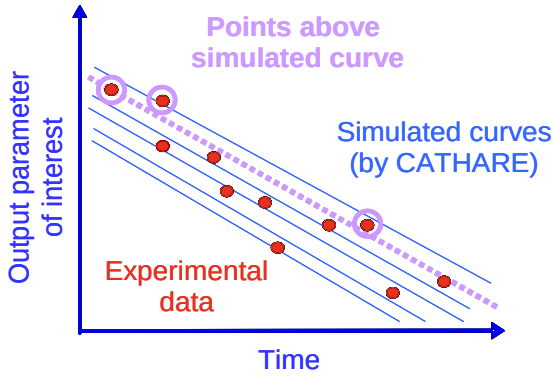

Figure F.3: calculation of the coverage rate $P(X_i)$

If the experimental data are not bounded by the entire simulated curves C(X), we try to enlarge the experimental design of X to do it.

Pseuso-CDF: If the 3 following assumptions are verified, the function P(X) obtained can be considered as an empirical pseudo-cumulative density function (CDF) of the input parameter X.

- *Assumption 1*: "Absence of measurement error"

The measurement error is negligible or not considered

- *Assumption 2*: "Random error of considered model"

At each time, it exists a calculated value $C(X_i)$ equal to Cexp, where the uncertain input parameter X_i is a random variable coming from an independent probability law

- *Assumption 3*: "Monotony"

At each time, the calculated curve C(X) is monotonous. The C(X) time curves must not cross.

Thus, we can represent it versus the value of the input parameter (see Figure F.4).

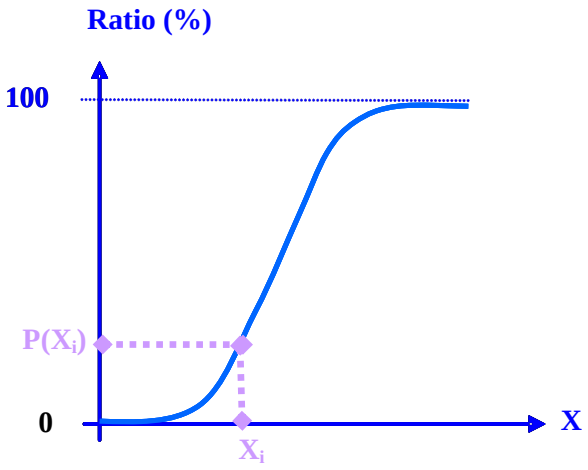

Figure F.4: pseudo-cumulative density function built with the coverage rate P(X)

Determination of the uncertainty interval**:** We seek to bind 95 % of the experimental data. It corresponds to search the curves C(X) having 2.5% of the experimental data above and another one having 2.5% of the experimental data below (see Figure F.5).

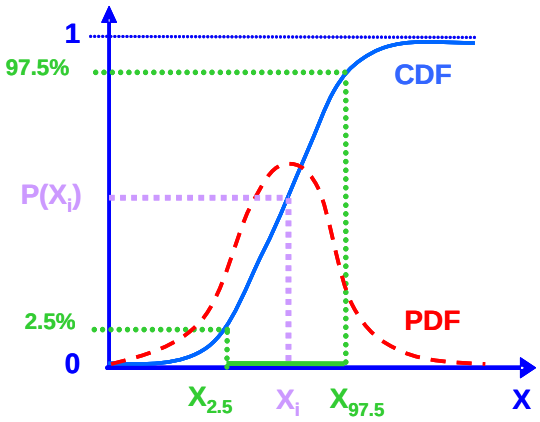

Figure F.5: determination of the range of the input parameter X

These correspond to the values of X for which P(X) takes values 0.025 and 0.975, i.e. the 2.5th and the 97.5th percentile. A pseudo probability distribution function (PDF) can be obtained by derivation of P(X).

Results aggregation: The aggregation of pseudo CDFs of X obtained from different experiments or for different output parameters is simply obtained by averaging of the individual curves.

F.1.2. Description of the 2D DIPE

When two parameters X and Y are considered, the 1D process is performed for the first parameter X with given values for the second Y (inside its range of variation). This gives a set of coverage rates curves C(X, Y_i) and permits the construction of coverage rate contour lines.

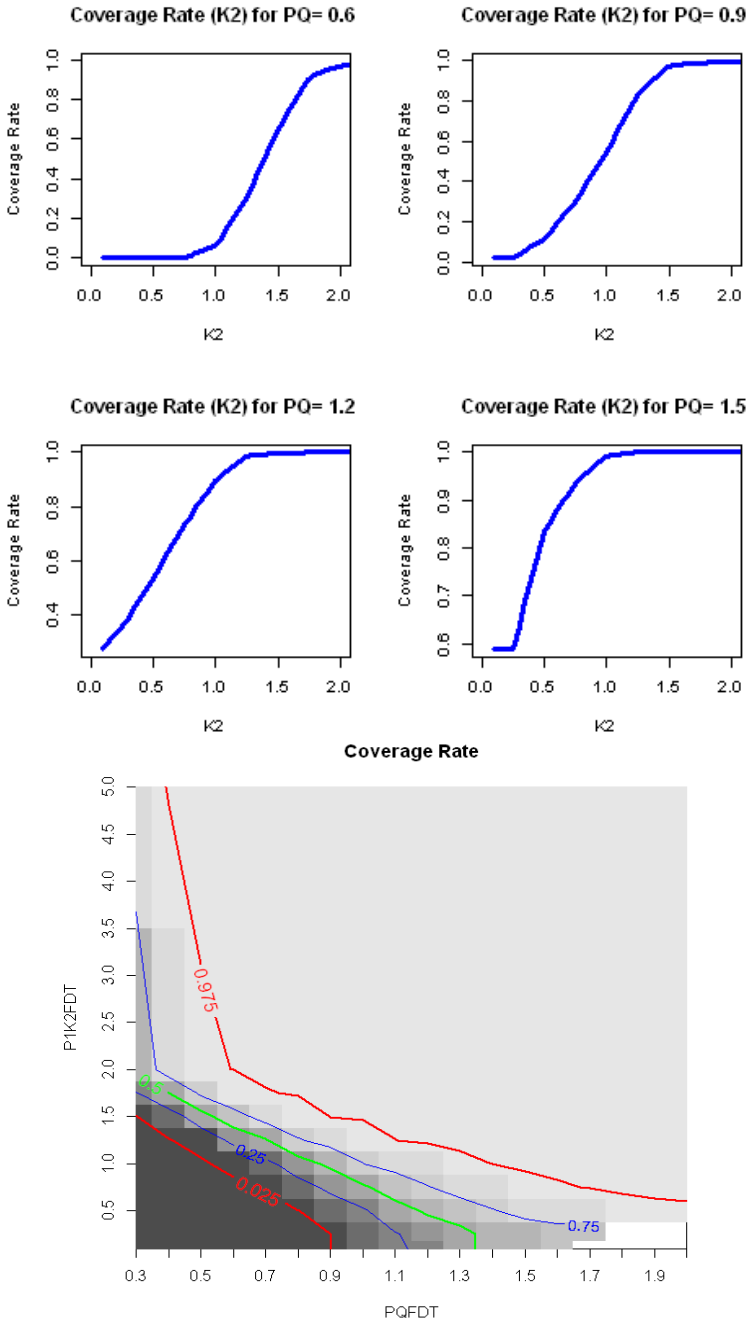

Figure F.6: coverage rates of X (K2) for different values Yi (PQ) and corresponding contour lines.

A similar approach may be used when more than two parameters are considered (2D+ DIPE), the coverage rate depending on the values of each parameter.

Comments:

1. It should be noted that these contour lines, showing the dependency between the variability of the two parameters, cannot be considered as a representation of a pseudo-joint cumulative density function.
2. DIPE gives information on uncertain input parameters permitting the "coverage" of selected output parameters of the selected experiments used in this method. This kind of method cannot give the intrinsic probability distribution of these input parameters.

3. More generally, the empirical PDF obtained during PREMIUM cannot be the intrinsic PDF of the parameters considered to be uncertain. This is due to the fact that the sampling both of the experimental test runs and of the experimental values of interest is not random.

Obviously, the test runs are chosen with deterministic boundary and initial conditions covering at best the whole space of experimental states, i.e. mainly at the corners of the hyper-cube of possible situations. They therefore cannot be random.

The experimental values of interest are deterministically chosen, at given locations or given times. They neither are random.

The lower and upper bounds obtained (kmin and kmax) may be representative of the corresponding range of variation for the FEBA experiments, if these experiments and the experimental values of interest have been well chosen to cover all the possible situations. These bounds are however FEBA specific.

APPENDIX G: DESCRIPTION OF THE SAMPLING-BASED INVERSE UNCERTAINTY QUANTIFICATION (IUQ) METHOD

G.1 INTRODUCTION

Tractebel has developed a sampling-based inverse uncertainty quantification (IUQ) approach with DAKOTA tool. Please find hereunder a description of our own methodology.

G.2 PRINCIPLE

Tractebel's IUQ approach is to use DAKOTA sampling based uncertainty quantification (UQ) functionality to quantify the model uncertainty.

The DAKOTA code has uncertainty quantification (UQ) functionality based on random sampling [G.1]. This approach should be in principle used for "propagation" of the "known" input uncertainties into the "unknown" output uncertainties, which can be quantified based on the desired probability and confidence level.

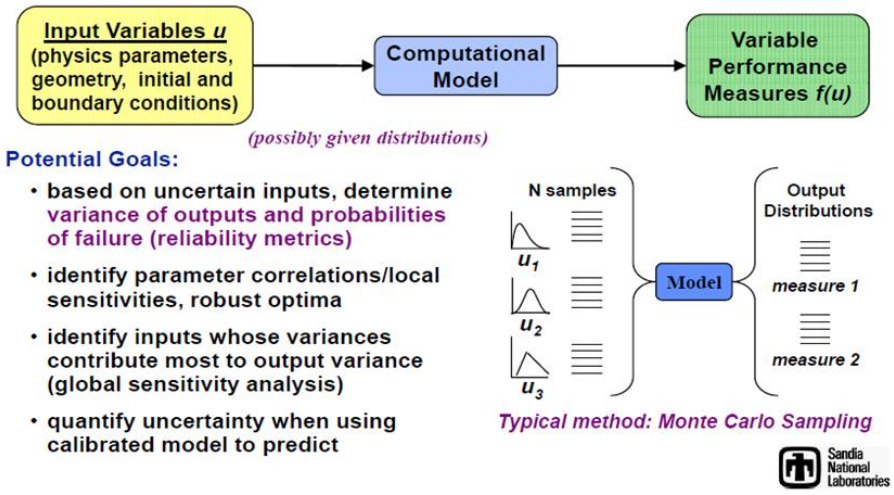

Figure G.1: DAKOTA Uncertainty Quantification Method [G.1]

In the current application, the key model input uncertainties are unknown. However, the output uncertainties are considered to be known from the experiments.

The quantification of the unknown key model uncertainties can be thus considered as an "inverse problem" of the uncertainty propagation, namely, how to define the key model input uncertainties (variation ranges and distribution) such that the code calculated output distributions match the given measured experimental data (like peak cladding temperature or rewetting time) within the measurement uncertainty ranges?

In principle, we can use the so-called "calibration (or optimization) under uncertainty" approach to find a statistical characterization of input parameters such that when propagated through the model, they match statistics on the output responses. The approach is described in a paper of the DAKOTA team from a few years ago [G.2]. Here, given information on response moments or distribution information, DAKOTA can combine any one of its UQ methods with any desired deterministic calibration method to perform this kind

of "uncertainty inversion". These kinds of approaches rely on nesting UQ analysis within a calibration loop and therefore can be computationally demanding, but can treat challenging engineering problems with nonlinearities.

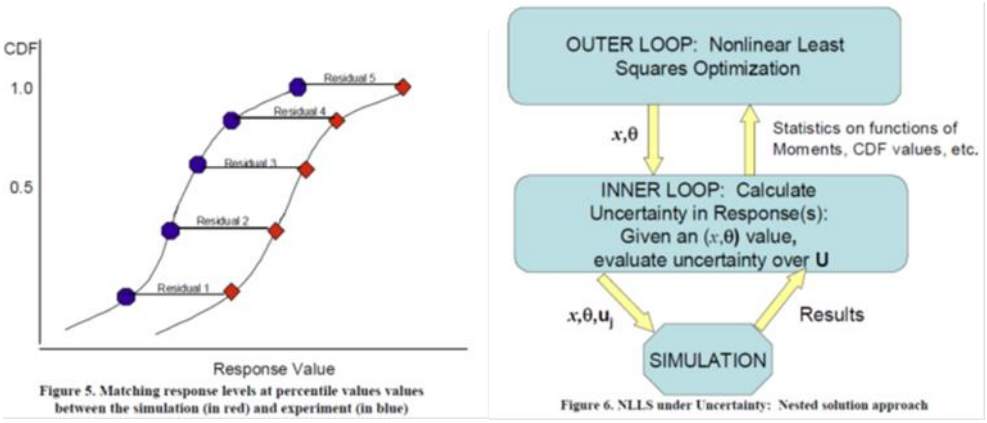

Figure 2: Model Uncertainty Calibration by Matching Distribution Information [G.2]

G.3 MAJOR STEPS

The inverse uncertainty quantification (IUQ) approach to determine the key model input uncertainties (variation ranges and distributions) consists in the following 4 major steps (following the identification of the key model input uncertainties, assessment of the code applicability, and choice of the Separate Effect Tests or Integral Effect Tests, i.e., SETs/IETs for UQ):

- Step 1, define the key model input uncertainty variation ranges and distributions;
- Step 2, sample each of the model input uncertainties to obtain the needed input decks, and run the code calculations for simulation of the selected tests;
- Step 3, check if the obtained upper and lower bounds of the calculated output parameters well cover the selected experimental data (including the experimental uncertainties and provision for different scales of tests and limitations in codes and data);
- Step 4, if necessary, adapt the key model input uncertainty variation ranges and distributions, and repeat steps 2-3 until a reasonable coverage is found. In case of various output parameters are targeted, a compromise may be needed to ensure the adequate coverage of all output parameters.

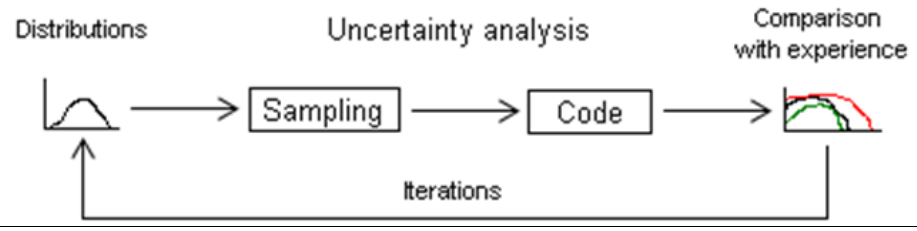

Figure 3: Illustration of the inverse uncertainty quantification (IUQ) approach

Remarks:

Step 1: The initial ranges can be defined on the basis of the code developmental assessment results, while a uniform distribution can be assumed.

The principle is thus different from the other methods. We identify one distribution of model parameters that permit to bound the chosen experimental data. This approach allows us to choose the distribution laws to be used; they are just tools in order to obtain code calculations that cover as close as possible the selected test data. The uncertainty quantification will not be impaired if there are better knowledge available about the distributions. Indeed, if there is a better function to represent the model uncertainty, it will permit to reduce the uncertainty ranges, while still covering the test data. Having a non-optimal distribution function will thus not impair the safety, because it will lead wider uncertainty ranges. From a safety point of view, this approach permits to guarantee that subsequent uncertainty analyses will be able to conservatively cover the output uncertainties.

Step 2: In order to be effective, the sample size has to be limited (say N=100) during iterations, but needs to remain statistically significant. Note that larger sample size with lower order will decrease the bounds, and hence a limited sample size with top and bottom rank is conservative (leading to larger uncertainties on the models, while less penalizing distribution could have covered the test data with a larger sample). Also uncertainty contributors are varying together, to be representative of the future uncertainty analysis. The principle is to perform the uncertainty analysis whose results represent the code uncertainties in simulation of the tests. It is an advantage to be able to easily treat the combined effects of different models.

Step 3: A quantitative criterion could be defined to measure the coverage.

Step 4: In the future applications, it is possible to define certain quantitative criteria to end the optimization, such as to reduce the uncertainty ranges. Note that the reduction of the ranges will often finish to be blocked by the calculations touching the experimental curve in one of the cases, or becoming overly dissymmetric. The loss of degrees of freedom is a good indicator of the progress of the optimization. When the ranges of the uncertain parameters can only be slightly reduced without causing difficulties, it can be considered that the process has converged.

The following assumptions were made to ensure the correctness of the approach:

- The other parameters are not important, or do not contribute significantly to the calculation results;
- There is neither bias in the used code, or in its inputs. This means that the uncertainty can be represented by random functions only and that the range of multipliers resulting from the optimization process will include the nominal value (1). If it is necessary to exclude the nominal value (1) in one of the model uncertainties, this means that either the optimization must be done in another direction or the models/inputs are biased and have to be improved. Compensating errors must be avoided.
- The true model uncertainty distributions (although unknown) are not distorted to the point that only over-conservative simple functions can bound the corresponding experimental results.
- There are no discontinuities that would prevent the optimization work.

Those assumptions must be verified in a final calculation for which the final distributions are applied to the sampling and the obtained upper and lower bounds of the selected calculated output parameters well cover the experimental data for all selected tests.

The IUQ approach can be applied to a matrix of selected SETs and IETs, in order to obtain the uncertainty ranges and distributions that include the effects of different scales of tests.

G.4 REFERENCES

[G.1] Adams, B.M., Bohnhoff, W.J., Dalbey, K.R., Eddy, J.P., Eldred, M.S., Gay, D.M., Haskell, K., Hough, P.D., and Swiler, L.P., "DAKOTA, A Multilevel Parallel Object-Oriented Framework for Design Optimization, Parameter Estimation, Uncertainty Quantification, and Sensitivity Analysis: Version 5.2 User's Manual," Sandia Technical Report SAND2010-2183, November 2011. (http://www.cs.sandia.gov/dakota)

[G.2] Laura P. Swiler, Brian M. Adams, and Michael S. Eldred, "Model Calibration under Uncertainty: Matching Distribution Information", SAND Report 2008-0632A, AIAA Paper AIAA-2008-5944. (http://dakota.sandia.gov/papers/AIAA-2008-5944.pdf)

APPENDIX H: METHODOLOGY USED BY PSI AS PART OF CONTRIBUTION TO PREMIUM

H.1 SCOPE OF PSI CONTRIBUTION

The PSI participation to the PREMIUM benchmark was made as part of the development of a new methodology, which is still at an early stage of development. The new methodology is essentially based on the use of Bayesian inference to derive the parameters of the PDF of relevant code input and parameters out of a set of representative experimental Separate-Effect-Test database for bottom reflooding [H.1].

The previous PSI methodology for the determination of code model parameter uncertainties [H.2] could not be readily employed with the TRACE code (it was implemented in the RETRAN-3D code, no more used at PSI), and the added-value of the method (clustering of the uncertainty parameters based on a wide range of test data) was of limited interest in the specific context of the PREMIUM benchmark, where only 6 FEBA reflood tests were proposed as the reference experiment database to infer closure model uncertainties.

The novelty of the new methodology is not in the use of Bayesian inference, but on the different aspects of its implementation for the specific case of time dependent problems using non-linear simulation models. Bayesian inference is a data assimilation procedure that employs a probabilistic framework to describe and update the model uncertainties. Bayesian inference procedure calls for a *prior* estimate of the PDF of the assumed uncertain model parameters which contains the available background information about the parameters.

This *prior* (PDFs estimate) serves as starting point of a calibration procedure based on a set of selected observable outcomes and a likelihood function. The calibration updates the *prior* into a *posterior* that maximizes the likelihood function of the set of selected uncertain parameters while taking into account all the uncertainties given by the *prior*.
By definition, a *prior* has to be defined with limited available information, and this is where engineering judgement is put into play in order to define a *prior* that is as sensible as possible.

Essentially, the PSI contribution PREMIUM Benchmark consisted in the determination phase of the *prior* for a Bayesian inference methodology that is being developed.

H.2 OUTLINE

- A set of input and model parameters for the TRACE code has been determined using engineering judgement based on available literature on the subject and prior experience of the authors.
- A *prior* estimate of the PDFs has been derived using information in available literature, and through local sensitivity analysis based uniquely on the provided FEBA experiment database (6 tests).
- The *prior* estimate has been verified through confirmatory uncertainty quantification for the 6 available FEBA tests, and has been submitted to the PREMIUM organizers [H.3].
- A blind analysis of the available PERICLES database (6 tests) has been done using the *prior* PDFs estimate [H.3] as part of Phase IV.

- A post-analysis of the available PERICLES database (6 tests) has been done using the same *prior* PDFs estimate, but corrected for the heater rods temperature initialization procedure [H.4], also as part of Phase IV.

H.3 METHOD DESCRIPTION

Simulation code

The thermal-hydraulics system code TRACE has been employed for PSI contribution to PREMIUM. With support of U.S.NRC, a prototypical version instrumented for propagation of uncertainties has been derived from the reference code version v5.0 Patch3 [H.5].

Input models

The TRACE input models for the FEBA and PERICLES tests facilities have been developed based on specifications provided by PREMIUM (GRS and CEA) and following whenever possible the modelling best-practices guidelines for the TRACE code [H.6].

Preliminary verification of the input models included sensitivity studies upon axial and radial nodalization, specific reflood input model options (e.g. fine-mesh parameters), time steps, and other aspects of the model that a trained TRACE user should verify.

Selection of the relevant parameters

The selection process differed depending on the type of parameter. Independently of its nature (aleatory/epistemic) or of its relevance (influential/not-influential), each of the selected parameters can fall in one of the two following categories:

- Input/parameter that is not specific to the TRACE code (e.g. initial and boundary conditions, material thermo-physical properties);
- Input/parameter that is specific to the TRACE code (e.g. implementation of the 2-phase momentum and heat transfer package for reflood conditions).

As for the parameters of the first category, these simply corresponded to the parameters recommended by the organizers and employed by most of the participants to Phase II.

As for the selection of the parameters specific to the TRACE code, one difficulty stems from the fact that TRACE is a relatively recent code (compared to codes like RELAP5, ATHLET or CATHARE), which has been essentially built out the different variants of the TRAC codes (TRAC-BF1, TRAC-P) to result in a single consolidated code applicable to both PWR and BWR reactors.

Another difficulty came from the fact that TRACE is currently undergoing significant developments and improvements, including modifications to the 2-phase closure models for momentum and heat transfer. As a consequence, the task of selecting a priori estimate of the PDFs was more difficult than for more established system codes.

In order to overcome this issue, the following principles have been followed to select the parameters:

a) The selection has been restricted to the physical models in the post-CHF package of the TRACE code (including reflood models), for the Inverted Annular Film Boiling (IAFB) and Dispersed Flow Film Boiling (DFFB) flow regimes [H.5];

b) The multiplication factors have been implemented at the highest-possible level of the structure of the post-CHF package, in order to allow using reference uncertainty information determined with system codes different from TRACE;

c) The spacer grids are known to have a significant impact on reflooding [H.7];

d) A parameter related to the minimum film boiling temperature should be selected, since it has (by design) a major impact on the quench time.

As a result of items a) and b), a set of 10 high-level parameters has been selected (5 per flow regime), namely for each flow regime: The wall-fluid HTC, the liquid-interface HTC, the vapour-interface HTC, the wall-fluid drag coefficient and the interfacial drag coefficient.

As for item c) 2 additional parameters have been selected. Namely, the spacer grids pressure loss coefficient model from Yao, Loftus, and Hochreiter and the convective heat transfer enhancement model from Yao, Hochreiter and Leech (see [H.5], pp. 425-429). These uncertainties were applied to all the spacer grids at once.

As for item d) the quench temperature parameter in TRACE (see [H.5], pp. 293-299) has been added to the list of uncertain parameter.

Preliminary determination of the uncertainty bands

A first determination of the uncertainty bands has been made following an internal selection process primarily based on use of information in available literature on uncertainties in physical models for large break LOCA analysis.

The main sources of information consisted of [H.8] and [H.9], which included uncertainty information for the closure models of system codes TRAC-PF1/MOD1, and ATHLET-Mod 2.1(Cycle B), respectively. Moreover, prior experience and knowledge of the closure model uncertainties of the CATHARE2 code (V1 .3L_1, Revision 5) has been used. Indeed, one of the co-authors of this work contributed in the late 90ies to the analysis by IPSN of the uncertainty quantification method “Méthode Déterministe Réaliste” for the PWR LB-LOCA, which has been proposed by EDF and has been evaluated in June 2000 as part of the “Groupe Permanent Réacteurs” [H.10]. As for the code RELAP5, no similar source of information could be found in available literature.

The high-level implementation of the multiplication parameters for uncertainties in the closure models for post-CHF interfacial/wall momentum and heat transfer, allowed using reference uncertainty information obtained from different codes. This approach was deemed adequate in the limited context of the determination of a prior estimate of the PDFs.

In order to simplify the following iterative procedure of the selection of the bounds of the PDFs, the uncertainty in the high-level multiplication factors to the physical models of the post-CHF heat transfer package has been devised following an empirical approach. The PDFs were assumed to follow a symmetric uniform or log-uniform law of the type [2-n, 2n], with n an integer. If n was strictly larger than 1, a log-uniform law was assumed, otherwise a uniform law was assumed.

Then, for each uncertain parameter of the second category (TRACE-specific parameters), n was determined so as to encompass the information available for a similar (or deemed related) parameter in [H.8] and [H.9]. This approach resulted sometimes in the selection of particularly large bounds of the multiplication factors (up to a factor 8). This was however found appropriate in the general context of the determination of a prior, especially in order to avoid mistakenly underestimating and thus potentially neglecting important influential parameters.

Moreover, in order to avoid any risk of code prediction distortions due to unrealistically large uncertainty bands of the parameters, a systematic verification of the model results has been conducted through local sensitivity analysis ("local" means that one parameter is changed at a time) where each parameter was set to its minimum or maximum values. The use of bounded PDF laws (uniform, log-uniform) allowed readily defining the minimum/maximum parameter values for the local sensitivity analysis. The verification was made by visual inspection of the model results (compared to experiment data from the 6 FEBA tests).

Refinement of the uncertainty bands based on FEBA experiment data

Once the initial set of uncertainty bands has been established, series of full uncertainty quantifications were to be executed (200 codes runs per test). The procedure was to iteratively modify the bounds of the most influential parameters (determined by the initial local sensitivity analysis) until a sufficient coverage ratio of the experiment results would be obtained. This coverage ratio was estimated visually. No special error estimators have been employed. Again, this approach was found adequate in the context of the search of a prior.

For this phase of the work, the use of integer power exponents to define the bounds of the PDFs was also deemed appropriate should several iterations of the uncertainty quantification study be necessary. Indeed, simply increasing or decreasing by one the value of n was deemed more efficient, in the context where only engineering judgement would be used (namely, a simple visual verification of the coverage of the experiment data).

Thus few adjustments to the prior estimates for the exponent n of the PDF of the most influential parameters were to be made iteratively using the FEBA experiment data, until obtaining an adequate coverage of the temperature and pressure evolutions from the FEBA tests (no other experiments data were employed). The determination of the most influential parameters was made based on the results of the local sensitivity analysis.

In fact, only two iterations have been required, since the first set of PDF estimate was already resulting in very satisfactory coverage results of the FEBA data, however relatively large. Thus, the only modification to the PDFs consisted in narrowing the uncertainty of the interfacial drag parameter for DFFB, which proved to be one of the most influential parameters of the model (the corresponding PDF band was narrowed from [0.125; 8] to [0.25; 4]).

The same modification was considered for the interfacial drag parameter for IAFB, essentially based on the consideration that the band ([0.125; 8]) was implausibly too large. However it has been decided not to modify this parameter for consistency with the employed methodology, since the local sensitivity study for this parameter did not show that this parameter was particularly influential for the prediction of the maximum heater rod outer temperatures.

Nevertheless, it should be added that from a related work carried out later in 2015 [H.11], it can be inferred that a narrowing of the PDF from [0.125; 8] to [0.25; 4] of the interfacial drag parameter for the IAFB flow regime should not significantly change the results of the uncertainty quantification analysis made as part of PREMIUM. Therefore, as a result of the determination of the uncertainty bands, the widest bands for the most influential parameters of the PREMIUM benchmark did not exceed [0.25; 4].

Uncertainty quantification for the PERICLES tests

The uncertainty quantification for the PERICLEs was composed of two phases, namely a blind phase and a later open phase, after release of the test data.

As for the blind phase, the uncertainties selected for the PERICLES model were identical to the ones determined and verified using the FEBA data, and the PDFs were also identical [H.3]. The nodalization of

the PERICLES using three parallel channels (using the three-dimensional VESSEL component in TRACE) only resulted in an increase of the number of parameters related to boundary conditions (inlet and outlet).

As for the following open phase, the same parameters and associated PDFs have been re-conducted. The only modification consisted in improving the initialization methodology to achieve a more accurate initial temperature distribution in the heater rods, compared to experiment data. It was however eventually found that this improvement to the model had a very limited impact on the uncertainty quantification results [H.4].

H.4 REFERENCES

[H.1] Wicaksono D., Pautz A. and Zerkak O.: *Research Plan: Bayesian Uncertainty Quantification of Physical Models in Thermal-Hydraulics System Codes*, Submitted to the EPFL Doctoral School on November 29 2013, and presented on December 9, 2013.

[H.2] Vinai P., Macian-Juan R. M. and Chawla R.: *"A statistical methodology for quantification of uncertainty in best estimate code physical models"*, Annals of Nuclear Energy 34, pp. 628–640, (2007).

[H.3] Wicaksono D., Zerkak O. and Pautz A.: *PSI Contribution to PREMIUM Phase IV*, EPFL-PSI Report (SB-RND-ACT-006-13.001), April 2014.

[H.4] Wicaksono D., Zerkak O. and Pautz A.: *PSI Contribution to PREMIUM Phase IV; Post-Test Uncertainty Quantification of FEBA and PERICLES Reflood Tests*, EPFL-PSI Report (SB-RND-ACT-006-13.002), September 2014.

[H.5] U.S.NRC: *TRACE V5.0 Theory Manual; Field Equations, Solution Methods, and Physical Models*, May 7 2012.

[H.6] U.S.NRC: *TRACE Pressurized Water Reactor Modeling Guidance*, Preliminary Draft Report, October 24 2012.

[H.7] Miller D. J., Cheung F. B. and Bajorek S. M.: *"Investigation of grid-enhanced two-phase convective heat transfer in the dispersed flow film boiling regime"*, Nuclear Engineering and Design, vol. 265, pp. 35-44, (2013).

[H.8] Wickett A. J., Birchley J. C. and Holmes B. J.: *Quantification of Large LOCA Uncertainties*, AEA Reactor Services Report, November 29, 1991.

[H.9] Glaeser H., Krzykacz-Hausmann B., Luther W., Schwarz S. and Skorek T.: *Methodenentwicklung und exemplarische Anwendungen zur Bestimmung der Aussagesicherheit von Rechenprogrammergebnissen*, Final Report of GRS Reactor Safety Research-Project RS1165, GRS-A-3443, November 2008.

[H.10] IPSN: *Rapport d'activité 2000 de l'IPSN*, (2001).

[H.11] Wicaksono D., Zerkak O. and Pautz A.: "*A Methodology for Global Sensitivity Analysis of Transient Code Output Applied to a Reflood Experiment Model using TRACE*", Accepted for oral presentation at the International Topical Meeting on Nuclear Reactor Thermal Hydraulics NURETH-16, Chicago, USA, August 30-September 4, 2015.